Evaluating immunotoxicity of oil sands process-affected waters using the RAW 264.7 macrophage cell line

By

Kendra Mary Woodall

A thesis submitted in partial fulfillment of the requirements for the degree of

Master of Science

in

Physiology, Cell and Developmental Biology

Department of Biological Sciences

University of Alberta

Abstract

Alberta's wide-ranging oil sands deposits are recovered via oil sands processes such as surface mining and in situ approaches. Oil sands processes use substantial volumes of water known as oil sands process-affected waters (OSPW) and as per a zero-discharge policy, this water needs to be stored on location. Tailings ponds have resulted as a temporary storage solution, and remediation strategies are being developed to treat and target contaminants. Naphthenic acids (NAs), polycyclic aromatic hydrocarbons, metals, and ions are all contaminants found in OSPW. OSPW toxicity is mainly attributed to NAs and exposure has resulted in deformities, reduction in growth, and impaired development in aquatic and terrestrial species as well as immunotoxicity in macrophages. Advanced oxidation processes degrade NAs, and treated OSPW must be evaluated to determine efficacy in reducing toxicity. I propose using RAW 264.7 macrophages in a cell-based *in vitro* biosensor system to evaluate immunotoxicity in untreated and treated waters. Taking this further, pharmacological inhibitors can be used to understand the activation of macrophage cells by OSPW and identify OSPW-mediated receptors and receptor pathways. Macrophages use numerous receptors, like Toll-like receptors (TLRs), to detect and rapidly respond to stimuli, like bacterial lipopolysaccharides (LPS). I found that OSPW upregulates pro-inflammatory genes and advanced oxidation treatments, like electrooxidation and solar oxidation, reduces this expression. I then explored how OSPW exposure results in immunotoxicity. I found that OSPW triggers pro-inflammatory responses comparable to activation by endotoxic stimuli such as LPS. Toll-like receptor 4 (TLR4) and intracellular signaling proteins associated with TLR signaling, such as NF-κB and IRAK1/4, are implicated in both LPS- and OSPW-mediated signaling. These similarities between LPS- and OSPW-activated signaling indicate a potential role for TLR4 in detecting the immunotoxic constituent(s)

of OSPW. This research enhances our understanding of how OSPW is perceived by mammalian cells and the immunotoxicity incited by OSPW. In addition, this research illustrates how RAW 264.7 macrophage cells successfully outline immunotoxicity resulting from exposure to contaminated waters and in the future, may be used to evaluate potential water treatments.

Preface

These are original experiments performed by Kendra Mary Woodall and no results of this thesis have been published.

Acknowledgements

Table of Contents

List of Tables

List of Figures

List of Abbreviations

Ang II	Angiotensin II
AOP	Advanced Oxidation Process
AP-1	Activator Protein 1
CD14	Cluster of Differentiation 14
DAMP	Damage-associated Molecular Pattern
DMEM	Dulbecco's Modified Eagle's medium
ELISA	Enzyme Linked Immunosorbent Assay
ERK1/2	Extracellular Signal-Related Kinase 1/2
FBS	Fetal Bovine Serum
HEK293	Human Embryonic Kidney 293
HIV	Human Immunodeficiency Virus
I-κBα	Inhibitor of Nuclear Factor kappa B
IC$_{10}$	10% Inhibitory Concentration
IFN-β	Interferon-β
IFNλ1/2	Interferon-λ1/2
IL-10	Interleukin 10
IL-1R	Interleukin 1 Receptor
IL-2	Interleukin 2
IL-6	Interleukin 6
iNOS	inducible Nitric Oxide Synthase
IP-10	Interferon-γ-induced Protein 10
IRAK1/4	Interleukin-1 Receptor-Associated Kinase 1/4
IRAK2	Interleukin-1 Receptor-Associated Kinase 2
IRF3	Interferon Regulatory Factor 3
IRF7	Interferon Regulatory Factor 7
LBP	LPS-Binding Protein
LC$_{50}$	50% Lethal Concentration
LPS	Lipopolysaccharide
MCP-1	Monocyte Chemoattractant Protein-1
MD-2	Myeloid Differentiation 2
MEK1/2	Mitogen Activated Protein Kinase Kinase 1/2
MIP-2	Macrophage Inflammatory Protein-2
MyD88	Myeloid Differentiation Primary Response 88
NA	Naphthenic Acids
NAFC	Naphthenic Acid Fraction Component
NF-κB	Nuclear Factor kappa B
NO	Nitric Oxide
OD$_{600}$	Optical Density
OSPW	Oil Sands Process-Affected Waters
PAC	Polycyclic Aromatic Compounds
PAH	Polycyclic Aromatic Hydrocarbons
PAMP	Pathogen-Associated Molecular Pattern
PBS	Phosphate-Buffered Saline
Pen-Strep	Penicillin-Streptomycin

PKCα	Protein Kinase C-α
PKCβ	Protein Kinase C-β
PRR	Pattern Recognition Receptor
qPCR	quantitative Polymerase Chain Reaction
RANTES	Regulated Upon Activation, Normal T cell Expressed and Secreted
REF	Relative Enrichment Factor
SEM	Standard Error of the Mean
TIR	Toll/IL-1R homology domain
TIRAP	TIR Domain-Containing Adaptor Protein
TLR	Toll-Like Receptor (1, 2, 3, 4, 6)
TNF-α	Tumor Necrosis Factor-α
TNFR1	Tumor Necrosis Factor-α Receptor
TRAF6	Tumor Necrosis Factor Receptor-Associated Factor 6
TRAM	TRIF-related Adaptor Molecule
TRIF	TIR domain-containing adaptor-inducing IFN-β
UV	Ultraviolet

Chapter I

General Introduction

1.1 Introduction

Alberta is well-recognized for its abundant oil sands deposits as three major deposits are found in northern Alberta: Athabasca, Peace River, and Cold Lake (Mahaffey and Dubé, 2017). As Alberta's proven oil reserves are the third greatest in the world (Hewitt et al., 2020), oil sands processing is a massive industry in Alberta. Bitumen can be extracted by surface mining or in situ methods depending on the mine depth (Allen, 2008). Surface mining is applied to shallow deposits, and the resulting slurry is transferred to a processing facility where it undergoes the Clark Hot Water Process which separates bitumen and removes other components (Allen, 2008; Mahaffey and Dubé, 2017). In situ methods are implemented for deep deposits and involve pumping steam into a deposit and collecting the released bitumen (Allen, 2008). Both bitumen extraction methods use water, and to create one barrel of oil, 3.1 barrels of water for surface mining or 0.4 barrels of water for in situ methods are required (Mahaffey and Dubé, 2017). This unsustainably results in oil sands process-affected water (OSPW), a term that encompasses all water exposed to oil sands (Li et al., 2017). OSPW must be stored on location due to a zero-discharge policy and has resulted in the creation of tailings ponds (Allen, 2008).

OSPW consists mainly of water as well as clay, sand, silt, and residual bitumen (Mahaffey and Dubé, 2017). OSPW is contaminated with organic compounds like naphthenic acids (NAs), polycyclic aromatic hydrocarbons (PAHs), and phenols as well as inorganic components like nitrate, fluoride, magnesium, and boron (Li et al., 2017; Phillips et al., 2020). This water must be remediated and then returned to the environment. Many remediation

methods are developed to address a major contaminant of interest, NAs (Quinlan and Tam, 2015). NA exposure has resulted in toxicity to a variety of organisms (Armstrong et al., 2007; Bartlett et al., 2017; Kavanagh et al., 2012; Kinley, McQueen, & Rodgers, 2016; Li et al., 2017; Scarlett et al., 2013). However, OSPW and remediated OSPW must be assessed for biological impacts. OSPW bioactivity has previously been assessed via changes in gene expression and protein secretion of RAW 264.7 macrophage cells (Lillico et al., 2023). Lillico et al. (2023) demonstrates changes in bioactivity before and after water capping oil sands-impacted waters using their immune cell-based bioactivity assay. This immune cell-based assay could be used to assess the efficacy of remediation methods in reducing bioactivity. Furthermore, understanding how bioactivity is perpetuated will further our understanding of the risk of OSPW contaminants and may guide future remediation strategies.

1.2 Research Objectives

Here, I intend to address the need to assess remediation strategies and explore how bioactivity is perpetuated. OSPW bioactivity has previously been demonstrated using an *in vitro* immune cell-based assay (Fu et al., 2017; Lillico et al., 2023; Phillips et al., 2020), and I aim to differentiate bioactivity before and after OSPW treatment. To understand how OSPW induces bioactivity, I want to investigate how cells are activated by OSPW and bridge the knowledge gap between cell activation and cell response.

RAW 264.7 mouse macrophage cells show a reduction in cell proliferation and viability with increasing NA concentration of whole OSPW (Fu et al., 2017) and increases in expression of pro-inflammatory markers like *tnfa* with exposure to the organic fraction of OSPW (Phillips et al., 2020). Here, I expand on previous work demonstrating OSPW exposure activates and

influences pro-inflammatory activities of macrophage cells. I aim to determine if bioactivity mediated by OSPW is decreased by electrooxidation or solar oxidation treatment. It has been shown that the organic fraction of OSPW, which includes NAs (Li et al., 2017), contributes to pro-inflammatory activities (Lillico et al., 2023; Phillips et al., 2020) and as advanced oxidation processes (AOPs) degrade NAs (Abdalrhman and El-Din, 2020; Abdalrhman, Zhang, and El-Din, 2019; Meng et al., 2021), a decrease in bioactivity after treatment suggests that OSPW-mediated pro-inflammatory effects may be facilitated by NAs. My goal is to examine differences in chemokine gene expression between solar- and electrooxidation-treated OSPW as compared to untreated OSPW. I aim to outline differences in *mip-2, ip-10,* and *mcp-1* expression between untreated and treated water. Ultimately, this will determine if treatments that remove NAs are successful in reducing bioactivity.

Additionally, I aim to explore how RAW 264.7 mouse macrophage cells are activated to result in pro-inflammatory changes in gene expression. Pharmacological inhibitors have previously been used to study cell signaling pathways and investigate their associated receptors and signaling proteins (Cheng et al., 2012; Israf et al., 2007; Koide et al., 2005; Takashima et al., 2009; Zhang et al., 2021). I applied this approach to explore how immune cells detect and respond to OSPW exposure and identify intracellular signaling proteins necessary for OSPW-mediated activation. Toll-like receptors (TLRs) are known to modulate pro-inflammatory gene expression when activated (Ciesielska, Matyjek, and Kwiatkowska, 2021; Liu et al., 2014; Takashima et al., 2009) and are potentially involved in OSPW-mediated macrophage cell activation. By understanding how OSPW activates cells and how changes in gene expression are occurring, we can elucidate the components of OSPW that contribute to bioactivity. In addition, I compare patterns of pro-inflammatory responses from OSPW stimulation to agonists of specific

receptors to further elucidate OSPW-induced response. This exploration of macrophage cell

response to OSPW stimulation will set a basis for OSPW-mediated bioactivity. This research

provides insight into cellular effects of OSPW exposure and may be used to evaluate and monitor

potential water treatments as well as guide future remediation strategies.

Chapter II

Literature Review

2.1 OSPW

OSPW classifies as all water that has been exposed to the oil sands or processing (Li et al., 2017). Water is involved in different aspects of oil sands processing for deep and shallow deposits (Allen, 2008; Mahaffey and Dubé, 2017). *In situ* processes address deep oil sands deposits and use steam injection to collect bitumen (Allen, 2008). Surface mining is utilized for shallow deposits, and a modified Clark Hot Water Process is used to extract bitumen and separate components (Allen, 2008; Giesy, Anderson, and Wiseman, 2010). A zero-discharge policy necessitates that tailings and process-affected waters are retained on site and this has resulted in the creation of tailings ponds (Allen, 2008; Giesy, Anderson, and Wiseman, 2010). One oil barrel needs 2-4 barrels of water during extraction (Giesy, Anderson, and Wiseman, 2010) and with Alberta's massive oil reserves, this process is not sustainable. Therefore, OSPW needs to be remediated and returned to the environment (Mahaffey and Dubé, 2017).

As OSPW includes a wide range of process-affected waters such as seepage from settling basins, active tailings ponds, and aged OSPW from reclaimed sites, it contains many different constituents and contaminants in varying proportions (Li et al., 2017). OSPW consists mainly of water as well as sand, clay minerals, silt, and residual bitumen (Allen, 2008; Mahaffey and Dubé, 2017). Among many others, OSPW contaminants comprise of naphthenic acids (NAs), polycyclic aromatic compounds (PACs), and metals (Hussain and Stafford, 2023; Li et al., 2017).

2.1.1 Naphthenic Acids (NAs)

NAs are recognized as a major source of OSPW-mediated toxicity and are responsible for acutely toxic effects on various species (Allen, 2008; Armstrong et al., 2007; Li et al., 2017). NAs are an assortment of carboxylic acids that have three structural characteristics: a carboxylic group, an aliphatic side chain, and cycloalkane ring or rings (Brown and Ulrich, 2015). Oil sands extraction processes allow for the release of NAs into OSPW (Mahaffey and Dubé, 2017). NAs may have more than one possible mechanism of toxicity and toxicity may depend on concentration, molecular weight, and/or structure (Brown and Ulrich, 2015; Rundle et al., 2021). Two proposed mechanisms of action include disrupting the cell membrane (Brown and Ulrich, 2015; Frank et al., 2008; Frank et al., 2009) and disruption of mitochondrial functions (Rundle et al., 2018; Rundle et al., 2021).

NAs display surfactant qualities and these qualities are thought to be linked to toxicity (Brown and Ulrich, 2015). NAs have both hydrophilic and hydrophobic characteristics due to a carboxyl functional group and an alicyclic end which results in surfactant qualities (Brown and Ulrich, 2015). Narcosis is thought to occur when this molecule interacts with the lipid bilayer, interferes with functioning, and can lead to cell death (Brown and Ulrich, 2015; Frank et al., 2008).

Another possible toxicity mechanism involves disrupting cell metabolism (Rundle et al., 2018; Rundle et al., 2021). NAs may impact mitochondrial function via oxidative uncoupling and hinder the electron transport system (Rundle et al., 2018; Rundle et al., 2021). The study by Rundle et al. (2018) provides evidence of the disruption of the electron transport system by NAs using mitochondria isolated from rainbow trout livers. They propose that NAs are protonated, transported into the mitochondrial matrix, and deposit the acquired proton, which effectively

disrupts the proton gradient (Rundle et al., 2018). The exact step in which NAs may interfere with the electron transport system is unknown (Rundle et al., 2018). Adamantane carboxylic acids have been shown to uncouple mitochondrial membrane potential in mitochondria from rainbow trout liver and the mechanism of specific adamantane NAs may be comparable to how OSPW-extracted NAs may interact with the mitochondria (Rundle et al., 2021).

The molecular weight and structure of NAs has been associated with differing toxicities (Anderson et al., 2012; Frank et al., 2008; Frank et al., 2009; Li et al., 2017; Lo, Brownlee, & Bunce, 2006). Acute toxicity is thought to be greater with lower molecular weight NAs as compared to higher molecular weight NAs (Anderson et al., 2012). OSPW acute toxicity decreases as it ages and NAs with multiple rings are not as easily degraded by microbes (Anderson et al., 2012; Holowenko, MacKinnon, and Fedorak, 2002; Lo, Brownlee, & Bunce, 2006). High molecular weight NA exposure to *Vibrio fisheri* has resulted in lower toxicity than low molecular weight NAs (Frank et al., 2008; Li et al., 2017). Another study demonstrated that the OSPW fraction containing multi-ring compounds in large proportions, and so corresponding to a higher molecular weight, resulted in reduced toxicity (Frank et al., 2008; Lo, Brownlee, & Bunce, 2006). However, this defies the idea that the higher hydrophobicity associated with high molecular weight molecules should demonstrate a larger narcotic impact (Li et al., 2017). A possible explanation is that the presence of more carboxylic acid groups in higher molecular weight NAs reduces hydrophobicity and the associated toxicity (Frank et al., 2009; Li et al 2017). The chronic toxicity of OSPW is an apparent concern as OSPW acute toxicity declines with age (Bartlett et al., 2017).

Microtox assays have been used to assess NA toxicity from OSPW fractions as well as from individual NAs (Jones et al., 2011; Morandi et al., 2015). High toxicity, as determined by

exposure to *Vibrio fischeri* in a Microtox assay, was detected in the OSPW fraction containing high proportions of NAs (Morandi et al., 2015). These results support the notion that NAs are a major source of acute toxicity. The Microtox assessment of individual NAs reflected that specific types of NAs were more toxic than others (Jones et al., 2011). Specifically, a bicyclic acid, 3-decalin-1-yl propanoic acid, was the most toxic of all acids tested and *n*-hexanoic acid was one of the least toxic acids (Jones et al., 2011). Overall, different types of NAs have varying toxicities (Jones et al., 2011) which influences the complexity and toxicity of OSPW.

The bioactivity of OSPW fractions that contain NAs or NAs extracted from OSPW have been previously assessed *in vitro* using mammalian cells (Garcia-Garcia et al., 2011; Leclair et al., 2015; Lillico et al., 2023). In mammalian cell lines, such as mouse macrophage cells, exposure to the OSPW organic fraction has resulted in bioactive changes (Lillico et al., 2023). For example, RAW 264.7 murine macrophage cells exposed to a treated OSPW organic fraction showed changes in pro-inflammatory gene expression as compared to RAW 264.7 cells exposed to a saline control. NAs may also impact hormone-related or receptor-mediated reproductive pathways (Leclair et al., 2015). H295R cells showed significantly elevated corticosterone production when exposed to the highest assessed concentration of an OSPW-extracted NA fraction and NAs from OSPW-extracted fractions also appear to have antiandrogenic or antiestrogenic properties (Leclair et al., 2015). Garcia-Garcia et al. (2011) shows immunotoxic effects of the organic fraction of OSPW as exposure resulted in reduced phagocytosis by bone marrow-derived macrophage cells and altered gene expression of specific cytokines like IL-1, IL-12, and TNF- α after exposure to an OSPW fraction containing 50 μg/mL NAs. In addition, the ability of NK cells to kill target cells decreased after exposure to the OSPW fraction containing 50 μg/mL NAs (Garcia-Garcia et al., 2011).

NA toxicity from both commercial and OSPW sources have also been investigated in plants and invertebrates (Armstrong et al., 2007; Bartlett et al., 2017; Kinley, McQueen, & Rodgers, 2016). Armstrong et al. (2007) found commercial NAs to be more phytotoxic than NAs extracted from OSPW when studying exposure in *Typha latifolia* (cattail) and *Phragmites australis* (common reed grass). In addition, higher molecular weight NAs seemed to be less phytotoxic than low molecular weight NAs (Armstrong et al., 2007). Higher toxicity is seen in invertebrates exposed to commercial NAs compared to NA fraction components (NAFCs) from OSPW (Bartlett et al., 2017). For example, *Hyalella azteca* (freshwater amphipod) survival was affected by exposure to commercial NAs as well as NAFCs from OSPW with commercial NA exposures demonstrating 10-30 times the toxicity of NAFCs as indicated by LC_{50} (Bartlett et al., 2017). *Lampsilis cardium* (freshwater mussel) glochidia viability was impacted by commercial NA exposure which showed 120 times the toxicity of NAFCs from fresh OSPW (Bartlett et al., 2017). In addition, the survival of *H. azteca* and viability of *L. cardium* glochidia were impacted at environmentally relevant concentrations of NAFCs (Bartlett et al., 2017). The structure, composition, and concentration of NAFCs influences toxicity (Bartlett et al., 2017) and this is apparent from the studies comparing commercial and OSPW-derived NAs (Armstrong et al., 2007; Bartlett et al., 2017). There is also a noticeable difference in the sensitivity of plants and invertebrates to NAs (Kinley, McQueen, & Rodgers, 2016). For instance, as commercial NA concentrations increase, the survival of *Ceriodaphnia dubia* (microcrustacean), *Hyalella azteca* (amphipod), and *Chironomus dilutus* (midge) decreases (Kinley, McQueen, & Rodgers, 2016). The root length of *Typha latifolia* (common cattail) decreases at higher commercial NA concentrations than invertebrate mortality occurs, demonstrating that invertebrates are more sensitive to commercial NA toxicity than plants (Kinley, McQueen, & Rodgers, 2016).

NA exposure has been shown to result in toxicity, deformities, and impaired reproduction in fish species (Kavanagh et al., 2012; Marentette et al, 2015; Scarlett et al., 2013). In larval zebrafish, acute toxicity was examined by exposure to an OSPW fraction containing classical alicyclic NAs or aromatic NAs (Scarlett et al., 2013). Researchers showed toxicity resulting from both aromatic, high molecular weight acids and alicyclic acid exposure, with the former being slightly more toxic. Marentette et al. (2015) found walleye and fathead minnow early-life stages demonstrated toxicities after exposure to NAFC concentrations that were equal to or lower than the concentrations in OSPW obtained from an active settling basin from which the NAFCs were extracted. Both walleye and fathead minnows showed a dose-response increase in deformities at hatch with increasing NAFC concentration (Marentette et al., 2015), which outlines the potential impact of NAFCs on organism development. NAFCs may especially impact fish species with lengthy embryonic periods (Marentette et al., 2015). Reproduction of fish is affected as there was a decrease in egg spawning by fathead minnow as well as decreased testosterone and 11-ketotestosterone in male fathead minnow after 21 days of exposure to NAs extracted from OSPW (Kavanagh et al., 2012).

Notably fewer studies have assessed NA exposure in vertebrates outside of fish, though NAs have displayed toxicity as indicated by altered behaviours, deformities, and genetic changes at a cellular level in other aquatic, terrestrial, and avian species (Elvidge et al., 2023; Garcia-Garcia et al., 2011; Melvin & Trudeau, 2012). Amphibians at earlier developmental stages are vulnerable to pollutants in water as their physiological development is coordinated by sensitive hormone signaling, and their growth occurs in water (Melvin & Trudeau, 2012). Early-life exposure of *Rana sylvatica* (wood frog) tadpoles exposed to NA fraction compounds extracted from OSPW resulted in changes in antipredator behaviours and chemical alarm cue production

(Elvidge et al., 2023). Commercial NA exposure to *Lithobates pipiens* (Northern Leopard frog) and *Silurana tropicalis* (Western-clawed frog) tadpoles induced morphological deformities including tail necrosis and bent tails (Melvin & Trudeau, 2012). In addition, *L. pipiens* and *S. tropicalis* exhibited significantly diminished development and growth after embryonic exposure to NAs (Melvin & Trudeau, 2012).

Terrestrial vertebrates like mice showed genetic changes in the liver, which is a prominent detoxifying organ (Garcia-Garcia et al., 2011). In the liver of mice gavaged with the organic fraction of OSPW, containing 100 mg/kg NAs, the downregulation of cytokine genes was reported, including *tnf-α*, *il-1*, and *ifn-γ* (Garcia-Garcia et al., 2011). However, some vertebrates are only minimally affected by acute NA exposure (Gentes et al., 2007). *Tachycineta bicolor* (tree swallows) nestlings demonstrated relatively unimpacted growth, blood biochemistry, and organ weights when dosed with environmentally relevant concentrations of NAs (Gentes et al., 2007). These results conflict with previous studies regarding NA impact on aquatic organisms which are vulnerable to NAs and at risk to their surfactant properties (Gentes et al., 2007). It is important to note that how NAs incur toxicity in terrestrial organisms, like *T. bicolor*, is not the same as aquatic organisms because exposure mainly occurs orally versus through direct contact (Gentes et al., 2007).

As OSPW is a complex mixture, other interactions may occur between OSPW constituents that may influence the resulting toxicity seen in OSPW studies (Kavanagh et al., 2012; Li et al., 2017). For example, the secondary sex characteristic, tubercles, and testosterone in male fathead minnows was impacted by NA extracts differently depending on the presence of $NaHCO_3$ (Kavanagh et al., 2012). Exposing male fathead minnows to NA extracts resulted in significantly less tubercles whereas when $NaHCO_3$ was added, tubercle number was comparable

to controls (Kavanagh et al., 2012). Testosterone concentration in male fathead minnows was also significantly lower when exposed to NA extracts whereas the addition of $NaHCO_3$ resulted in no significant difference from the controls. Thus, the addition of $NaHCO_3$ may interfere with the reproductive toxicity invoked by NA extracts. $NaHCO_3$ may also impact bioaccumulation as less NA accumulation occurred in fathead minnow tissues when treated with both $NaHCO_3$ and NA extracts compared to just NA extracts (Kavanagh et al., 2012). Overall, it may be possible that $NaHCO_3$ decreases NA extract toxicity and tissue accumulation.

It has been reported that not all OSPW toxicity may be attributed to NAs (Klamerth et al., 2015). For example, Klamerth et al. (2015) showed that even after organic fractions were extracted from OSPW and treated with ozonation to degrade NA content, toxicity was still seen in *Vibrio fischeri* via Microtox assessments. Thus, NAs may not be entirely accountable for toxicity from OSPW, and it is important to move forward with investigating other OSPW constituents that may have toxic effects.

2.1.2 Polycyclic Aromatic Compounds

Another contaminant implicated in oil sands toxicity is polycyclic aromatic compounds (PACs) (Hussain and Stafford, 2023). PAHs are encompassed within PACs and have a structure of more than one aromatic ring that may have three different types of positioning: linear, angular, or cluster (Folwell, McGenity, and Whitby, 2016; Hussain and Stafford, 2023). PACs as well as PAHs are referred to as either high or low molecular weight (Folwell, McGenity, and Whitby, 2016; Hussain and Stafford, 2023). High molecular weight PACs have four or more aromatic rings whereas low molecular weight PACs have two to three aromatic rings (Hussain and Stafford, 2023). It's thought that carcinogenic PAHs have decreased solubility and increased

molecular weight (Folwell, McGenity, and Whitby, 2016). Surface water located near Albertan oil sands contain specific PACs which levels surpassed the Canadian Council of Ministers of the Environment guidelines (Hussain and Stafford, 2023). PAHs are listed on the US Agency for Toxic Substances and Disease Registry (Kurek et al., 2013) and OSPW contains about 1000 times the amount of PAHs listed in Canadian Environmental Quality Guidelines (Folwell, McGenity, and Whitby, 2016). Thus, PAHs are a cause for concern regarding OSPW toxicity.

PAHs are known for their toxicity, and more specifically, their carcinogenic effects due to their ability to enter cells and form metabolites that can interact with DNA, resulting in mutagenicity (Honda and Suzuki, 2020). PAHs have been implicated in effects including oxidative stress, genotoxicity, immunotoxicity, and developmental toxicity (Honda and Suzuki, 2020). Varanasi et al. (1987) found that *Parophrys vetulus* (English sole) readily uptakes aromatic hydrocarbons, and that juvenile *P. vetulus* was reported to have 10 times the binding of benzo[a]pyrene intermediates to hepatic DNA as compared to adults.

Median and maximum PAH levels are generally elevated in the sediment of experimental wetlands as well as in invertebrates which leads to the concern of bioavailability (Wayland et al., 2008). Wayland et al. (2008) assessed PAH levels in larval and adult insects as well as in sediment from experimental, reclaimed, and reference wetlands. Experimental wetland sediment generally had the greatest PAH concentrations (Wayland et al., 2008). Larvae from experimental ponds had higher maximum and median amounts of alkylated PAHs as compared to larvae from reference or reclaimed ponds (Wayland et al., 2008). However, there was no substantial increase in PAH levels in adult insects from experimental wetlands as compared to those from reclaimed or reference sites (Wayland et al., 2008). The lack of association between wetland type and PAH levels may be due to adult insects migrating and feeding elsewhere (Wayland et al., 2008). In

addition, the PAH content adult insects encounter as larvae may only contribute to a limited degree (Wayland et al., 2008). Nevertheless, the PAH content of the environment, and consequently invertebrate larvae, highlights the need to further investigate the variables dictating PAH bioavailability (Wayland et al., 2008).

Adverse effects, including deformities, have been documented in vertebrates exposed to oil sands-impacted sediment containing considerably high concentrations of alkyl-substituted PAHs (Colavecchia et al., 2004). Colavecchia et al. (2004) explored the impact of oil sands-affected sediment on the early life stages of *Pimephales promelas* (fathead minnows) and evaluated PAH concentrations from the sediment of natural and anthropogenic sites. Increased malformations and larval mortality as well as decreased hatching success and size were reported in *P. promelas* after exposure to oil sands and sediment from an oil sands-impacted wastewater pond (Colavecchia et al., 2004). Oil sands process-impacted sediment from a wastewater pond was reported to contain substantial amounts of PAHs with total PAH concentration of 1300 μg/g (Colavecchia et al., 2004). The levels of PAHs in the oil sands-influenced areas potentially played a role in the reported toxicological outcomes (Colavecchia et al., 2004).

PACs and PAH metabolites have been detected within the bile, feces, and muscles of vertebrate species exposed to oil sands process-affected areas with consumption as the most likely route of exposure (Fernie et al., 2018; Gurney et al., 2005). Gurney et al. (2005) reared *Anas platyrhynchos* (mallard) ducklings on oil sands-impacted wetlands and detected PAH metabolites in their bile. Significantly greater concentrations of pyrene and naphthalene were found in the bile of ducklings reared on oil sands-impacted wetlands as compared to reference wetlands (Gurney et al., 2005). This is indicative that ducklings encountered greater amounts of PAHs on oil sands-impacted wetlands and the route of exposure may have been consumption

(Gurney et al., 2005). Fernie et al. (2018) evaluated PAC exposure of nestling *Tachycineta*

bicolor (tree swallows) in oil sands mining-related sites and compared to nestlings at reference

locations. Sixty percent of *T. bicolor* nestlings had discernable amounts of six PAHs: C1-

phenanthrenes, C1-fluorenes, C2-fluorenes, naphthalene, C1-naphthalenes, and C2-naphthalenes

(Fernie et al., 2018). Greater concentrations of most PACs were found in the feces and muscle of

T. bicolor nestlings at the oil sands mining-related sites compared to nestlings from reference

sites (Fernie et al., 2018). Like how Gurney et al. (2005) suggests exposure may be through

ingestion, the study by Fernie et al. (2018) implicates the route of exposure of select PACs may

be diet and that water and air sources may also contribute to PAC exposure.

Microbial transformation of high molecular weight PAHs has been investigated (Folwell,

McGenity, and Whitby, 2016). Folwell, McGenity, and Whitby (2016) explored the

transformation of high molecular weight PAHs by microbes from OSPW and identified a change

in the community composition of bacteria to support *Pseudomonas*, *Microbacterium,* and

*Bacillu*s species. Of the three PAHs studied, pyrene was found to be more highly eliminated

than benzo[b]fluoranthene and benzo[a]pyrene (Folwell, McGenity, and Whitby, 2016). This

study shows that microbes in OSPW are able to transform high molecular weight PAHs and

further research is needed to explore the biodegradation of PAHs (Folwell, McGenity, and

Whitby, 2016).

2.1.3 Metals and Metalloids

Metals and metalloids were identified as constituents of concern by McQueen et al.

(2017) in OSPW obtained from an active settling basin. Specifically, copper, aluminum,

selenium, iron, nickel, boron, and zinc were all found to have concentrations greater than water

quality guidelines/toxicity study endpoints (McQueen et al., 2017). Even though elemental

constituents and their proportions vary depending on the source of OSPW, the range of element

concentrations in OSPW from the Athabasca oil sands region demonstrate relative consistency

among samples from the same area (McQueen et al., 2017). Lari et al. (2016) showed that three

separate OSPW samples had comparable proportions of nickel, vanadium, copper, zinc, and

cadmium, and of the assessed elements, found vanadium to have the greatest concentration.

OSPW can be separated into an inorganic fraction, containing elemental metals such as

aluminum, lithium, and vanadium as well as fluoride, sulfate, chloride, and nitrate while the

organic fraction can contain NAs, PAHs, and phenol (Phillips et al., 2020). Phillips et al. (2020)

demonstrated that inorganic constituents separated from whole, unfractionated OSPW show

similar toxic effects via RAW 264.7 cell viability as whole OSPW whereas the organic fraction

does not. Phillips et al. (2020) attributes the decrease in cell viability associated with the

inorganic fraction, which contributes to whole OSPW, to possible metal components within this

fraction as well as potential metal-salt complexes. In addition, Phillips et al. (2020) found the

organic fraction of OSPW noticeably increased *tnf-α* expression but the unfractionated as well as

the inorganic fraction did not impact this cytokine gene expression to the same extent which

leads to the possibility of metallo-organic complexes and their dissociation influencing cell

bioactivity. The fractionation could break up these complexes and within the organic fraction,

the organic components may stimulate immune cells as indicated by the *tnf-α* expression

changes. Metals or their associations with other components in OSPW may also influence

OSPW toxicity (Phillips et al., 2020).

Metals have been detected in organisms exposed to oil sands-impacted materials (Baker

et al., 2012). *Chara* (alga) species exposed to consolidated tailings within microcosms

demonstrated generally greater concentrations of lanthanum and yttrium in a tissue analysis than other oil sands-associated sediment treatments (Baker et al., 2012). Of the surface sediment treatments, *Lymnaeidae* (snails) exposed to sediment from a constructed wetland in a reclaimed area had consistently greater concentrations of nickel, vanadium, lanthanum, and yttrium than those from the reference site (Baker et al., 2012). In addition, Aeshnid dragonfly nymphs had a heightened vanadium concentration after exposure to the petroleum coke microcosm treatment which demonstrates the potential for elemental accumulation (Baker et al., 2012). Overall, the metals detected in alga and invertebrate species reflect the potential for metal accumulation.

The bioaccumulation of heavy metals may be involved in the toxicity of OSPW (Li et al., 2017). However, data exploring the effects of metals from OSPW is limited (Li et al., 2017). Less focus has been placed on the possible toxic effects by metals even though it has been suggested that select metals such as manganese and uranium in OSPW may play a role in toxicity (Anderson et al., 2012; Li et al., 2017). Arsenic, chromium, and copper in OSPW have been previously documented to surpass the Canadian Council of Ministers of the Environment water quality guidelines (Li et al., 2017). Anderson et al. (2012) proposes that alongside NAs, specific metals may be involved in OSPW toxicity, and that the acute and chronic toxicity seen in *Chironomus dilutus* (benthic invertebrate) may be due to the array of metals found in OSPW. It has previously been noted that the presence of metals can impact adult emergence, and Anderson et al. (2012) found a decrease in emergence rates with OSPW exposure.

However, in discrepant studies, the exposure of vertebrates to oil sands-impacted areas, and the presumed elemental metals/metalloids they may contain, showed mild and seemingly inconsequential impacts (Godwin, Smits, and Barclay, 2016). McQueen et al. (2017) did not show that cationic metals contribute to toxicity via process-based manipulations though they

were recognized as a possible ecological risk and proposed wetland treatment to allow for the conversion of metals/metalloids into stable forms to restrict their re-distribution and bioavailability. Nestling *Tachycineta bicolor* (tree swallow) located close to oil sands processes were studied to assess metal and metalloid content in tissues and their diet (Godwin, Smits, and Barclay, 2016). Researchers found no significant difference in concentration of the assessed elements in kidney, liver, or stomach contents of nestlings between locations close to and far from oil sands mining processes (Godwin, Smits, and Barclay, 2016). Overall, researchers found that the metal content in *T. bicolor* near oil sands operations and their diet did not breach thresholds of concern (Godwin, Smits, and Barclay, 2016).

2.2 *In vitro* Studies of Toxicity

OSPW toxicity has been assessed using a range of cellular assays, from yeast estrogen screen assays to mammalian cell bioassays (Barrow et al., 2023; He et al., 2010). *In vitro* studies can be high throughput, are not costly, are reproducible, and straightforward whereas animal studies need consistent upkeep and may be high cost (Li et al., 2017; Lillico et al., 2023). OSPW contains compounds with structures resembling estrogens and *in vitro* assays reflecting estrogenicity have been used to examine OSPW (Barrow et al., 2023). The yeast estrogen screen assay is low maintenance and straight-forward, but it has lower sensitivity than the Erα-GeneBLAzer assay (Barrow et al., 2023). OSPW exposure resulted in elevated estrogenicity in the yeast and mammalian cell-based assays (Barrow et al., 2023). He et al. (2010) studied how OSPW impacts sex steroid production and found that H295R cells exposed to OSPW resulted in significantly higher 17β-estradiol production and significantly reduced testosterone production.

The Microtox assay is a useful monitoring tool that is commonly utilized to quantify bioluminescence from *Vibrio fischeri* which reflects narcosis, the mechanism of action thought to be enacted by NAs and result in acute toxicity (Bartlett et al., 2017; Jones et al., 2011; Li et al., 2017). OSPW-induced cytotoxicity assessed using *Aliivibrio fischeri* resulted in an IC_{10} of 0.98 ± 0.66 relative enrichment factor (REF) which demonstrates the acute toxicity of OSPW (Barrow et al., 2023). Though *Vibrio fischeri* have been used to assess OSPW and NA toxicity (Jones et al., 2011; Li et al., 2017; Scott et al., 2008), its environmental relevance is controversial as a marine bacterium is used to depict the impact on freshwater organisms (Bartlett et al., 2017). The UMU-ChromoTest assay is another standardized bacteria-based assay that evaluates the induction ratio of *umu*-C in *Salmonella typhimurium* TA1535 after exposure to contaminated samples to estimate mutagenicity and has previously been used to assess OSPW (Barrow et al., 2023).

Mammalian cell-based assays have also been developed and optimized as useful *in vitro* tools to explore the impact of OSPW (Barrow et al., 2023; Lillico et al., 2023). The PPARγ-GeneBLAzer assay assesses the activation of a mammalian transcription factor, PPARγ, which is involved in glucose and lipoprotein metabolism regulation (Barrow et al., 2023). Compounds like benzothiazole sulfonic acid have been known to activate this receptor and it may be activated by compounds present in OSPW (Barrow et al., 2023). OSPW induced a high response in this bioassay, which is unsurprising as many compounds in OSPW have previously resulted in PPARγ activation (Barrow et al., 2023). Immune cell-based bioactivity assays use mammalian macrophage cells to identify the bioactivity of OSPW by assessing changes in gene expression (Lillico et al., 2023). *mip-2* and *mcp-1* expression in RAW 264.7 mouse macrophage cells was higher after exposure to treated OSPW, with or without a water cap, as compared to the control

(Lillico et al., 2023). As these genes encode cytokines that are not basally expressed, this demonstrates that OSPW exposure induces expression of these pro-inflammatory genes and demonstrates changes in bioactivity (Lillico et al., 2023). The inducible nitric oxide synthase (iNOS) pathway contributes to antimicrobial response and leads to the production of iNOS, an enzyme that facilitates reactive nitrogen intermediate generation, after the upregulation of *inos* expression (Lillico et al., 2023). *inos* expression and iNOS levels were higher after exposure to OSPW as compared to the control, which further demonstrates bioactivity resulting from OSPW exposure (Lillico et al., 2023). OSPW bioactivity was demonstrated by RAW 264.7 macrophages which reflects potential as a water monitoring tool (Lillico et al., 2023).

2.3 *In vivo* Studies of Toxicity

2.3.1 Invertebrates

Many different aquatic invertebrates are used in toxicity testing including *Daphnia magna* (water flea) and *Ceriodaphnia dubia* (water flea) (Connors et al., 2022; Lari et al., 2016; McQueen et al., 2017). *D. magna* are often used in toxicity testing as *D. magna* is a bioindicator organism that is sensitive to pollutants, simple to culture, and are incorporated in regulatory guidelines (Connors et al., 2022; Lari et al., 2016). *D. magna* has been used to assess the impact of chronic exposure in toxicity testing for decades and is an appealing bioindicator to assess OSPW (Connors et al., 2022; Lari et al., 2016). Three samples of OSPW, at 1% and 10% concentrations, all significantly decreased the reproductive rate and growth of *D. magna* after 21 days of exposure (Lari et al., 2016). This suggests that OSPW may hinder *D. magna* reproduction and potentially impact population levels. However, OSPW did not demonstrate acute lethality in *D. magna* (Lari et al., 2016). *D. magna* exposed to 100% concentration of

OSPW from three separate sources for 48 hours did not result in a definitive LC_{50} value which demonstrates that OSPW may not substantially contribute to acute lethality (Lari et al., 2016). This is consistent with results from McQueen et al. (2017) that reported the LC_{50} of *D. magna* exposure to OSPW to be >100% OSPW after 48 hours of exposure.

Ceriodaphnia dubia (water flea) is an alternative model organism in toxicity testing to *D. magna* with similar reproductive habits and a quicker generation time (Connors et al., 2022). *C. dubia* neonates were found to be more sensitive to OSPW exposure than *D. magna* neonates as *C. dubia* demonstrates 20% survival whereas *D. magna* demonstrates 100% survival in 100% OSPW (McQueen et al., 2017).

Chironomids have been used as freshwater bioindicators as they demonstrate behavioural and morphological changes after exposure to pollutants (Reyes-Maldonado, Marie, & Ramirez, 2021). Chironomid survival reflected as LC_{50} and deformities in mouth parts have previously been used to evaluate toxicity (Reyes-Maldonado, Marie, & Ramirez, 2021). Anderson et al. (2012) evaluated acute effects of OSPW exposure by assessing survival and growth of *Chironomus dilutus* (benthic invertebrate). They found significantly lower larvae mass after exposure to OSPW from an active settling basin as compared to the controls (Anderson et al., 2012). Anderson et al. (2012) assessed the effects of chronic exposure to OSPW by examining pupation and emergence of *C. dilutus* after exposure to OSPW from an active settling basin. There was significantly lower pupation and emergence rates after exposure to OSPW as compared to a freshwater control (Anderson et al., 2012).

2.3.2 Aquatic Vertebrates

The sensitivity of fish to OSPW is greater than or equal to the sensitivity of aquatic invertebrates (McQueen et al., 2017). *P. promelas* larvae had 85% survival in 100% OSPW after 7 days of exposure and *D. magna* neonates had 100% survival when exposed to 100% OSPW for 48 hours (McQueen et al., 2017). In addition, Zubot et al. (2012) reported *D. magna* to have an LC_{50} of more than 100% concentration of OSPW after 48 hours of exposure whereas rainbow trout had an LC_{50} of 35% concentration of OSPW after 96 hours of exposure. This evidence outlines fish to be more sensitive to OSPW than aquatic invertebrates. However, *C. dubia* neonates had 20% survival after 7-8 days of exposure to 100% OSPW and were found to be somewhat more sensitive (McQueen et al., 2017). It is important to note exposure factors, such as test duration, and how they may influence the comparison of taxonomic groups (McQueen et al., 2017).

The impact of OSPW exposure to fish has varied in effects from impairment of senses to endocrine disruption to deformities (Lari et al., 2019; Peters et al., 2007; Van den Heuvel et al., 2012). *Oncorhynchus mykiss* (rainbow trout) exposed to OSPW at increasing concentrations diminishes olfactory response to chemical cues in a concentration-dependent manner (Lari et al., 2019). Olfaction is necessary for fish to assess predator danger and detect food (Lari et al., 2019). After exposure to 22% OSPW, olfactory system impairment increased from 59.4% at 3 hours of exposure to 86.1% after 96 hours of exposure (Lari et al., 2019). This study found particulate matter collecting on the olfactory epithelium in *O. mykiss* exposed to 22% OSPW and as pollutants may trigger necrosis or apoptosis, it is proposed that the inhibitory impact on the olfactory system may be due to the death of olfactory sensory neurons (Lari et al., 2019). Hormones in male *Perca flavescens* (yellow perch) were reported to be altered after exposure to

an experimental pond created in 1993 containing tailings as opposed to a natural, boreal forest lake (Van den Heuvel et al., 2012). Male *P. flavescens* demonstrated significantly decreased testosterone and 11-ketotestosterone after exposure to the pond containing tailings as compared to the boreal forest lake (Van den Heuvel et al., 2012). Changes in larvae size and deformities in early life stages of fish have also resulted from OSPW exposure and are comparable to the effects of NA exposure (Peters et al., 2007). Exposure to increasing NA concentrations from dilutions of OSPW resulted in declining larval length at hatch of *Orizias latipes* (Japanese medaka) and *Perca flavescens* as well as an increase in incidence of deformity in embryos (Peters et al., 2007).

Lithobates sylvaticus (wood frog) tadpoles have been used to investigate the impact of oil sands process-affected materials in reclaimed wetlands as they are responsive to pollutants, local to the oil sands area, and the developmental stages are ideal for evaluating contaminated wetland toxicity (Hersikorn and Smits, 2011). *L. sylvaticus* tadpoles required significantly more time to undergo metamorphosis, or possibly did not undergo successful metamorphosis, when exposed to reclaimed oil sands wetlands less than or equal to 7 years old as compared to the references (Hersikorn and Smits, 2011). The ability of tadpoles to complete metamorphosis and survive reflects reclaimed wetland viability as they are consistently exposed to contaminants in their aquatic habitat via ingestion and physical contact (Hersikorn and Smits, 2011).

2.3.3 Terrestrial and Avian Vertebrates

Mammals have been used for in situ experiments to assess the viability of OSPW-impacted wetlands (Gurney et al., 2005). Traits of waterfowl used to assess wetlands containing oil sands effluent include bill depth, length of bill and tarsus, and body mass whereas metabolite

analysis did not appear to suitably reflect OSPW impact by indicating nutritional status, which may be potentially due to the free roaming environment of waterfowl (Gurney et al., 2005). Skeletal size and body mass were reported to be decreased in *Anas platyrhynchos* (mallard) ducklings raised on wetlands formed from tailings water seepage as compared to reference wetlands (Gurney et al., 2005). Also, significantly higher concentrations of PAH metabolites were reported in the bile of ducklings exposed to OSPW-influenced wetlands as compared to reference wetlands (Gurney et al., 2005). The presence of PAH metabolites may be due to potential consumption of PAHs from OSPW-impacted wetland debris and overall, this is consistent with how impacted duckling growth is likely from OSPW toxicant exposure (Gurney et al., 2005). Gurney et al. (2005) concluded that wetlands formed from oil sands effluent are not an ideal environment for waterfowl.

Movasseghi, Rodriguez-Estival, & Smits (2017) present *Peromyscus maniculata* (deer mice) as a sensitive bioindicator organism to assess the viability of reclaimed oil sands-impacted sites. *P. maniculata* abundantly inhabit North American woodlands and have previously exhibited sensitivity to reclaimed sites formerly involved in oil sands processes (Movasseghi, Rodriguez-Estival, & Smits, 2017). Thyroid physiology has already been acknowledged as ideal for reflecting biological impacts of contaminant exposure (Movasseghi, Rodriguez-Estival, & Smits, 2017). A range of differences in thyroid histopathology has been reported in *P. maniculata* local to a reclaimed site that borders active oil sands processing areas as compared to a reference site (Movasseghi, Rodriguez-Estival, & Smits, 2017). In addition, plasma T4 in deer mice from the reclaimed site was significantly elevated as compared to the reference site (Movasseghi, Rodriguez-Estival, & Smits, 2017). These findings support that *P. maniculata* collected from reclaimed oil sands sites may have atypical thyroid activity and in combination

with previous reports, it is deemed that reclaimed areas comparable to this study site are not a suitable habitat for *P. maniculata* (Movasseghi, Rodriguez-Estival, & Smits, 2017).

Tachycineta bicolor (tree swallows) have previously been included in environmental evaluations as a model species and have demonstrated a decline in reproductive performance when exposed to environments containing anthropogenic contaminants (Gentes et al., 2006). Considering the extent of exposure to pollutants, the sensitivity of this organism may be low as the impact on the tree swallows was unexpectedly minimal and some studies noted indiscernible results regarding reproductive performance (Gentes et al., 2006). The reproductive performance of *T. bicolor* from reclaimed, oil sands process-affected wetlands distinctly decreased when challenged with stormy weather, an environmental stressor, as compared to the control site (Gentes et al., 2006).

Besides birds, other animals have been used as a model species to assess oil sands process-affected environments such as *Lontra canadensis* (North American river otter), which are widespread in marine and freshwater habitats in North America (Thomas et al., 2021). This organism is recognized as a sentinel species for aquatic environments because of their sensitivity to pollutants in their surroundings as well as their high trophic position which leaves them vulnerable to adverse impacts from the biomagnification of contaminants (Thomas et al., 2021). Baculums typically displayed decreased stiffness and peak load values from *L. canadensis* sampled from sites affected by oil and gas processing (Thomas et al., 2021). Previously, four ring PACs have demonstrated the ability to influence hormonal pathways, both estrogenic and androgenic, and this study demonstrates that baculum bone material properties are negatively impacted by alkylated four ring PACs (Thomas et al., 2021). Hormone levels impact bone

formation and resorption, and it is suggested that the possible impact of this compound on the baculum may be exerted by influencing hormone levels (Thomas et al., 2021).

2.4 Remediation

OSPW treatment strategies have been extensively investigated (Abdalrhman and El-Din, 2020; Abdalrhman, Zhang, and El-Din, 2019; Alberts et al., 2021; Afzal et al., 2012; Balaberda and Ulrich, 2021; Clemente et al., 2004; Ganiyu and El-Din, 2020; Meng et al., 2021; Quinlan and Tam, 2015). NAs have been the focus for removal or degradation, and many OSPW remediation strategies have been explored (Abdalrhman, Zhang, and El-Din, 2019; Alberts et al., 2021; Meng et al., 2021; Quinlan and Tam, 2015). Remediation technologies include coagulation/flocculation procedures, AOPs, biodegradation, and phytoremediation (Alberts et al., 2021; Quinlan and Tam, 2015).

2.4.1 Coagulation and Flocculation

Coagulation/flocculation processes have been explored for NA elimination from OSPW (Quinlan and Tam, 2015). Initially, microflocs are constructed from the coagulation of particles by electrostatic attraction (Quinlan and Tam, 2015). In the next phase, microflocs come together to create flocs (Quinlan and Tam, 2015). These larger units can be removed by sedimentation or flotation (Quinlan and Tam, 2015). These processes have had materials like alum incorporated which becomes positively charged aluminum hydroxide precipitates that interact with NAs as they have a negative charge (Quinlan and Tam, 2015). These interactions contribute to the creation of microflocs (Quinlan and Tam, 2015). These procedures are straightforward and

energy efficient, but it can be costly and lead to more waste products that need to be treated (Quinlan and Tam, 2015).

2.4.2 Advanced Oxidation Processes

Advanced oxidation refers to procedures for the breakdown of chemical components using hydroxyl radicals during oxidation reactions (Quinlan and Tam, 2015). The interaction of H_2O_2 with a stimulus, like UV light, results in the generation of hydroxyl radicals, which contributes to the oxidation of organic compounds like NAs (Quinlan and Tam, 2015). AOPs include electrooxidation, where oxidation of organic components occurs using an anode, and solar oxidation, which utilizes photocatalysts such as TiO_2 and Bi_2WO_6 (Abdalrhman and El-Din, 2020; Meng et al., 2021; Quinlan and Tam, 2015). AOPs are already used in regular practices such as wastewater treatment and have been reported to be effective in treating OSPW and removing NAs (Abdalrhman and El-Din, 2020; Abdalrhman, Zhang & El-Din, 2019; Ganiyu and El-Din, 2020; Meng et al., 2021; Quinlan and Tam, 2015). Drawbacks of AOPs include just partial degradation of chemical components, which, in treating OSPW, may be more toxic than the starting NAs, and the process itself is often quite costly (Quinlan and Tam, 2015).

2.4.2.1 Electrooxidation

Electrooxidation is known to effectively breakdown organic components that can be found in wastewater (Abdalrhman and El-Din, 2020; Abdalrhman, Zhang, & El-Din, 2019). Electrooxidation oxidizes organic compounds using an anode to facilitate electron transfer, resulting in the production of reactive oxygen species (Abdalrhman and El-Din, 2020). Different anode materials can be used, such as graphite or boron-doped diamond, which can dictate the

oxidants created and influence process efficiency (Abdalrhman, Zhang, and El-Din, 2019; Abdalrhman and El-Din, 2020). Anode material affects the extent of oxidation of organic compounds and are categorized based on oxygen evolution potential as active or non-active (Abdalrhman, Zhang, and El-Din, 2019). Active anodes have minimal oxygen evolution over-potential, encourage partial oxidation of contaminants, and include graphite and dimensionally stable anodes (Abdalrhman, Zhang, & El-Din, 2019; Abdalrhman and El-Din, 2020). Graphite anodes are quite conductive and inexpensive whereas dimensionally stable anodes are useful in chlorine and oxygen production and are very stable (Abdalrhman and El-Din, 2020). Non-active anodes have elevated oxygen evolution over-potential, permit full organic compound mineralization, and include lead dioxide and boron-doped diamond (Abdalrhman, Zhang, & El-Din, 2019). Boron-doped diamond effectively produces secondary oxidants that promote organic compound mineralization (Abdalrhman and El-Din, 2020; Ganiyu and El-Din, 2020). Electrooxidation requires no extra chemicals, is straightforward, and effective (Abdalrhman and El-Din, 2020). Electrooxidation treatment of OSPW does not face the same limitations as other treatment options such as how OSPW permits minimal light transmittance which impedes UV-based AOPs or how OSPW alkalinity limits Fenton processes (Abdalrhman and El-Din, 2020; Abdalrhman, Zhang, & El-Din, 2019).

Electrooxidation has been reported to be effective in treating OSPW by breaking down organic components (Abdalrhman and El-Din, 2020). Abdalrhman and El-Din (2020) reported that NAs from OSPW with higher carbon numbers and more rings were more reactive toward oxidation via electrooxidation using either a dimensionally stable anode or graphite. Both anodes were effective in removing NAs from OSPW, though the graphite anode operated more efficiently at low current densities as compared to the dimensionally stable anode (Abdhalrman

and El-Din, 2020). As well, treatment of OSPW NAs with electrooxidation using the dimensionally stable anode showed preference for removing compounds with aromatic rings (Abdalrhman and El-Din, 2020). OSPW treatment with electrooxidation utilizing a non-active anode, boron-doped diamond, is reported to be successful in fully degrading NAs and PAHs (Abdalrhman, Zhang, & El-Din, 2019; Ganiyu and El-Din, 2020). Overall, electrooxidation with both active and inactive anodes have demonstrated the ability to degrade NAs from OSPW (Abdalrhman and El-Din, 2020; Ganiyu and El-Din, 2020).

2.4.2.2 Solar/UV Oxidation

Solar photocatalytic treatment is reported to reduce NAs in OSPW (Meng et al., 2021). Photocatalytic AOPs can function by creating electron-hole pairs on metal oxide catalysts through UV light (Quinlan and Tam, 2015). Subsequently, hydroxyl radicals are produced as the holes facilitate the oxidation of OH^- and H_2O (Quinlan and Tam, 2015). Photocatalytic AOPs offer an environmentally friendly option as they make use of solar energy and reusable materials (Meng et al., 2021). However, regarding OSPW treatment, the turbidity of this waste product interferes with light penetration (Abdalrhman, Zhang, and El-Din, 2019). Therefore, a pre-treatment stage is necessary (Abdalrhman, Zhang, and El-Din, 2019).

Photocatalysts such as TiO_2 and Bi_2WO_6 have been used to treat OSPW (Meng et al., 2021). TiO_2 has been used as a photocatalyst in OSPW photocatalytic treatment though it is restricted by its low visible light absorption (Meng et al., 2021). Bi_2WO_6 is another photocatalyst that uses visible light, and its qualities and structure largely aid in the breakdown of organic components (Meng et al., 2021). Meng et al. (2021) evaluated three different

structures of Bi_2WO_6 in their ability to degrade NAs and reported that flower-like Bi_2WO_6 breaks down NAs quicker than swirl-like and nanoplate Bi_2WO_6.

Solar and UV oxidation treatments have successfully degraded NAs from OSPW (Afzal et al., 2012; Meng et al., 2021). Solar photocatalytic treatment via Bi_2WO_6 significantly decreased classical NA content and eliminated S-NAs in OSPW (Meng et al., 2021). UV light has been used in combination with H_2O_2 in AOPs for NA removal and this UV light/H_2O_2 treatment significantly improved the efficiency of NA degradation from OSPW (Afzal et al., 2012). Ninety-two percent of NAs from OSPW were eliminated after one hour of treatment (Afzal et al., 2012). Taken together, this demonstrates how different forms of solar and UV treatments may be feasible in OSPW remediation (Afzal et al., 2012; Meng et al., 2021).

2.4.3 Biodegradation

Biodegradation involves using microorganisms to degrade organic compounds like NAs using metabolic processes (Quinlan and Tam, 2015). Microbes such as *Pseudomonas putida* and *Acinetobacter anitratum* are capable of NA metabolization (Quinlan and Tam, 2015). Using microbes found in OSPW, Clemente et al. (2004) demonstrated a decrease in NA concentration after biodegradation to under 10 mg/L from ~100 mg/L. Biodegradation successfully removed NAs, and low molecular weight NAs were found to be more susceptible which contrasts AOPs (Clemente et al., 2004; Quinlan and Tam, 2015). A drawback is that larger NAs with rings and branching are less susceptible to biodegradation (Quinlan and Tam, 2015). In addition, bioremediation occurs gradually and may take a long period of time which is why it is appealing to combine this process with another (Abdalrhman, Zhang, and El-Din, 2019; Balaberda and Ulrich, 2021; Quinlan and Tam, 2015).

2.4.4 Phytoremediation

Phytoremediation methods harness plants and affiliated microorganisms to mitigate pollutants from the environment (Alberts et al., 2021). This low-input, economical method has previously been implicated in the dissipation and translocation of NAs (Alberts et al., 2021). From solution and OSPW-contaminated soil, *Salix interior* (sandbar willow) and *Elymus trachycaulus* (slender wheatgrass) have been reported to take up different classes of NAs including diamondoid and single-ring structures (Alberts et al., 2021). Alberts et al. (2021) demonstrates how NAs and/or their associated molecules can be redistributed in plants and that plants are able to remove NAs from soil exposed to OSPW and hydroponic solution. This presents phytoremediation strategies as a potential approach in removing NAs and treating OSPW.

2.4.5 Combined Treatments

Remediation methods have been combined to increase efficiency (Balaberda and Ulrich, 2021). It has been reported that ozonation, a form of chemical oxidation, does not result in a proportional decrease in NAs over time (Balaberda and Ulrich, 2021). Biodegradation is unable to break down all types of NAs though it is very cost-effective (Balaberda and Ulrich, 2021). Treatment of a NA fraction with chemical oxidation improves bioremediation as it allows for degradation into simple components for microbes to interact with and lowers the degree of toxicity by reducing the contaminants concentration (Balaberda and Ulrich, 2021). Pairing these two methods bypasses their associated drawbacks while making use of their advantages (Balaberda and Ulrich, 2021). Balaberda and Ulrich (2021) demonstrate that persulfate oxidation combined with biodegradation is successful in lowering toxicity and eliminating NAs.

2.5 Aging of OSPW

NA content and proportions in OSPW changes over time (Holowenko, MacKinnon, and Fedorak, 2002; Li et al., 2017). Biodegradation of NAs by the native microbial community in OSPW selectively breaks down NAs with low carbon numbers and fewer rings and leads to elevated concentrations of NAs of high carbon number (Clemente et al., 2004; Holowenko, MacKinnon, and Fedorak, 2002; Li et al., 2017; Quinlan and Tam, 2015). Holowenko, MacKinnon, and Fedorak (2002) demonstrate reduced NA content in older OSPW as they report OSPW aged for 7 and 11 years to contain 36 mg/L and 24 mg/L NAs, respectively, as compared to OSPW from an active settling basin containing 49 mg/L NAs.

Aged OSPW contains NAs of higher carbon numbers and aged tailings samples are reported to contain greater adamantane NA content (Holowenko, MacKinnon, and Fedorak, 2002; Li et al., 2017; Rundle et al., 2021). Holowenko, MacKinnon, and Fedorak (2002) showed a higher percentage of high carbon number NAs in aged OSPW as compared to OSPW from an active settling basin. It was reported that adamantane NAs exist in greater proportions in aged tailings aliquots and have been documented to be the most prevalent type of NA found in aged tailings (Rundle et al., 2021). Adamantane NA content potentially could be utilized in the evaluation of the aging and microbial breakdown of OSPW (Rundle et al., 2021).

Acute toxicity has been seen in newly generated OSPW and this toxicity naturally lessens over time as it is thought to be due to NA biodegradation (Holowenko, MacKinnon, and Fedorak, 2002; Kavanagh et al., 2011). The decrease in the acute toxicity is evidenced via Microtox bioassay by an IC_{50} of 100% concentration of aged OSPW and an IC_{50} of 32% concentration of OSPW from an active settling basin (Holowenko, MacKinnon, and Fedorak, 2002). The decrease in OSPW toxicity is also reflected in invertebrate species diversity of new versus aged

wetlands (Li et al., 2017). Newer wetlands impacted by OSPW demonstrate a smaller variety of invertebrate species as compared to aged OSPW-affected wetlands (Li et al., 2017). This change in toxicity may be attributed to inhabitation by more resilient organisms, or the biodegradation of NAs may be occurring in older wetlands (Li et al., 2017).

Though no longer demonstrating acute toxicity, aged OSPW may still be implicated in adverse effects on organisms (Kavanagh et al., 2011). Exposure to aged OSPW resulted in a significant decrease in the number of spawn and average fecundity rate in *Pimephales promelas* (fathead minnow) as opposed to reference water (Kavanagh et al., 2011). Reduced plasma steroid levels were found in *Carassius auratus* (goldfish) exposed to aged OSPW as compared to fish exposed to control water (Kavanagh et al., 2011; Lister et al., 2008). However, NAFCs derived from aged OSPW had similar or increased toxicity as compared to NAFCs derived from fresh OSPW (Bartlett et al., 2017). It is important to note that the toxicity of NAFCs is influenced by factors including concentration and composition, and that separate sources may impact results (Bartlett et al., 2017).

2.6 Summary

With the development of OSPW treatments, it is necessary to evaluate their efficacy in reducing the adverse effects of OSPW. Bioassays using *Vibrio fischeri* are recognized as a conventional toxicity assessment (Klamerth et al., 2015) and evaluates toxicity via bioluminescence, which reflects membrane disruption or narcosis (Bartlett et al., 2017; Klamerth et al., 2015). Microtox assays previously have outlined differences between untreated and treated OSPW (Arslan et al., 2023). Microtox results demonstrate that sulfate radical AOP treatment with biofiltration reduces OSPW toxicity (Arslan et al., 2023). However, the

environmental relevance is controversial as *V. fischeri* is used to anticipate effects on freshwater organisms and it is a marine bacterium (Bartlett et al., 2017). In addition, bioluminescence indicates narcosis of *V. fischeri* and therefore does not assess impact on processes of higher-level organisms (Bartlett et al., 2017). Aquatic organisms like rainbow trout have previously been used to assess the impacts of OSPW treatment (Zubot et al., 2012). However, animal studies may need consistent care and can be high cost (Lillico et al., 2023). This leads to the need for a quick and efficient biosensor system that accurately reflects biological impact to distinguish between untreated and treated OSPW.

RAW 264.7 mouse macrophage cells present as a sensitive bioindicator and have previously been used in a macrophage cell biosensor assay to identify and monitor OSPW bioactivity and immunotoxicity (Arslan et al., 2023; Fu et al., 2017; Lillico et al., 2023; Phillips et al., 2020). As an *in vitro* assay, the RAW 264.7 cell bioindicator system has the benefits of being low cost, rapid, reproducible, and reliable (Li et al., 2017; Lillico et al., 2023). Fu et al. (2017) used RAW 264.7 cells to show how OSPW exposure can impact cell proliferation, cell morphology, and cell viability. Fu et al. (2017) was able to differentiate effects from different OSPW fractions as whole OSPW significantly impacted cytokine protein secretion while the organic fraction did not. Phillips et al. (2020) also demonstrated differences in gene expression in RAW 264.7 cells from exposure to OSPW fractions and showed gene expression of cytokines to be significantly affected by the OSPW inorganic fraction.

RAW 264.7 cells have also been used to monitor OSPW bioactivity (Lillico et al., 2023) and to differentiate between untreated and treated OSPW samples (Arslan et al., 2023). The RAW 264.7 cell line allowed Lillico et al. (2023) to track changes in pro-inflammatory cytokine gene expression for the duration of OSPW exposure and compare bioactive changes in gene

expression between OSPW fractions. This macrophage biosensor system has also successfully been used to assess OSPW fractions before and after the introduction of a water cap and showed that OSPW with a water cap results in significant bioactive changes in gene expression (Lillico et al., 2023). In addition, RAW 264.7 cell nitric oxide (NO) response distinguished untreated OSPW from OSPW treated by sulfate radical AOPs combined with post-biofiltration (Arslan et al., 2023). Moving forward, this biosensor system has the potential to assess OSPW treatment options by identifying changes in pro-inflammatory gene expression and ultimately, bioactivity.

RAW 264.7 cells have been successful in distinguishing untreated and treated OSPW (Arslan et al., 2023; Lillico et al., 2023) and with this basis, RAW 264.7 cells are a sound candidate to assess OSPW treatment. Moving forward, it is important to establish a difference in RAW 264.7 cell response between untreated and treated OSPW. From there, we can explore how OSPW interacts with and activates RAW 264.7 cells, the cell signaling pathways or proteins involved in the bioactive response, and the component(s) responsible for RAW 264.7 cell bioactivity. This allows us to fully comprehend how OSPW exerts its effects on mammalian cells and the component(s) responsible for these effects. It is important to fully understand the consequences of OSPW contaminants as this sets a basis for remediation strategies and may guide future remediation technologies.

Chapter III

Materials & Methods

3.1 Cell Culture

RAW 264.7 murine macrophage cells were incubated at 37°C and 5% CO_2 in high glucose Dulbecco's Modified Eagle's medium (DMEM; Cytiva) with 10% fetal bovine serum (FBS; Avantor) and 1% penicillin-streptomycin (Pen-Strep; Gibco) in 75cm^2 vented flasks. Cell seeding and passaging occurred at confluency in 75cm^2 vented flasks. Passaging consisted of removing previous media, washing with phosphate-buffered saline (PBS; Cytiva), adding 2mL 25% trypsin-EDTA (Gibco), and rinsing with 3mL DMEM/10% FBS/1% Pen-Strep before transferring 1 mL into a new 75cm^2 vented flask containing 9mL DMEM/10% FBS/1% Pen-Strep. RAW 264.7 cells were stored in 90% FBS/10% DMSO (Sigma-Aldrich) at -80°C.

3.2 Gene Expression

3.2.1 Cell Seeding

Twenty-four well plates were seeded with 300 000 cells/well in 500 μL DMEM/10% FBS/1% Pen-Strep and incubated overnight at 37°C and 5% CO_2.

3.2.2 OSPW

OSPW was provided by Syncrude from a Northern Albertan tailings pond. This water underwent electrooxidation treatment for 2 hour and 6 hours, and solar oxidation treatment using a zinc oxide catalyst for 2 hour and 4 hours (Suara et al., 2022) by the El-Din laboratory (University of Alberta). Waters were stored at 4°C in the dark.

3.2.3 Exposure

After overnight incubation, seeded cells were washed with 200 μL PBS and exposed to 500 μL colorless DMEM F12 (Gibco) with 5% FBS, and either 50% v/v PBS, 1 hour solar oxidation-treated OSPW, 4 hour solar oxidation-treated OSPW, 1 hour electrooxidation-treated OSPW, or 6 hour electrooxidation-treated OSPW. OSPW was passed through a 0.45 μM filter before use. Exposed cells were incubated for 2 or 6 hours before RNA extraction occurred.

3.2.4 RNA Extraction

Cells were harvested using 200 μL TRIzol (Invitrogen) and transferred to tubes containing 120 μL chloroform. Samples were vortexed and incubated for 10 minutes at room temperature before centrifugation for 15 minutes at 12 000 rcf. 500 μL isopropanol was added to the aqueous layer before tubes were inverted and incubated for 10 minutes at room temperature then centrifuged for 10 minutes at 12 000 rcf. Supernatant was removed and pellets were washed with 75% ethanol (Sigma Aldrich) before centrifugation for 5 minutes at 12 000 rcf. This was repeated two times before supernatant was removed and pellets were dried. Pellets were dissolved in nuclease-free water (IDT DNA) overnight at 4°C. NanoDrop 1000 Spectrophotometer (Thermo Fisher) identified RNA concentration and relative quality.

The experiment proceeded with RNA samples with 260/280 and 260/230 ratios higher than 1.8, and if lower, the sample underwent ethanol precipitation. Ethanol precipitation involved adding 10% sample volume of sodium acetate (pH 5.2) and 100% ethanol. Samples were incubated at -80°C and centrifuged for 20 minutes at 7600 rcf. Pellets were washed with 70% ethanol and centrifuged for 15 minutes at 12 000 rcf. Pellets were dried and dissolved in nuclease-free water (IDT Technologies).

3.2.5 cDNA Synthesis

Superscript III First-Strand Synthesis System kit (Invitrogen) was used to create cDNA from RNA samples according to the manufacturer's protocol.

3.2.6 Quantitative PCR (qPCR)

Three technical replicates of each qPCR reaction were run and contained the following: 2 µL nuclease-free water, 1 µL primer, and 5 µL SYBR^{TM} green master-mix (MBSU, University of Alberta), and 2 µL cDNA. qPCR cycle parameters are found in Table 3.1. qPCR determined fold change using *gapdh* as the endogenous control and 2 hours of 50% v/v PBS exposure as the reference sample. Results were analyzed by calculating fold change, which compares experimental sample to the endogenous control and reference sample. Applied Systems' 7500 Fast Real-Time PCR system and the manufacturer's software were used to assess samples.

3.2.7 qPCR Primers

Primer sequence and concentration was determined by Choo-Yin (2021) and outlined in Table 3.2.

Table 3.1. qPCR cycling parameters.

Cycle Stage	Time	Temperature
Holding Stage	2 minutes	95°C
Cycling Stage (40 cycles)	Alternating between:	
	15 seconds	95°C
	1 minute	50°C
Melt Curve Stage	15 seconds	95°C
	1 minute	50°C
	30 seconds	95°C
	15 seconds	50°C

Table 3.2. qPCR primer sequences and concentrations. The *gapdh* primer sequences are from Girbl et al. (2018)[1]. The *mip*-2, *ip-10*, and *mcp-1* primer sequences are from Bandow et al. (2012)[2].

Gene	Forward Primer	Reverse Primer	Concentration (Combined Forward and Reverse Primers)
gapdh[1]	TCGTGGATCTGACGTGCC GCCTG	CACCACCCTGTTGCTGTAG CCGTA	3 μM
mip-2[2]	GAAGTCATAGCCACTCTC AAGG	TTCCGTTGAGGGACAGCA	3 μM
ip-10[2]	GGATCCCTCTCGCAAGGA	ATCGTGGCAATGATCTCAA CA	3 μM
mcp-1[2]	AGCACCAGCCAACTCTCA CT	CGTTAACTGCATCTGGCTG A	3 μM

3.2.8 Statistics

GraphPad Prism 10.0.2 software was used to calculate statistics. Fold change significance was analyzed using the Shapiro-Wilk test for normality. If data distribution was Gaussian ($\alpha=0.05$), significance was determined via unpaired t-test. If distribution was not Gaussian ($\alpha=0.05$), significance was determined via Mann-Whitney test. Significance was determined if $p<0.05$.

3.3 Nitric oxide (NO) Assays

3.3.1 Cell Seeding

Ninety-six well plates were seeded with 25 000 or 100 000 RAW 264.7 cells per well in 100 μL DMEM/10% FBS/1% Pen-Strep. 25 000 cells per well were seeded for Cu-CPT22 inhibition. These plates were incubated overnight at 37°C and 5% CO_2.

3.3.2 OSPW

Suncor provided OSPW from an active tailings pond at Suncor Base Plant. This pond receives coarse tailings and the water is constantly recycled. This water was received on April 17, 2023 and stored at 4°C in the dark.

3.3.3 Exposure

After overnight incubation, cells were washed with 75 μL PBS and exposed to 100 μL colorless DMEM F12 (Gibco), 5% FBS, and/or either 6.25% v/v OSPW, PBS, or pre-treatment with DMEM/5% FBS and varying concentrations of Aminoguanidine (TOCRIS), Cardamonin (TOCRIS), IRAK1/4 Inhibitor I (TOCRIS), Go 6976 (Selleck Chem), U0126 (TOCRIS),

TAK242 (TOCRIS), or Cu-CPT22 (TOCRIS). OSPW was passed through a 0.45 µM filter

before use. Inhibitor concentrations were determined by serial dilutions (Appendix Fig. 1) as

well as previous literature as shown in Table 3.3 (Cheng et al., 2012; Israf et al., 2007; Jin, Liu,

and Nelin, 2015; Koide et al., 2005; Takashima et al., 2009; Wolff, Lubeskie, and Li, 1997; Wu

et al., 2003; Zhang et al., 2021). Cell viability assays were not performed; however,

concentrations used here are consistent with previous literature. Cell stimulation occurred with

either 12.5 ng/mL LPS, 1.25 µL of heat-killed *E. coli* with OD_{600} of 0.6, 2.5 µg/mL Pam_3CSK_4,

62.5 µg/mL Zymosan, or 6.25% v/v OSPW in DMEM with 5% FBS. Controls were stimulated

for 24 hours and experimental groups were stimulated for 22 hours or 24 hours.

Table 3.3. Pharmacological inhibitor concentrations in thesis and from previous literature.

Pharmacological Inhibitor	Concentration in Thesis	Concentration from Previous Literature
Aminoguanidine	31.25 µM – 125 µM	0.3 mM - 5 mM (Wolff, Lubeskie, and Li, 1997)
Cardamonin	3.125 µM – 12.5 µM	0.78 µM – 50 µM (Israf et al., 2007)
IRAK1/4 Inhibitor I	45 µM - 180 µM	N/A
Go 6976	2 µM - 8 µM	1 µM – 5 µM (Wu et al., 2003)
U0126	5 µM – 20 µM	1.25 – 7.5 µM (Koide et al., 2005) 10 µM (Jin, Liu, and Nelin, 2015)
TAK242	12.5 nM – 200 nM	0 nM – 100 nM (Takashima et al., 2009)
Cu-CPT22	1 µM - 4 µM	1 µM (Zhang et al., 2021) 2 µM – 8 µM (Cheng et al., 2012)

3.3.4 Griess Reaction

Nitric oxide production was analyzed via Griess reaction (Lillico et al., 2023; Gagioti et al., 2000). Cells were centrifuged at 300g for 5 minutes before supernatant was collected. Nitrite was assessed by colorimetric reaction using 5% Phosphoric Acid (Sigma-Aldrich)/1% Sulfanilamide (Sigma-Aldrich) solution and 0.1% N-1-naphthylethylenediamine dihydrochloride (Aldrich Chemistry) solution. Samples were analyzed using the BioTek Synergy H1 Microplate Reader at 570nM and concentration was calculated using a standard curve of 0.1mM sodium nitrite solution.

3.3.5 Statistics

GraphPad Prism 10.0.2 software was used to calculate statistics. Statistical significance was determined via one-way ANOVA and Tukey's multiple comparisons test.

3.4 Cytokine Secretion

3.4.1 Cell Seeding

Twenty-four well plates were seeded with 300 000 RAW 264.7 cells per well in 500 μL DMEM/10% FBS/1% Pen-Strep. These plates were incubated overnight at 37°C and 5% CO_2.

3.4.2 OSPW

Suncor provided OSPW from an active tailings pond at Suncor Base Plant. This pond receives coarse tailings and the water is constantly recycled. This water was received on April 17, 2023 and stored at 4°C in the dark.

3.4.3 Exposure

After overnight incubation, cells were washed with 100 μL PBS and exposed to 100 μL colorless DMEM F12 (Gibco), 5% FBS, and either 6.25% v/v OSPW, or PBS. OSPW was passed through a 0.45 μM filter before use. Cell stimulation occurred with either 12.5 ng/mL LPS, OD_{600} of 0.6 heat-killed *E. coli*, 2.5 μg/mL Pam_3CSK_4, 62.5 μg/mL Zymosan, or 6.25% v/v OSPW in DMEM with 5% FBS. Cells were stimulated for 24 hours before 100 μL cell supernatant was collected.

3.4.4 Cytokine Analysis

After exposure, 100 μL of cell supernatant was collected and stored at -20°C. Samples were sent to Eve Technologies Inc. (Calgary, Canada) on dry ice for Mouse Cytokine Proinflammatory Focused 10-Plex Discovery Assay Array (MDF10).

3.4.5 Statistics

Statistics were calculated using GraphPad Prism 10.0.2 software. Statistical significance was determined via one-way ANOVA and Tukey's multiple comparisons test.

Chapter IV

In vitro Indication of RAW 264.7 cell Bioactivity Before and After AOP Treatments

4.1 Introduction

Prior to allowing treated OSPW to be returned to the environment, it must be evaluated for potential bioactivity. Immune cells possess various receptors that have the capacity to detect environmental stimuli, and innate immune cells acutely respond via changes in gene expression or protein secretion (Lillico et al., 2023; Taylor et al., 2005; Varol, Mildner, and Jung, 2015). Macrophage cells play a role in innate immunity as the first line of defense to detect and respond to foreign entities (Varin & Gordon, 2009). Their inherent sensitivity to foreign bodies makes them an ideal bioindicator for evaluating the effects of OSPW at a cellular level (Burger & Gochfeld, 2001; Kong, Smith, and Hao, 2019; Lillico et al., 2023). Changes in gene expression and protein secretion after exposure to mixtures containing contaminants, such as OSPW, can indicate bioactivity (Lillico et al., 2023). Bioactivity is reflective of macrophage cell activation from a basal, resting state as cells are challenged by OSPW constituents, which is evidenced by changes in pro-inflammatory gene expression and cytokine production (Lillico et al., 2023). These changes enable us to monitor the ability of OSPW to impact the cellular level and assess treatment efficacy from pre- and post-exposure. To indicate treatment success, OSPW should demonstrate decreased or no effect at the cellular level. RAW 264.7 murine macrophages show changes in gene expression and protein secretion within hours after exposure to stimuli (Lillico et al., 2023), which is advantageous as this assay can be performed in a timely manner. Using

cellular responses to assess contamination is not a new idea, and has been used to assess crude particulate matter, contaminated river water, and even treated sewage (Jankowska-Kieltyka et al., 2021; Makene and Pool, 2015; Pool and Magcwebeba, 2009). *In vitro* assays offer a reproducible, minimal cost, and high throughput option that bypasses the use of live animals as well as their associated constraints, while still producing demonstrable and measurable results (Li et al., 2017; Lillico et al., 2023).

Chemokines and cytokines are released by activated immune cells to regulate cellular movement and are released during injury or infection or in response to various stimuli such as lipopolysaccharides (LPS) (Qin et al., 2017; Singh, Anshita, and Ravichandiran, 2021). Monocyte chemoattractant protein-1 (MCP-1), interferon-γ-induced protein 10 (IP-10), and macrophage inflammatory protein-2 (MIP-2) are cytokine proteins released by activated macrophages (Lei et al., 2019; Phillips et al., 2020; Qin et al., 2017; Singh, Anshita, and Ravichandiran, 2021). MCP-1 regulates monocyte recruitment during osteoarthritic inflammation and is implicated in various conditions such as cancer, respiratory tract infections, and rheumatoid arthritis (Singh, Anshita, and Ravichandiran, 2021). IP-10 is notably expressed by monocytes but also released by other cells such as natural killer cells and endothelial cells (Lei et al., 2019). IP-10 is associated with HIV infection (Lei et al., 2019) and Coronavirus disease-2019 severity (Singh, Anshita, and Ravichandiran, 2021). MIP-2 is involved in polymorphonuclear neutrophil recruitment and contributes to the regulation of inflammation, specifically in liver disease (Qin et al., 2017). *mip-2, ip-10,* and *mcp-1* are pro-inflammatory genes related to antimicrobial response and immune cell coordination during inflammation (Choo-Yin et al., 2021). These genes have previously demonstrated increased expression after

OSPW exposure and effectively reflected the bioactive effects of OSPW (Choo-Yin et al., 2021; Lillico et al., 2023).

Many AOPs have been explored for the treatment of OSPW (Abdalrhman, Zhang, and El-Din, 2019; Meng et al., 2021; Quinlan and Tam, 2015). NAs are believed to contribute to toxicity as they have surfactant characteristics that may result in a narcotic mode of action (Brown and Ulrich, 2015; Frank et al., 2009; Giesy, Anderson, and Wiseman, 2010) and may ultimately interfere with the cell membrane (Brown and Ulrich, 2015; Phillips et al., 2020). The negative impacts of NAs and NAFCs on growth, development, and reproduction (Kavanagh et al., 2012; Marentette et al., 2015; Melvin and Trudeau, 2012) further suggests NA toxicity. Electrooxidation is currently at the forefront of OSPW treatment options as minimal chemicals are necessary, it's environmentally friendly, and it is highly adaptable as there are many anode options (Abdalrhman, Zhang, and El-Din, 2019; Ganiyu and El-Din, 2020). Solar oxidation is another AOP that is currently being explored and has previously demonstrated successful NA degradation (Meng et al., 2021). Solar oxidation boasts the benefits of being potentially less expensive than other AOP options due to the ecofriendly nature of solar energy and the use of recyclable materials (Meng et al., 2021). Electrooxidation and solar oxidation treatments are successful in NA removal (Abdalrhman and El-Din, 2020; Abdalrhman, Zhang, and El-Din, 2019; Meng et al., 2021). Previously, AOP treatment with biofiltration has demonstrated a reduction in NAs which was consistent with a decrease in RAW 264.7 cell bioactivity as indicated by NO production (Arslan et al., 2023). NAs are suggested as a bioactive component within OSPW.

I use a macrophage-based *in vitro* assay that works as a biosensor system by responding to OSPW and treated OSPW with distinct changes in pro-inflammatory gene expression to

indicate bioactivity (Choo-Yin et al., 2021; Lillico et al., 2023). Since solar and electro-oxidation procedures degrade NAs in OSPW (Abdalrhman and El-Din, 2020; Abdalrhman, Zhang, and El-Din, 2019; Meng et al., 2021), I wanted to determine if the bioactivity of OSPW changes after treatment. To determine the efficacy of solar and electrooxidation-treated OSPW, immune cells were exposed to both types of treated OSPW as well as untreated OSPW to analyze changes in bioactivity between samples. If treatment is successful, untreated OSPW will induce high expression of pro-inflammatory genes and treated OSPW will induce low expression of pro-inflammatory genes. This will reflect that OSPW treatment reduces the bioactivity of OSPW and ultimately, this assay will be useful for assessing bioactivity in OSPW treated using various methods. Thus, the changes in bioactivity reflect the success of the AOP treatment, which is defined as less immune cell activation as indicated by less changes in pro-inflammatory gene expression.

4.2 Results

4.2.1 Immune gene expression of RAW 264.7 cells before and after electrooxidation treatment of OSPW

RAW 264.7 cells were treated with 50% v/v untreated OSPW, 2 hour electrooxidation-treated OSPW, 6 hour electrooxidation-treated OSPW, or PBS for either 2 or 6 hours. Gene expression was normalized to the endogenous control, *gapdh,* after exposure to PBS for 2 hours. Statistical significance is determined by p-value<0.05 or p-value<0.01.

After 2 hours and 6 hours of exposure to untreated OSPW, *mip-2* expression increased to an average fold change of 450.85 and 507.6, respectively (Fig. 4.1a). However, after a 2 hour and 6 hour exposure to 2 hour electrooxidation-treated OSPW, *mip-2* expression showed a

reduction that is reflected by a percent inhibition of 66% and 79%, respectively (Fig. 4.1b). OSPW treated with electrooxidation for 6 hours showed an even further decrease, reflecting a percent inhibition of 96% and 99% at 2 and 6 hours of exposure, respectively (Fig. 4.1b). It appears that the longer OSPW is treated with electrooxidation, the lower the expression of *mip-2*.

ip-10 expression after exposure to untreated OSPW at both 2 and 6 hours showed significantly higher fold changes than the respective control for each time point (Fig. 4.1c). At both 2 and 6 hours, exposure to 2 hour electrooxidation-treated OSPW had a lower *ip-10* fold change corresponding to percent inhibitions of 71% and 62%, respectively (Fig. 4.1d). Exposure to 6 hour electrooxidation-treated OSPW resulted in the lowest fold change at both 2 and 6 hours of 2.63 and 7.58 (Fig. 4.1c) with corresponding percent inhibitions of 94% and 97%, respectively (Fig. 4.1d). After 6 hours of exposure to both 2 hour and 6 hour electrooxidation-treated OSPW, there is a significant difference in fold change as compared to the 6 hour control whereas after 2 hours of exposure, only the 2 hour electrooxidation-treated OSPW results in a significantly different fold change as compared to the 2 hour control (Fig. 4.1c).

Untreated OSPW exposure for 2 hours shows a significant difference when compared to the control (Fig. 4.1e). Exposure to untreated OSPW for 6 hours showed a higher *mcp-1* average fold change of 119.19 whereas the 2 hour exposure showed a lower *mcp-1* average fold change of 17.56 (Fig. 4.1e). OSPW treated for 2 hours with electrooxidation treatment showed a lower *mcp-1* fold change at both 2 and 6 hours of 10.93 and 59.55, respectively (Fig. 4.1e), than untreated OSPW, which corresponds with a percent inhibition of 37% and 50%, respectively (Fig. 4.1f). OSPW treated for 6 hours with electrooxidation showed an even lower fold change reflecting a percent inhibition of 57% and 93% (Fig. 4.1f).

4.2.2 Immune gene expression of RAW 264.7 cells before and after solar oxidation treatment of OSPW

RAW 264.7 cells were treated with 50% v/v untreated OSPW, 2 hour solar oxidation-treated OSPW, 4 hour solar oxidation-treated OSPW, or PBS for either 2 or 6 hours. Gene expression was normalized to the endogenous control, *gapdh,* after exposure to PBS for 2 hours. Statistical significance is determined by p-value<0.05.

Untreated OSPW induced a much higher *mip-2* fold change at both 2 and 6 hours of exposure than the corresponding control (Fig. 4.2a). 2 hour solar oxidation-treated OSPW exposure showed a lower fold change than untreated OSPW exposure (Fig. 4.2a), which is reflected by 70% inhibition at 2 hours and 80% inhibition at 6 hours (Fig. 4.2b). *mip-2* fold change was even lower after exposure to 4 hour treated OSPW at both exposure times (Fig. 4.2a), which corresponds to 84% inhibition at 2 hours and 88% inhibition at 6 hours (Fig. 4.2b).

ip-10 fold change after exposure to untreated OSPW at both 2 and 6 hours is 28.85 and 107.45, respectively (Fig. 4.2c). OSPW treated for 2 hours with solar oxidation showed a lower fold change at both 2 and 6 hours of 5.74 and 16.34 (Fig. 4.2c), which corresponds to a percent inhibition of 65% and 82% (Fig. 4.2d). OSPW treated for 4 hours with solar oxidation showed an even lower fold change of 1.85 and 10.97 (Fig. 4.2c) corresponding with even higher percent inhibitions of 88% and 87% (Fig. 4.2d).

mcp-1 expression is highest at 2 hours and 6 hours after exposure to untreated OSPW (Fig. 4.2e). OSPW treated with solar oxidation for 2 hours showed a lower fold change of 5.76 and 8.96 (Fig. 4.2e), which corresponds to percent inhibitions of 9% and 59% (Fig. 4.2f). OSPW treated with solar oxidation for 4 hours showed an even larger reduction in fold change at both 2

hours and 6 hours of 2.59 and 5.01, respectively (Fig. 4.2e), corresponding to percent inhibitions of 43% and 74% (Fig. 4.2f).

4.3 Discussion

I used a RAW 264.7 macrophage cell-based *in vitro* biosensor system to detect changes in bioactivity between untreated and treated OSPW via immune gene expression. Untreated OSPW demonstrates high bioactivity as indicated by all genes assessed, and both solar and electrooxidation-treated OSPW show a decrease in bioactivity as compared to untreated OSPW. In general, untreated OSPW demonstrates high bioactivity, as indicated by the large difference in fold change as compared to the control, whereas electrooxidation and solar oxidation treatment at both time points demonstrate lower bioactivity as indicated by the much smaller difference in fold change. Though significance is only seen in *ip-10* expression after exposure to electrooxidation-treated OSPW, the decrease in bioactivity is clearly visible in all genes with both treatments. The macrophage cell-based *in vitro* biosensor system effectively differentiated treated OSPW from untreated OSPW by changes in gene expression, thus demonstrating OSPW bioactivity and treatment efficacy in reducing OSPW-mediated bioactivity. Therefore, this work supports that electro- and solar oxidation are effective in reducing OSPW-mediated bioactivity.

As whole OSPW or fractions containing NAs are previously known to have bioactive effects (Choo-Yin et al., 2021; Lillico et al., 2023; Phillips et al., 2020) and both electro- and solar oxidation treatment degrade NA content (Abdalrhman, Zhang, and El-Din, 2019; Meng et al., 2021), this supports that the bioactivity is perpetuated by NAs as bioactivity decreases after treatment. AOP treatments are effective in decreasing NA content (Abdalrhman and El-Din, 2020; Abdalrhman, Zhang, and El-Din, 2019; Meng et al., 2021) and as OSPW bioactivity

decreases after treatment, this suggests NAs may potentiate bioactivity in RAW 264.7 cells. This effect has been previously seen as Suara et al. (2022) shows a decrease in NA species over time with ZnO-catalyzed solar oxidation treatment and pre- and post-treatment exposure demonstrates a reduction in THP-1 cell pro-inflammatory gene expression. In addition, sulfate advanced radical AOP treatment with biofiltration previously demonstrated a reduction in NA types which was consistent with a decrease in NO released by RAW 264.7 cells which reflects decreased bioactivity (Arslan et al., 2023). As my results are consistent with previous literature, this further supports NAs as a potentiator of bioactivity. Furthermore, it is also seen that the longer the treatment, the lower the bioactivity as the longer treatment time reflects less bioactivity in both electrooxidation and solar oxidation treatments. This is consistent with previous research showing that the longer solar oxidation treatment occurred, the lower the NA concentration (Suara et al., 2022), which again further suggests that NAs potentiate bioactivity.

In general, the fold changes of gene expression of treated and untreated OSPW are slightly higher after six hours of exposure as compared to the respective treatment at two hours of exposure, even though fold changes of treated waters continue to be lower than untreated water. This may suggest that exposure time influences bioactivity, and the higher exposure time leads to higher bioactivity. However, the induction profile over time may also contribute to this result as previous exposure to 50% v/v untreated OSPW led to the highest *mip-2* expression at 2 hours before continuously decreasing whereas *mcp-1* expression continuously increased up until 10 hours of exposure (Choo-Yin, 2021). Choo-Yin (2021) details a fluctuating pattern of *ip-10* expression as OSPW exposure results in increasing *ip-10* expression until 6 hours of exposure when expression decreases until 10 hours of exposure. The decreasing pattern of *mip-2* expression is perpetuated here as exposure to both OSPW treatments show a lower fold change

after 6 hours of exposure as compared to 2 hour exposures. However, untreated OSPW in Fig. 4.1a demonstrates higher *mip-2* expression after 6 hours of exposure which contradicts the pattern of decreasing expression whereas Fig. 4.2a demonstrates lower *mip-2* expression after 6 hours of exposure which is consistent with the decreasing *mip-2* expression profile. The increasing pattern of *mcp-1* expression is also perpetuated here as untreated and treated OSPW show a higher fold change after 6 hours of exposure as compared to 2 hour exposures. As the highest exposure time shown here is 6 hours, *ip-10* demonstrates a similar pattern to *mcp-1* expression, though Choo-Yin (2021) demonstrates a decrease in expression after 6 hours of exposure. Overall, the induction profiles demonstrated by Choo-Yin (2021) are almost completely maintained here and this suggests that the induction profile of specific genes may influence the gene expression during the exposure time.

It should be noted that though replicates retained a consistent pattern of treated OSPW having lower bioactivity than untreated OSPW, the magnitude was very different between each replicate as reflected by the SEM. This was seen across all genes and may reflect differences in the number of passages of cells (Taciak et al., 2018). The expression of specific genes in RAW 264.7 cells has previously been found to change over the number of passages, and at different passage numbers there is significantly different gene expression (Taciak et al., 2018). This also may have impacted statistical significance as even though there is a clear reduction in bioactivity after treatment, significant differences after treatment are only seen in *ip-10* expression and not *mip-2* or *mcp-1* after electrooxidation treatment and no significant differences are seen with any gene after solar oxidation treatment. As the trend of decreased bioactivity after treatment persisted in each replicate, this work effectively maintains that the AOP treatments were successful in reducing bioactivity.

As OSPW contains many contaminants (Li et al., 2017), it is possible other contaminants within this mixture may be stimulating cells and potentially be impacted by OSPW treatment. First, filtration of OSPW samples before exposures may not remove all bacterial components such as LPS and peptidoglycan which are known to activate Toll-like receptors (TLRs) (Choo-Yin, 2021; Liu et al., 2014). Environmental microbial components existing within OSPW may contribute to the bioactivity observed here and may further complicate the detection of OSPW bioactivity (Choo-Yin, 2021). Other constituents may also contribute to bioactivity prior to treatment as there are changes in *il-1β* expression and induction time after exposure to inorganic and whole fractions containing different concentrations of NAs that are not seen when exposed to the organic fraction of OSPW with corresponding NA concentrations (Phillips et al., 2020). NAs are a part of the organic fraction (Li et al., 2017) and changes in gene expression after exposure to the inorganic fraction is indicative of other bioactive constituents (Phillips et al., 2020). Transition metals are proposed to have the capacity to activate dendritic cells via TLR4 (Rachmawati et al., 2013) and as OSPW has been known to contain metals like copper (Phillips et al., 2020), they present as a potential bioactive constituent. In addition, potential contaminants of OSPW may mimic ligands of receptors as, for example, Feng et al. (2019) creates a mimic of a TLR2 agonist that can activate TLR2 on macrophage cells. Therefore, NAs are likely not the only potential agonist for OSPW bioactivity.

4.4 Future Directions

This *in vitro* bioindicator assay can be used to analyze and compare other OSPW treatments that target NAs. The reduction in bioactivity from solar and electrooxidation treatment could be compared to changes in bioactivity from other treatments such as

biodegradation (Quinlan and Tam, 2015). Treatment success and effectivity could be reflected by assessing changes in post-treatment bioactivity and assessing bioactivity from treatments for different periods of time. With further research, this assay may potentially be used as a standard in comparing OSPW treatments.

Previously, the bioactive effects of OSPW have been explored at the level of gene expression as well as protein secretion (Lillico et al., 2023). Here, this assay only assesses bioactivity by gene expression, and this could be expanded to also explore the associated protein expression or secretion. This would provide further depth to my research as OSPW bioactivity would be explored at both the genetic and protein levels. Further research is required to identify how OSPW impacts protein expression and if protein expression differs from gene expression.

How RAW 264.7 cells are stimulated to result in changes in gene expression could be further explored by pharmacological or antibody inhibition. As this research suggests NAs have a role in potentiating bioactivity, identification of the receptor detecting and activating in response to OSPW exposure could elucidate how bioactivity is occurring. This can be pursued using pharmacological inhibitors or antibodies to target specific receptors. As TLR4 can recognize a wide range of ligands (Ciesielska, Matyjek, and Kwiatkowska, 2021; Liu et al., 2014), pharmacological inhibitors or antibodies that target this receptor may act as a good starting point for furthering this research.

a)

b)

c)

ip-10

d)

ip-10

e)

mcp-1

f)
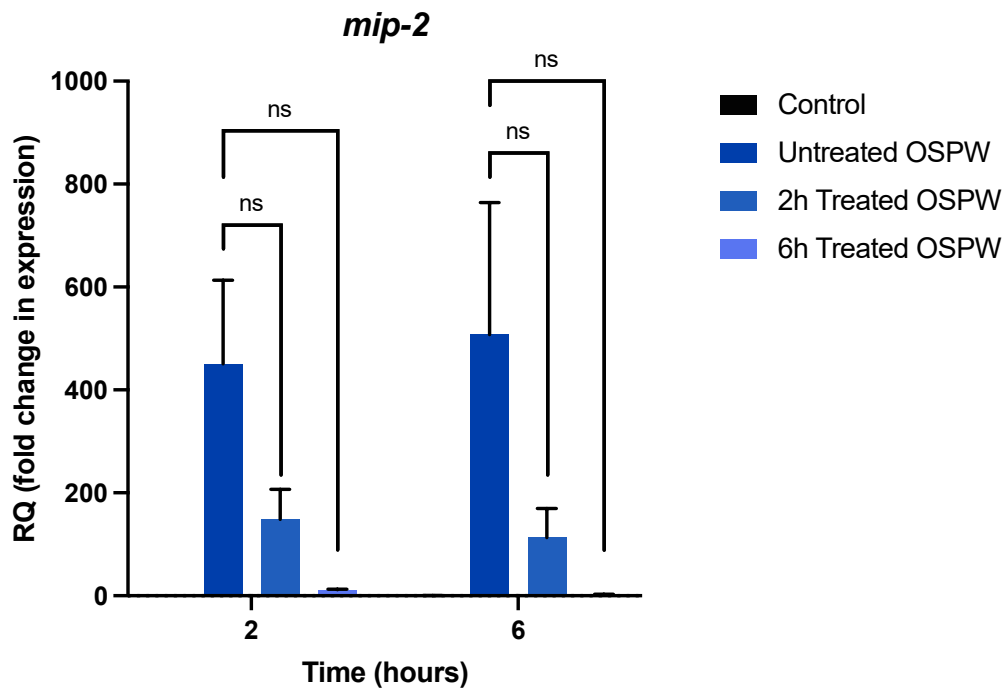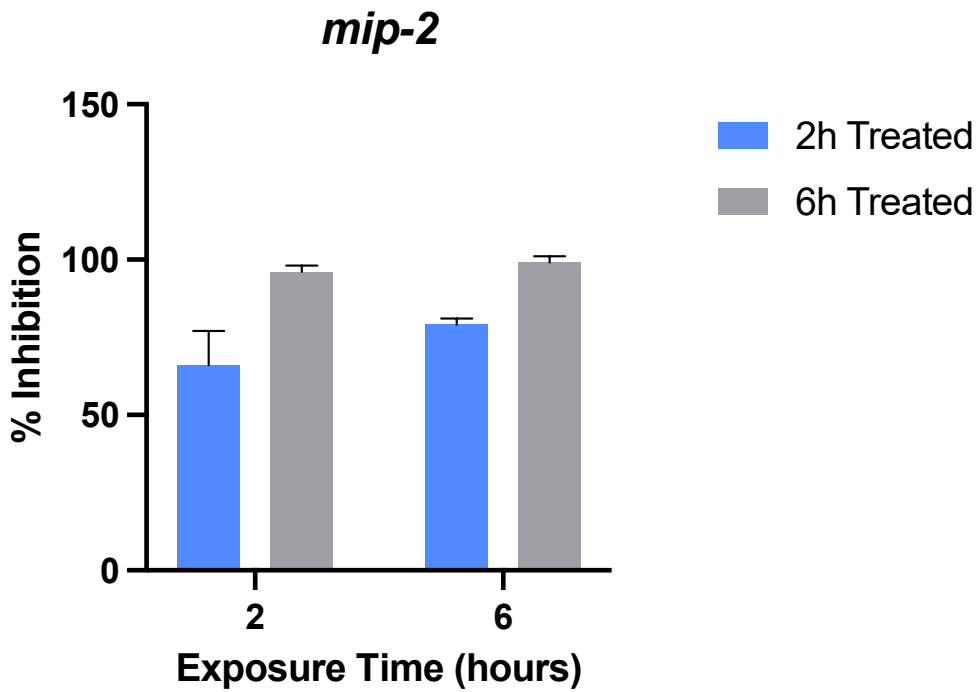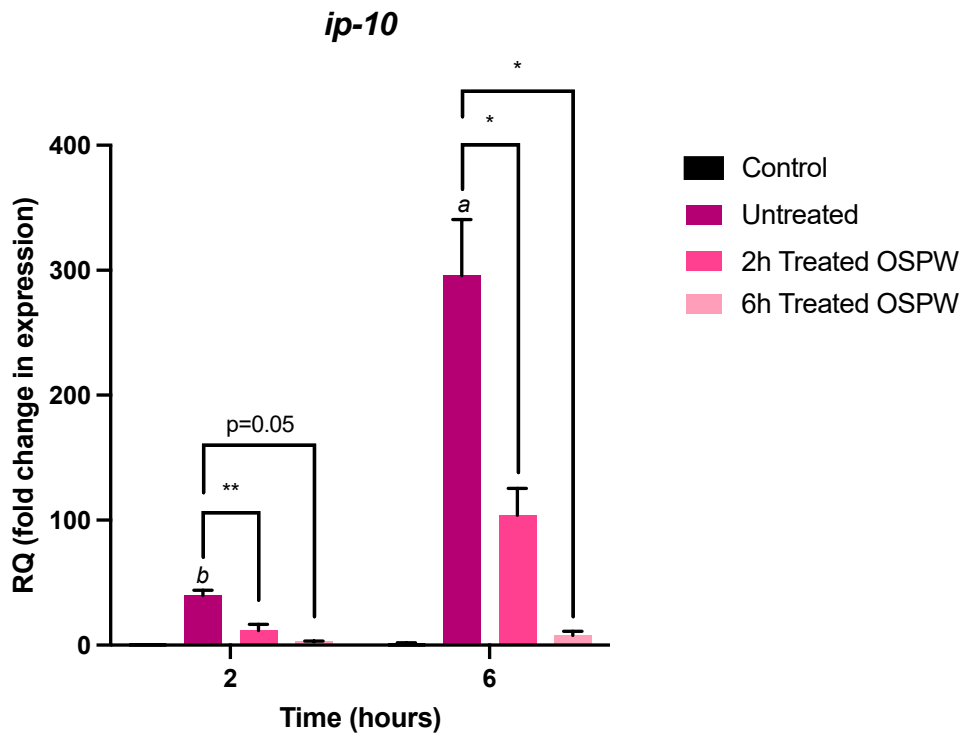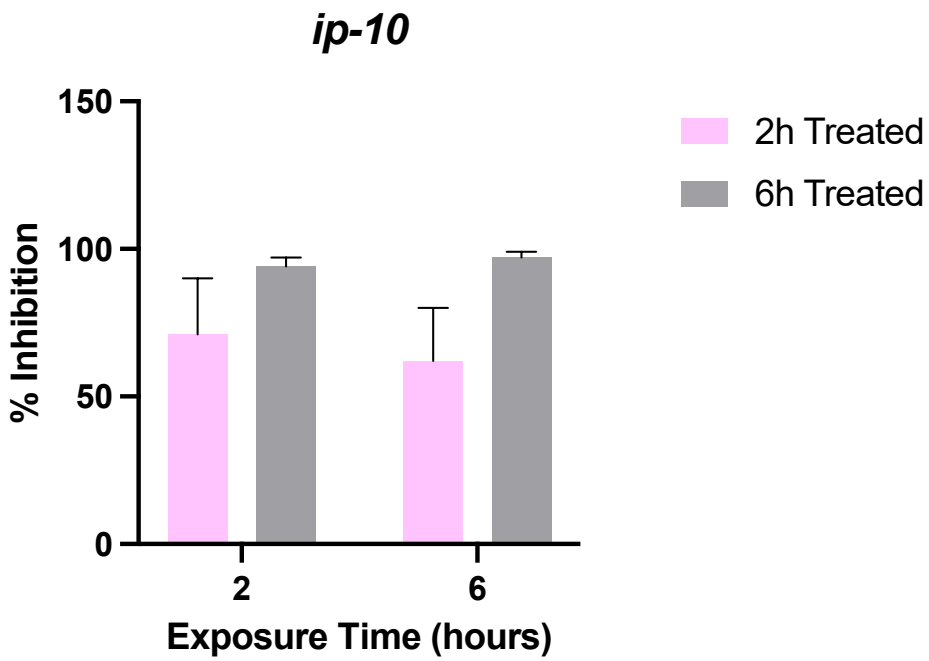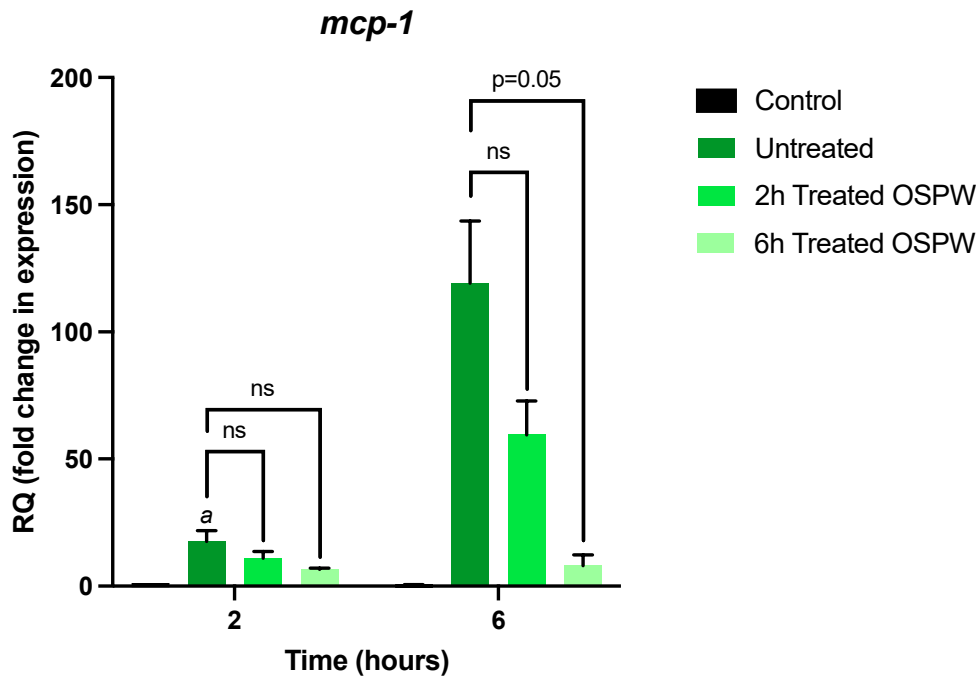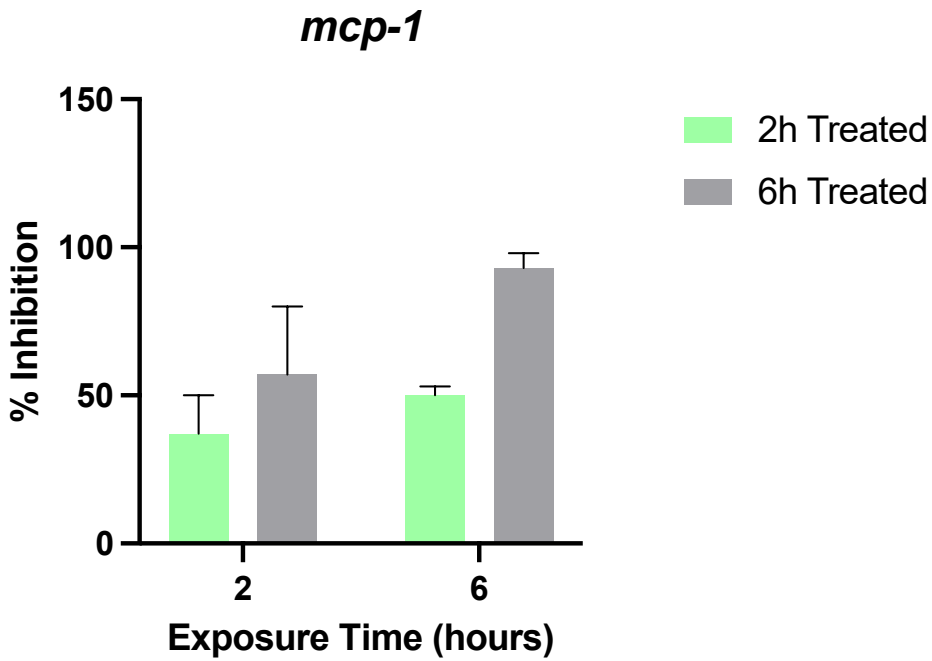
mcp-1

Figure 4.1. Electrooxidation reduces bioactivity as indicated by *mip-2*, *ip-10*, and *mcp-1* expression. RAW 264.7 cells (3 x 10^5 cells/well) were exposed for 2 or 6 hours to 50% v/v PBS (Control), 50% v/v OSPW, or 50% v/v 2 hour or 6 hour electrooxidation-treated OSPW before *mip-2* (a; n=3), *ip-10* (c; n=3), or *mcp-1* (e; n=3) expression was analyzed using RT-qPCR. Corresponding percent inhibition of *mip-2* (b; n=3), *ip-10* (d; n=3), and *mcp-1* (f; n=3) after 2 hour or 6 hour exposure to 2 hour or 6 hour electrooxidation-treated OSPW. Fold change is determined by comparison to the reference sample (control at 2 hours of PBS exposure) and endogenous control (*gapdh*). Based on the Shapiro-Wilk normality test, significance was determined by either an unpaired t test or Mann-Whitney t test. Bars display the average, error bars reflect SEM, * (p<0.05) or ** (p<0.01) depicts significance compared to untreated OSPW of respective time points, and *a* (p<0.05) or *b* (p<0.01) depicts significance compared to the control of respective time points.

a)

mip-2

b)

mip-2

c)

d)

e)

mcp-1

RQ (fold change in expression) vs Time (hours)

Legend:
- Control
- Untreated OSPW
- 2h Treated OSPW
- 4h Treated OSPW

f)

mcp-1

% Inhibition vs Exposure Time (hours)

Legend:
- 2h Treated
- 4h Treated
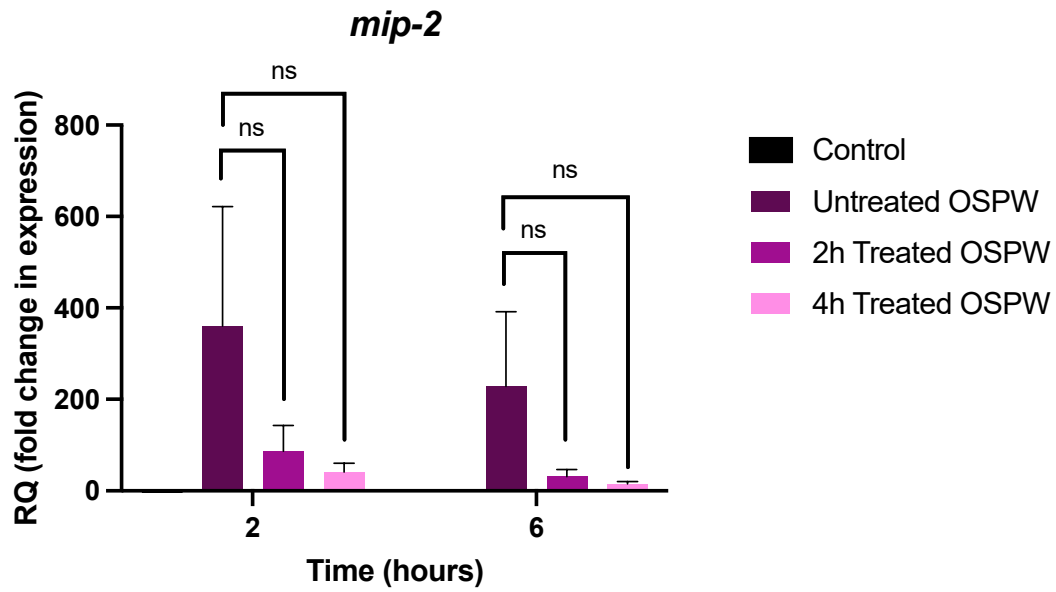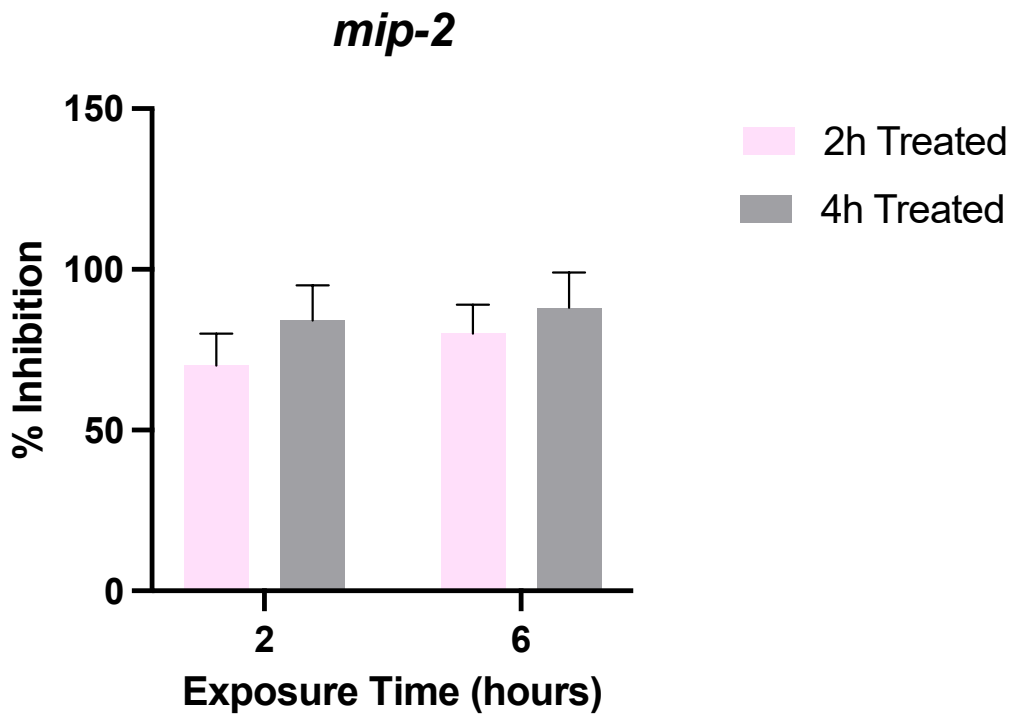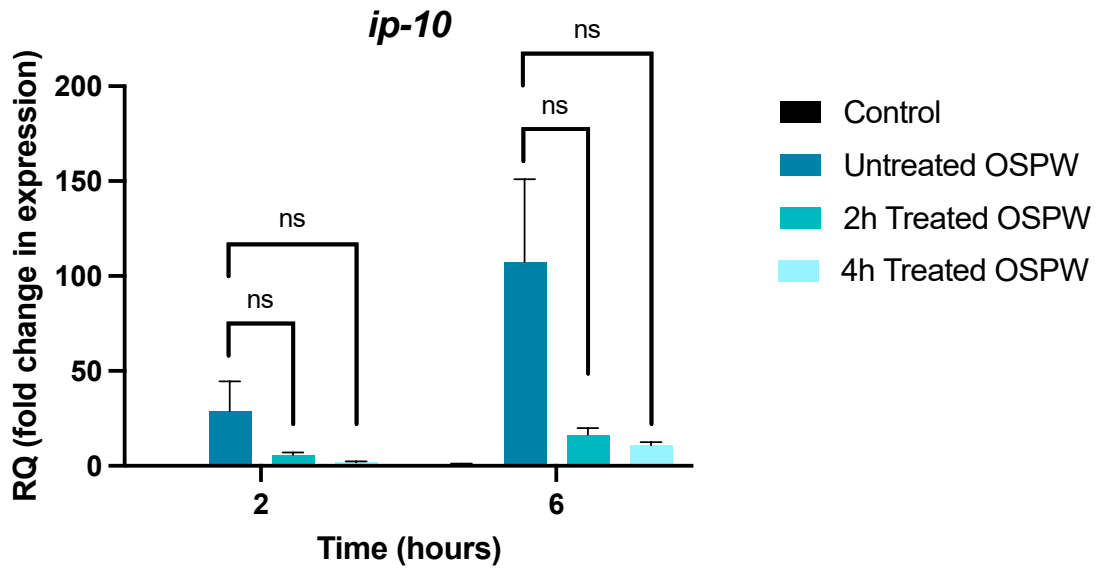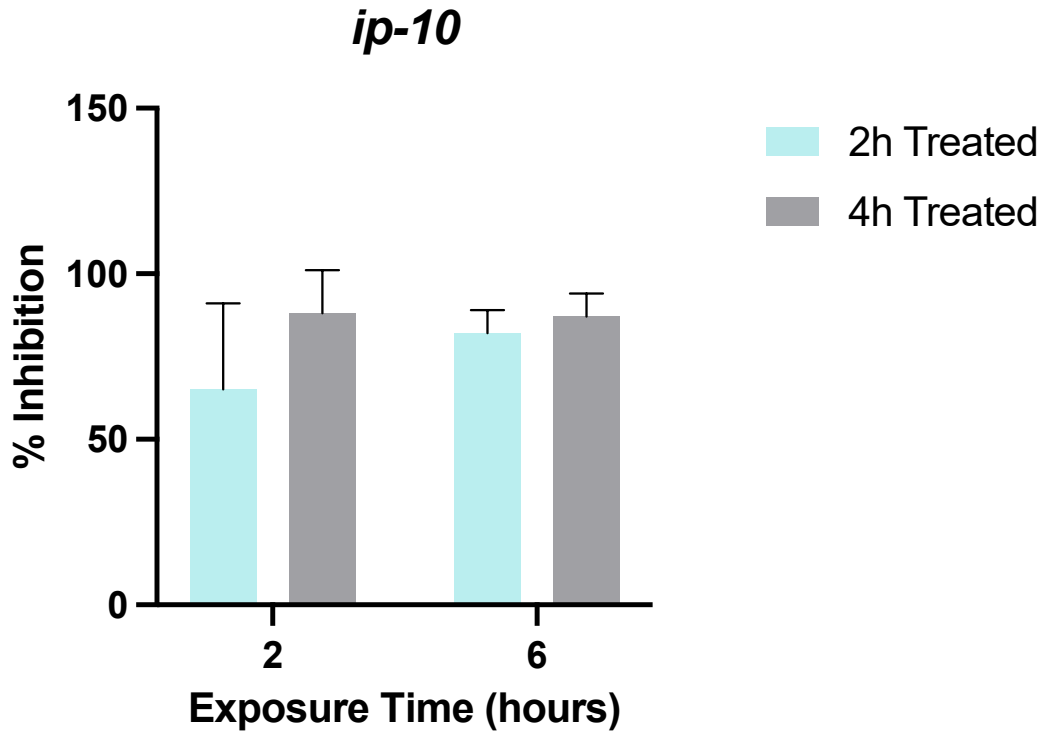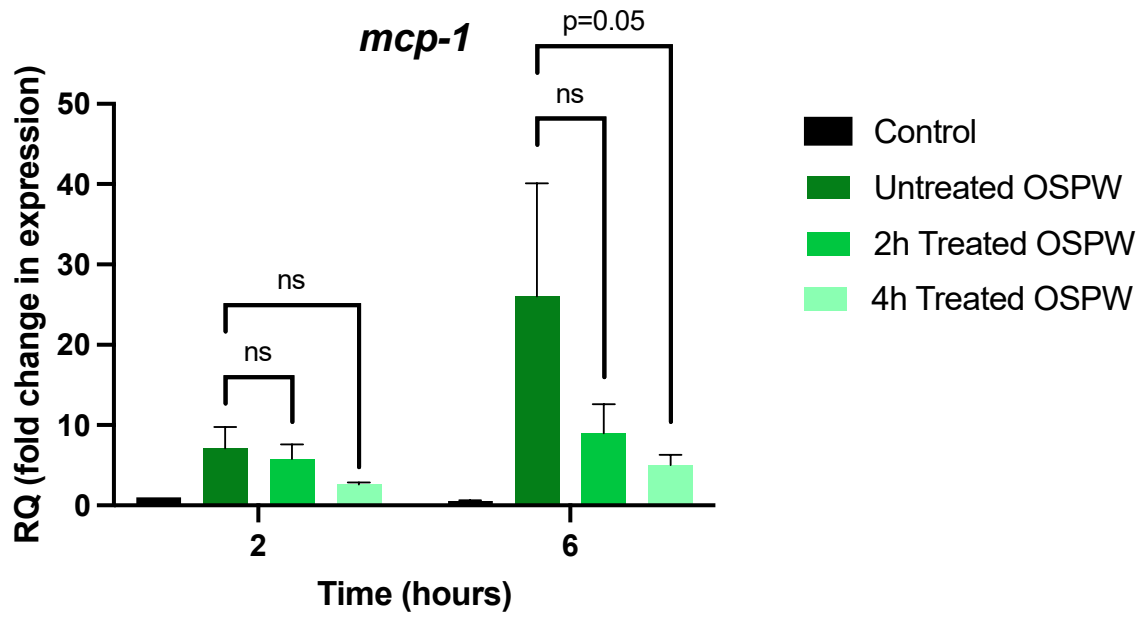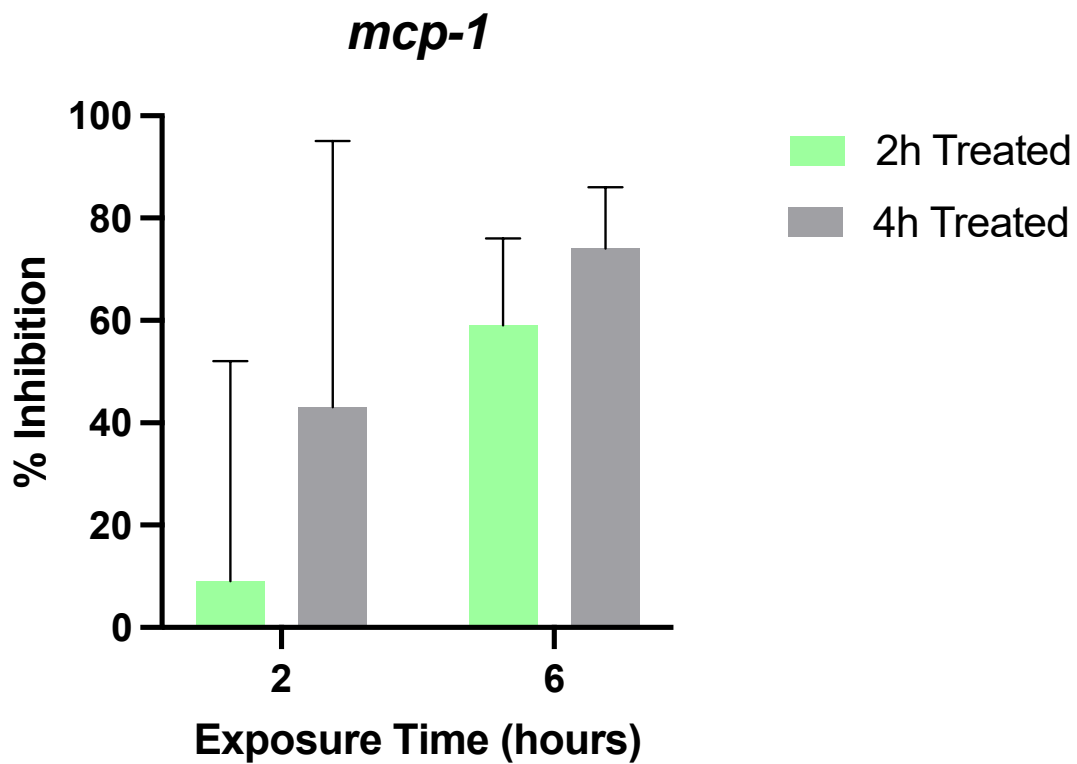
Figure 4.2. Solar oxidation reduces bioactivity as indicated by *mip-2*, *ip-10*, and *mcp-1* expression. RAW 264.7 cells (3 x 10^5 cells/well) were exposed for 2 or 6 hours to 50% v/v PBS (Control), 50% v/v OSPW, or 50% v/v 2 hour or 4 hour solar oxidation-treated OSPW before *mip-2* (a; n=3), *ip-10* (c; n=3), or *mcp-1* (e; n=3) expression was analyzed using RT-qPCR. Corresponding percent inhibition of *mip-2* (b; n=3), *ip-10* (d; n=3), and *mcp-1* (f; n=3) after 2 hour or 6 hour exposure to 2 hour or 4 hour solar oxidation-treated OSPW. Fold change is determined by comparison to the reference sample (control at 2 hours of PBS exposure) and endogenous control (*gapdh*). Based on the Shapiro-Wilk normality test, significance was determined by either an unpaired t-test or Mann-Whitney t-test. Bars display the average, error bars reflect SEM, * (p<0.05) depicts significance compared to untreated OSPW of respective time points, and *a* (p<0.05) depicts significance compared to the control of respective time points.

Chapter V

Examination of OSPW-mediated activation of RAW 264.7 macrophages and implications of TLRs and MyD88 signaling

5.1 Introduction

In Chapter 4, I showed that OSPW stimulation increases pro-inflammatory gene expression and that AOP treatments that degrade NAs (Abdalrhman, Zhang, and El-Din, 2019; Meng et al., 2021; Suara et al., 2022) reduce OSPW-mediated bioactivity. Arslan et al. (2023) assessed the bioactivity of an AOP treatment that degrades NAs in OSPW using NO production by RAW 264.7 macrophage cells and suggests that NA concentration may be a contributing factor to cell activation. In response to OSPW exposure, Paul et al. (2023) also recently showed that changes in immune gene transcriptional activity and secretion of pro-inflammatory cytokines by macrophages are reduced with NA-degrading AOP treatments. Ultimately, Paul et al. (2023) hypothesized that human THP-1 macrophage cells detect NAs within OSPW as reflected by the observed immunotoxic effects. Moving forward, exploring how NA-containing OSPW may interact with macrophage cells to induce changes in gene expression and protein secretion will allow us to further understand the immunotoxic effects of exposure.

Macrophages have an array of innate immune receptors that recognize a broad range of ligands (Lillico et al., 2023; Taylor et al., 2005; Varol, Mildner, and Jung, 2015). Pattern recognition receptors (PRRs) have the capacity to detect various microbial products referred to as pathogen-associated molecular patterns (PAMPs) and facilitate pro-inflammatory responses that are a part of innate immunity (Ciesielska, Matyjek, and Kwiatkowska, 2021). Toll-like receptors (TLRs) are a family of mammalian receptors that are classified as PRRs and when

activated, can upregulate pro-inflammatory gene expression to secrete pro-inflammatory proteins called cytokines (Ciesielska, Matyjek, and Kwiatkowska, 2021; Liu et al., 2014). For example, TLR4 is a cell surface receptor that binds LPS via a well-established mechanism where LPS is sequestered by LPS-binding protein (LBP) which allows CD14, a cell surface protein, to aid in the transfer of LPS to the TLR4/MD-2 complex, as MD-2 is required for LPS-induced TLR4 activation (Ciesielska, Matyjek, and Kwiatkowska, 2021). TLR4 activation by LPS results in a pro-inflammatory response and LPS-triggered macrophages synthesize and release pro-inflammatory cytokines such as Tumor Necrosis Factor-α (TNF-α) (Ciesielska, Matyjek, and Kwiatkowska, 2021; Liu et al., 2014; Stow et al., 2009). TLR4 recognizes a broad range of molecules including bacterial LPS and viral glycoproteins as well as various host molecules referred to as damage-associated molecular patterns (DAMPs), such as fibrinogen and fibronectin (Ciesielska, Matyjek, and Kwiatkowska, 2021; Liu et al., 2014). TLR4 can even recognize elemental stimuli like nickel ions (Schmidt et al., 2010) and is implicated in cell activation by other metals like palladium and cobalt (Rachmawati et al., 2013). Synthetic molecules have also been designed to activate TLR4, as Peri & Calabrese (2014) describes a synthetic TLR4 agonist, CCL-34, that can induce TNF-α production, which demonstrates how TLR4 can be activated by a specific pattern in a lab-designed compound. As this TLR recognizes a broad range of seemingly unrelated ligands (Ciesielska, Matyjek, and Kwiatkowska, 2021; Liu et al., 2014), TLR4 is a potential candidate receptor that may detect the bioactive components of OSPW, which are proposed to be NAs (Arslan et al., 2023; Paul et al., 2023), and result in the observed bioactivity seen in Chapter 4.

TLR4 is not the only receptor that can initiate pro-inflammatory signaling (Kawai and Akira, 2010) and it is important to consider other potential candidate receptors that may be

activated following OSPW exposures. Interestingly, *tlr2* mRNA expression has been reported to be significantly elevated in THP-1 cells after 6 hours of OSPW exposure as compared to the control (Paul et al., 2023), and it is proposed that TLR2 heterodimers evolved to expand the repertoire of PAMPs recognized (Farhat et al., 2008) as TLR2 can also detect a wide variety of PAMPs and DAMPs (Liu et al., 2014). TLR2 is known to form a heterodimer with TLR1 or TLR6, with TLR2/6 recognizing diacylated lipopeptides and TLR1/2 recognizing triacylated lipopeptides and distinguishes ligands via the presence of a hydrophobic channel in the TLR1/2 complex that the TLR2/6 complex lacks (Kawai and Akira, 2010). TLR2/6 recognizes zymosan (Underhill, 2003) whereas TLR1/2 recognizes Pam_3CSK_4 and lipoproteins derived from *E. coli* (Kawai and Akira, 2010; Tükel et al., 2010). Synthetic molecules have also previously been designed to activate TLR2, as Feng et al. (2019) designed a glucomannan polysaccharide with a particular structure that can activate TLR2 on macrophages, which demonstrates how specific lab-designed structures can mimic PAMPs. As this TLR can recognize an extensive ligand repertoire (Liu et al., 2014) and as specific structures can mimic PAMPs (Feng et al., 2019), TLR2 may potentially also be able to detect one or more ligands in OSPW.

TLR4, TLR1/2, and TLR2/6 activate the MyD88-dependent intracellular signaling pathway in immune cells (Ciesielska, Matyjek, and Kwiatkowska, 2021; Liu et al., 2014; Schenk, Belisle, and Modlin, 2009). TLR4 associates with two adaptor proteins: first TIR domain-containing adaptor protein (TIRAP), which then associates with MyD88 (Ciesielska, Matyjek, and Kwiatkowska, 2021). MyD88 interacts with interleukin-1 receptor-associated kinase (IRAK) ¼ and IRAK2 to form the myddosome (Ciesielska, Matyjek, and Kwiatkowska, 2021; Liu et al., 2014). Tumor necrosis factor receptor-associated factor 6 (TRAF6), an E3 ubiquitin ligase, then interacts with the myddosome to activate a signaling cascade that

ultimately results in the activation of IκB kinases α/β, which allows transcription factor NF-κB to translocate to the nucleus (Ciesielska, Matyjek, and Kwiatkowska, 2021; Liu et al., 2014). MyD88-dependent signaling leads to the upregulation of TNF-α, cyclooxygenase 2, IL-6, and IFNλ1/2 (Ciesielska, Matyjek, and Kwiatkowska, 2021). TLR4 also activates MyD88-independent signaling where TLR4 alternatively interacts with TRIF-related adaptor molecule (TRAM), an adaptor molecule, that activates TIR domain-containing adaptor-inducing IFN-β (TRIF) (Ciesielska, Matyjek, and Kwiatkowska, 2021; Liu et al., 2014). This pathway can lead to NF-kB translocation or interferon regulatory factor 3 (IRF3) translocation (Ciesielska, Matyjek, and Kwiatkowska, 2021; Liu et al., 2014). IRF3 and IRF7 activation can lead to the induction of genes encoding RANTES, IP-10, and IL-10 (Ciesielska, Matyjek, and Kwiatkowska, 2021).

Cytokines are produced during inflammatory responses from TLR-activated immune cells (Ciesielska, Matyjek, and Kwiatkowska, 2021; Liu et al., 2014; Qin et al., 2017) and as we saw in Chapter 4, OSPW exposure increases *mcp-1, ip-10,* and *mip-2* expression in RAW 264.7 macrophage cells. Also, OSPW exposure to THP-1 cells have previously been shown to result in increases in MCP-1, TNF-α, and IL-6 secretion (Paul et al., 2023). MCP-1, TNF-α, IL-6, and iNOS regulation have previously been associated with NF-κB activation (Brasier, 2010; Falvo et al., 2010; Jones et al., 2007). MCP-1 is produced by macrophages/monocytes and is involved in the recruitment of monocytes during inflammation (Yadav, Saini, and Arora, 2010). TNF-α is a major pro-inflammatory cytokine that plays a role in the activation of macrophage cells as well as regulation of pro-inflammatory cytokine generation (Parameswaran and Patial, 2010). IL-6 is important in coordinating inflammatory response and is known to induce the production of antibodies (Tanaka, Narazaki, and Kashimoto, 2014). iNOS is involved in the production of NO, a free radical that is released during inflammatory responses and in response to stimuli such as

LPS (Israf et al., 2007; Jones et al., 2007). Immune cell cytokine and NO response can be used to assess LPS- (Jones et al., 2007; Samarpita et al., 2020) and OSPW-stimulated cells (Arslan et al., 2023; Paul et al., 2023).

OSPW activation of macrophages can be compared with TLR4, TLR1/2, and TLR2/6 activation by LPS, Pam_3CSK_4, and zymosan, respectively (Cheng et al., 2012; Ciesielska, Matyjek, and Kwiatkowska, 2021; Kawamoto et al., 2008; Underhill, 2003), to identify similarities or differences in cytokine release between OSPW and TLR agonists. After demonstrating the bioactive effects of OSPW on cytokine secretion and comparing OSPW stimulation to stimulation with TLR agonists, I studied OSPW activation of TLRs in RAW 264.7 cells by pharmacologically inhibiting TLR4 and TLR1/2. Pharmacological inhibitors target and prevent activation of receptors by various mechanisms as Cu-CPT22 inhibits TLR1/2 by competitively binding with PAM_3CSK_4 (Cheng et al., 2012) whereas cell-permeable TAK242 inhibits TLR4 by binding the intracellular domain and is thought to prevent scaffold formation between the TIR domain and signaling proteins like TIRAP and TRAM (Matsunaga et al., 2011; Samarpita et al., 2020; Takashima et al., 2009). Cu-CPT22 has previously been found to decrease pro-inflammatory response from TLR1/2 activation (Cheng et al., 2012) and TAK242 has previously demonstrated inhibition of NO and TNF-α generation after LPS stimulation (Kawamoto et al., 2008; Samarpita et al., 2020). To identify the activation of TLRs by OSPW, I pharmacologically inhibited TLR4 or TLR1/2, stimulated with OSPW, and assessed NO response which can be analyzed using the colorimetric Griess reaction which assesses nitrite (Arslan et al., 2023). For example, OSPW stimulation of RAW 264.7 cells results in NO production (Arslan et al., 2023; Lillico et al., 2023) but if Cu-CPT22 is used to inhibit TLR1/2 (Cheng et al., 2012) and we no longer see a NO response, this would indicate a role for TLR1/2

in OSPW-mediated macrophage activation. Pharmacological inhibitors are widely used to study

cell signaling (Cheng et al., 2012; Samarpita et al., 2020; Zhang et al., 2021) and by directly

targeting TLR2 and TLR4 receptors with the above inhibitors, we can assess their role in OSPW-

mediated cell signaling and response.

Next, I applied the above idea to explore the activation of cell signaling proteins located

proximally and distally to TLR4 and TLR2 by OSPW as compared to TLR agonists using

pharmacological inhibitors. This allows us to examine the involvement of TLR cell signaling

proteins in OSPW-stimulated signaling and identify differences in OSPW- vs. TLR agonist-

mediated signaling. Furthermore, inhibiting proteins at different locations along a cell signaling

pathway will allow us to determine where divergence in signaling occurs, if any, which may

further elucidate differences in OSPW-mediated signaling. OSPW exposure increases TNF-α

secretion (Paul et al., 2023) and as TNF-α is regulated by NF-κB (Falvo et al., 2010), which is

activated by the MyD88-dependent signaling pathway (Ciesielska, Matyjek, and Kwiatkowska,

2021; Liu et al., 2014), this suggests that the MyD88-dependent signaling pathway, and by proxy

NF-κB, may be activated by OSPW. I explored the activation of IRAK1/4, PKCα/βI, MEK1/2,

and NF-κB by OSPW and compared to TLR4-mediated activation using pharmacological

inhibitors and the same approach as outlined above. As iNOS is regulated by NF-κB and is

directly involved in NO production (Jones et al., 2007), I used Aminoguanidine, an inhibitor that

competes with the iNOS substrate L-arginine (Griffiths et al., 1993; Salinas-Carmona et al.,

2020), as a pharmacological control for macrophage cell activation by OSPW in comparison to

the TLR4 agonist, LPS (Kawamoto et al., 2008; Liu et al., 2014).

Signaling proteins proximal to TLR4 and TLR2 include IRAK1/4 (Liu et al., 2014) and

PKCα, which is known to interact with the signaling complex formed at TLR2 and is implicated

in MyD88-dependent signaling (Loegering and Lennartz, 2011). IRAK4 is thought to be necessary for Toll and interleukin-1 receptor (TIR) domain signaling and blocking IRAK4 should inhibit mainly the MyD88-dependent pathway (Wang et al., 2009). IRAK4 can be inhibited via aminobenzimidazole inhibitors, which can bind at the ATP-binding site (Powers et al., 2006; Wang et al., 2009). IRAK1/4 can interact with MyD88 (Liu et al., 2014; Wang et al., 2009) and Wang et al. (2009) theorizes that MyD88-dependent signaling is prevented when TLR-activated IRAK4 function is blocked which means that inhibition of OSPW-activated IRAK4 should reflect inhibition of the MyD88-dependent signaling pathway, especially if TLR activation mediates OSPW-induced cell response. Protein Kinase C (PKC) has been implicated in TLR signaling and PKC isoforms may interact with TLRs, such as how PKCα can interact with TLR2 (Loegering and Lennartz, 2011). PKC represents a group of proteins that are subdivided into three categories (conventional isoforms, including PKCα and PKCβ, novel isoforms, and atypical isoforms (Loegering and Lennartz, 2011)) and are involved in various cellular processes such as apoptosis, differentiation, secretion, and growth (Loegering and Lennartz, 2011). Go 6976 is a potent inhibitor of PKCα/βI via competitive inhibition of the ATP binding site (Qatsha et al., 1993; Wu et al., 2003). PKCα is known to be involved in TLR2 and TLR4 signaling (Loegering and Lennartz, 2011; Zhou et al., 2015) and if OSPW-induced cell response ceases with PKCα inhibition, then this indicates a role for PKCα in OSPW-mediated signaling. We can compare IRAK1/4 and PKC activation by TLR agonists with OSPW and examine the involvement of IRAK1/4 and PKC in OSPW-mediated signaling to identify potential signaling differences between TLR stimuli and OSPW.

TLR4 stimulation activates distal signaling proteins like mitogen activated protein kinase kinase (MEK), which is proposed to occur via triggering the RAS-RAF-MEK1/2 signaling

cascade (Bauerfeld and Samavati, 2017). MEK1/2 is located after the Ras-Raf signaling

pathway and phosphorylates extracellular signal-regulated kinases (ERK) ½, which leads to AP-

1 activation (Bauerfeld and Samavati, 2017; Duncia et al., 1998). U0126 noncompetitively

inhibits MEK1/2 (Duncia et al., 1998) and as MEK/ERK can be activated by LPS (Bauerfeld and

Samavati, 2017), we can contrast LPS and OSPW stimulation with MEK1/2 inhibition to

identify differences in TLR4- and OSPW-mediated signaling. NF-κB is a transcription factor

activated by TLR4 and TLR2 and is located near the end of the MyD88-dependent signaling

pathway (Israf et al., 2007; Liu et al., 2014). When inactive, NF-κB is bound to I-κBα in the

cytoplasm and phosphorylation of I-κBα allows for the translocation of NF-κB to the nucleus

(Israf et al., 2007). Cardamonin inhibits the phosphorylation of I-κBα (Israf et al., 2007).

Previously, Cardamonin had reduced NO production from RAW 264.7 cells after LPS

stimulation (Takahashi, Yamamoto, and Murakami, 2011), and if Cardamonin decreases OSPW-

induced NO response, then this indicates a role for NF-κB in OSPW-mediated signaling.

Ultimately, we will elucidate the activation of signaling proteins central to MyD88-dependent

signaling by OSPW stimulation and by inhibiting proteins located at different positions proximal

and distal to TLRs, we will understand the point of divergence, if any, between OSPW and TLR

ligand signaling.

Lastly, I compared the IRAK1/4- and TLR4-inhibited NO response profile with

stimulation by OSPW to stimulation with a singular PAMP using LPS (Kawamoto et al., 2008;

Liu et al., 2014) and stimulation with more than one PAMP using heat-killed *E. coli* (Alexander

and Rietschel, 2001; Coorens et al., 2017; Tükel et al., 2010). By contrasting stimulation with

OSPW to LPS and heat-killed *E.coli*, I can compare the pattern of NO response to indicate if the

pattern induced by OSPW stimulation is more similar to one PAMP or multiple PAMPs. OSPW

is a complex mixture (Li et al., 2017; Phillips et al., 2020) and this explores the possibility that OSPW may contain more than one bioactive component resulting in bioactive effects that may be mediated through more than one receptor. Inhibition of TLR4 at varying concentrations and stimulation with one or more agonists allows for comparison of TLR4-induced NO response. We expect LPS stimulation to result in less NO production at increasing TAK242 concentrations because TLR4 recognizes LPS (Kawamoto et al., 2008; Matsunaga et al., 2011; Takashima et al., 2009) and TAK242 inhibits TLR4 (Matsunaga et al., 2011; Samarpita et al., 2020; Takashima et al., 2009) whereas heat-killed *E. coli* will likely maintain consistently high NO response regardless of TAK242 concentration because it contains other PAMPs that may activate alternative TLRs (Alexander and Rietchel, 2001; Coorens et al., 2017; Tükel et al., 2010). If OSPW contains one bioactive component, I expect the response profile with increasing TAK242 concentrations to look similar to LPS whereas the presence of more than one bioactive component would likely elicit an NO response more similar to heat-killed *E. coli*. IRAK4 is integral to TLR signaling (Wang et al., 2009) and as IRAK1/4 is downstream of TLR4 (Liu et al., 2014), I expect the inhibition of IRAK1/4 with LPS stimulation to elicit a minimal NO response. Conversely, stimulation with heat-killed *E. coli*, which contains other PAMPs that activate other TLRs (Alexander and Rietschel, 2001; Coorens et al., 2017; Tükel et al., 2010), may elicit a graded response as MyD88-dependent signaling via TLR activation is expected to be abrogated with IRAK4 inhibition (Wang et al., 2009). Therefore, it is reasonable to assume that if OSPW activates multiple TLRs, the NO response is likely to reflect a similar pattern to what is seen with heat-killed *E. coli* stimulation; however, if OSPW is detected only by TLR4, the NO response is likely to reflect a similar pattern to LPS stimulation.

OSPW exposure alters pro-inflammatory response of immune cells (Arslan et al., 2023; Paul et al., 2023) and NAs are proposed as the bioactive component that mediates these effects (Arslan et al., 2023; Paul et al., 2023). How OSPW components impact immune cells is poorly understood, and in this chapter, I explore immune cell detection and response of the bioactive component of OSPW. I investigate OSPW stimulation of RAW 264.7 mouse macrophage cells and the potential detection of OSPW by TLRs. If cell signaling from TLR4 activation is comparable to OSPW-mediated cell signaling, this may indicate TLR4 as a potential receptor in recognizing OSPW. Here, I compare OSPW-mediated bioactivity and signaling to TLR-mediated activation using various TLR agonists and an array of pharmacological inhibitors that target cell signaling proteins associated with TLR signaling.

5.2 Results

5.2.1 Comparison of cytokine secretion with TLR agonist and OSPW stimulation

Pro-inflammatory cytokine secretion from OSPW exposure was assessed. Heat-killed *E. coli*, Pam_3CSK_4, zymosan, LPS, and 6.25% v/v OSPW were used to stimulate RAW 264.7 cells and cell response was assessed by TNF-α, MCP-1, and IL-2 secretion.

Significantly higher levels of TNF-α are found when cells are stimulated with Pam_3CSK_4, zymosan, heat-killed *E. coli*, and 6.25% v/v OSPW as compared to medium (Fig. 5.2a) but not with LPS stimulation (Fig. 5.2b). The unstimulated control shows a significant difference when compared to OSPW stimulation (Fig. 5.2). MCP-1 secretion shows elevated but not significant levels with heat-killed *E. coli,* Pam_3CSK_4, zymosan, OSPW, and LPS stimulation (Fig. 5.3ab). There is no significant difference in MCP-1 concentration among different stimuli (Fig. 5.3). IL-2 secretion is significantly higher with zymosan, and heat-killed *E. coli* stimulation as compared

to the control (Fig. 5.4). Zymosan and heat-killed *E. coli* stimulation show significantly higher

IL-2 concentrations as compared to Pam$_3$CSK$_4$ and OSPW stimulation (Fig. 5.4).

5.2.2 OSPW-stimulated NO production after TLR1/2 and TLR4 inhibition

Positive controls for Cu-CPT22 were established and cell response to OSPW exposure

with various Cu-CPT22 concentrations and TAK242 was assessed. Heat-killed *E.coli*,

Pam$_3$CSK$_4$, zymosan, and 6.25% v/v OSPW were used to stimulate RAW 264.7 cells inhibited

by either TAK242 or serial diluted Cu-CPT22 and cell response was assessed by nitrite

concentration.

Pam$_3$CSK$_4$, heat-killed *E. coli,* zymosan, and OSPW significantly increase nitrite

response compared to medium (Fig. 5.5). Zymosan, heat-killed *E. coli,* and OSPW stimulation

demonstrate significantly reduced nitrite concentration between the highest and lowest

concentrations of Cu-CPT22 (Fig. 5.5bcd), whereas Pam$_3$CSK$_4$ treatment showed no significance

between concentrations (Fig. 5.5a). 4 µM Cu-CPT22 significantly reduces nitrite response when

stimulated with Pam$_3$CSK$_4$, Zymosan, and 6.25% v/v OSPW (Fig. 5.5e). 2 µM Cu-CPT22

significantly reduces nitrite response when stimulated with 6.25% v/v OSPW or Pam$_3$CSK$_4$ (Fig.

5.5e). LPS and 6.25% v/v OSPW significantly increase nitrite production as compared to the

medium and 200 nM TAK242 significantly reduces nitrite response when stimulated with LPS

or OSPW (Fig. 5.5f).

5.2.3 Involvement of TLR-activated signaling proteins in OSPW-mediated NO response

RAW 264.7 cells were exposed to Aminoguanidine, Cardamonin, IRAK1/4 Inhibitor I,

Go 6976, and U0126 in full, half, and quarter doses to assess the attenuation of cell response

with LPS stimulation as compared to 6.25% v/v OSPW as well as to avoid completely inhibiting cell response. From the concentrations assessed, an optimal concentration was selected and compared to the effects of the drug treatments on LPS- and OSPW-stimulated cells. Nitrite production assessed via Griess reaction reflects NO response.

LPS and OSPW stimulation induce significantly high nitrite concentrations (Fig. 5.6-5.10). Nitrite concentration shows a visible dose-response decrease with increase in pharmacological inhibitor concentration for all inhibitors assessed (Fig. 5.6-5.10). The highest concentration of each inhibitor results in a pronounced decrease in nitrite production as compared to the lowest concentration (Fig. 5.6-5.10), though only Cardamonin, and IRAK1/4 Inhibitor I show significantly less nitrite between the highest and lowest concentrations following OSPW stimulation (Fig. 5.7a, 5.8a). Aminoguanidine, Cardamonin, and IRAK1/4 Inhibitor I inhibition results in a significant decrease in NO response when stimulated with LPS or OSPW (Fig. 5.6b, 5.7b, 5.8b). 32.74 µM nitrite is produced with OSPW stimulation whereas Aminoguanidine reduces nitrite to 9.09 µM, Cardamonin reduces to 1.79 µM, and IRAK1/4 Inhibitor I reduces to 9.6 µM (Fig. 5.6b; 5.7b, 5.8a). Go 6976 significantly inhibits nitrite production from 32.74 µM to 14.55 µM with OSPW stimulation whereas the same concentration of inhibitor does not result in significant inhibition from LPS stimulation (Fig 5.9b). U0126 inhibition significantly reduces nitrite production from 32.74 µM to 13.81 µM with OSPW stimulation (Fig. 5.10b). Inhibitors of iNOS, NF-κB, IRAK1/4, PKC, and MEK1/2 all effectively reduce nitrite concentrations from OSPW stimulated cells (Fig. 5.6-5.10).

5.2.4 Pattern of OSPW-mediated NO production as compared to heat-killed E. coli and LPS

OSPW stimulation with either TAK242 or IRAK1/4 Inhibitor I exposure was paralleled with stimulation by heat-killed *E. coli* or LPS. Varying concentrations of TAK242 or IRAK1/4 Inhibitor I were exposed to RAW 264.7 macrophage cells that were stimulated with heat-killed *E. coli*, LPS, and 6.25% v/v OSPW. Cell stimulation and response was assessed by nitrite concentration.

Cells treated with serially diluted TAK242 and stimulated with heat-killed *E. coli* or LPS demonstrate significantly reduced nitrite concentration between the highest and lowest doses (Fig. 5.11ab), whereas there is no significant difference between the highest and lowest TAK242 concentrations with OSPW stimulation despite 80% inhibition (Fig. 5.11c). TAK242 treatment with LPS shows obvious dose-response effects that are reflected by a 94% inhibition between the highest and lowest concentrations (Fig. 5.11b). Nitrite response with heat-killed *E. coli* stimulation shows a much higher magnitude at each TAK242 concentration that is reflected by the 23% inhibition between the highest and lowest concentrations (Fig. 5.11a), as compared to LPS (Fig. 5.11b) and OSPW (Fig. 5.11c). For example, at 200 nM TAK242, heat-killed *E. coli* stimulation results in 13.97 µM nitrite (Fig. 5.11a), whereas nitrite is 0.72 µM with LPS stimulation (Fig.5.11b) and 1.6 µM with OSPW (Fig. 5.11c).

Heat-killed *E. coli*, LPS, and 6.25% OSPW stimulation of serially diluted IRAK1/4 Inhibitor I-treated cells show significantly inhibited nitrite response between the highest and lowest concentrations (Fig. 5.12). The nitrite response profile of LPS shows a much lower magnitude at each inhibitor concentration with 78% inhibition between the highest and lowest concentrations (Fig. 5.12b) as compared to heat-killed *E. coli* (Fig. 5.12a) and OSPW (Fig. 5.12c). Heat-killed *E. coli*-stimulated cells demonstrates 77% inhibition (Fig 5.12a) and OSPW

treated cells demonstrates 81% inhibition between the highest and lowest concentrations (Fig. 5.12c). Though the percent inhibition is similar for each stimulus, the magnitude varies as, for example, at 100 µM IRAK1/4 Inhibitor I, LPS stimulation results in 4.62 µM nitrite (Fig. 5.12b) whereas heat-killed *E. coli* stimulation is 17.37 µM nitrite (Fig. 5.12a) and OSPW stimulation is 16.05 µM nitrite (Fig. 5.12c).

5.3 Discussion

5.3.1 Pro-inflammatory cytokine secretion from TLR ligands

Firstly, I compared OSPW-mediated pro-inflammatory cytokine response to stimulation by known TLR agonists (Cheng et al., 2012; Ciesielska, Matyjek, and Kwiatkowska, 2021; Coorens et al., 2017; Kawamoto et al., 2008; Underhill, 2003). Stimulation by zymosan, heat-killed *E. coli*, LPS, and Pam_3CSK_4 results in increased TNF-α and MCP-1 secretion, which exemplifies macrophage activation by the respective TLRs. OSPW stimulation also increases TNF-α and MCP-1 concentrations, which reflects the capacity of OSPW to activate immune cells and thus induce bioactivity. Pro-inflammatory cytokine induction by OSPW exposure is not significantly different from TLR agonist exposure. This indicates that OSPW can induce effects on pro-inflammatory cytokines that are comparable to effects by TLR agonists. As TNF-α and MCP-1 are regulated by NF-κB, which can be activated by the MyD88-dependent signaling pathway (Brasier, 2010; Ciesielska, Matyjek, and Kwiatkowska, 2021; Falvo et al., 2010), the increased secretion of these cytokines with OSPW stimulation suggests OSPW may be activating MyD88-dependent signaling.

My results are consistent with previous literature demonstrating that zymosan, LPS, and Pam_3CSK_4 increase TNF-α production (de Campos et al., 2020; Sato et al., 2003). My results

are also consistent with previous literature demonstrating that Pam$_3$CSK$_4$ increases MCP-1

production (Sang et al., 2018). Heat-killed *E. coli* is known to contain LPS, among other TLR

stimuli (Alexander and Rietschel, 2001; Coorens et al., 2017; Tükel et al., 2010), and therefore it

is expected that it will increase TNF-α and MCP-1 concentration. Untreated OSPW was

previously noted to increase secretion of pro-inflammatory cytokines like TNF-α and MCP-1 as

well as IL-6 in THP-1 human macrophage cells (Paul et al., 2023). Here, the increased TNF-α

and MCP-1 secretion from RAW 264.7 mouse macrophage cells is consistent with what is seen

in human THP-1 cells (Paul et al., 2023). Overall, the comparable elevation of pro-inflammatory

cytokines between OSPW and TLR agonists demonstrates the bioactivity of OSPW and suggests

the possibility of TLR involvement in OSPW signaling.

IL-2 is known to be involved in T cell development as it contributes to T cell proliferation

and subsequent memory and effector cell production (Abbas et al., 2018). In monocytes, IL-2 is

thought to induce the secretion of cytokines and growth factors as well as be involved in

microbicidal functions (Masztalerz et al., 2003). IL-2 secretion is significantly increased by

heat-killed *E. coli* and zymosan stimulation whereas PAM$_3$CSK$_4$ or OSPW stimulation does not

have the same effect. This is interesting as TLR2/6 and TLR1/2 are previously known to signal

through the MyD88-dependent pathway (Schenk, Belisle, and Modlin, 2009) and this difference

in cytokine production indicates potential differences in signaling. Regardless, while OSPW

does not significantly modulate IL-2 secretion, the difference in cell response to other TLR

stimuli like zymosan and heat-killed *E. coli* is worth noting.

IL-2 secretion is unexpected, as to my knowledge, no reports have previously outlined

secretion of IL-2 from RAW 264.7 cells. In fact, it has previously been determined that

macrophage cells do not produce IL-2 (Zelante et al., 2012). Granucci et al. (2001) showed that

bone marrow-derived macrophage cells do not produce IL-2 whereas bone marrow-derived dendritic cells do. However, this study used an ELISA assay to analyze IL-2 secretion whereas this thesis uses a Luminex multiplex analysis. Luminex assays are known to be more sensitive than ELISA assays (Platchek et al., 2020) and as Granucci et al. (2001) used an ELISA assay, it is possible their approach may not detect the low levels of IL-2 production observed in this thesis. Cross-reactivity has been another possibility considered though due to the significance and consistency seen with all three replicates, it is unlikely. Using the Luminex assay performed by the same company, Arunachalam et al. (2023) also found low, but significant levels of IL-2 produced by RAW 254.7 mouse macrophage cells. Though IL-2 response and production from mouse macrophage cells is largely unknown, the changes in IL-2 concentration from TLR agonist and OSPW stimulation are noted here.

5.3.2 OSPW stimulation of TLR1/2 and TLR4

After recognizing how OSPW bioactivity induces effects comparable to TLR stimuli, I explored the involvement of TLR4 and TLR1/2 in OSPW stimulation of RAW 264.7 macrophage cells. Pam$_3$CSK$_4$, zymosan, heat-killed *E. coli,* and 6.25% v/v OSPW were independently used to stimulate RAW 264.7 cells and determine if different concentrations of TAK242 or Cu-CPT22 could inhibit NO response. The reduction in OSPW-mediated NO production with TAK242, which inhibits TLR4 (Matsunaga et al., 2011; Samarpita et al., 2020; Takashima et al., 2009), and Cu-CPT22, which inhibits TLR1/2 (Cheng et al., 2012), reflects that more than one TLR may be activated by OSPW and that both TLR1/2 and TLR4 may contribute to OSPW-mediated activation of mouse macrophage cells.

As TLR4 can recognize a broad range of seemingly unrelated PAMPs (Ciesielska, Matyjek, and Kwiatkowska, 2021; Liu et al., 2014; Peri & Calabrese, 2014; Rachmawati et al., 2013; Stow et al., 2009), I investigated the involvement of TLR4 in OSPW-mediated signaling. Kawamoto et al. (2008) previously showed TAK242 inhibition of LPS-stimulated NO response by RAW 264.7 cells, which is consistent with the significant reduction in LPS-stimulated NO response seen here. Inhibition of TLR4 significantly inhibits NO response with 6.25% v/v OSPW stimulation which implicates TLR4 in OSPW-mediated cell signaling. Arslan et al. (2023) and Paul et al. (2023) both hypothesized NAs to perpetuate OSPW bioactive or immunotoxic effects, and as TLR4 is implicated in OSPW stimulation of RAW 264.7 cells, this data suggests TLRs may present a possible route of activation by OSPW.

TLR4 is not the only receptor implicated in pro-inflammatory signaling and as elevated *tlr2* mRNA expression has been associated with OSPW exposure (Paul et al., 2023), I also investigated the involvement of TLR2 in OSPW activation of mouse macrophage cells. The highest assessed concentration of the TLR1/2 inhibitor resulted in significantly reduced NO response from zymosan, heat-killed *E. coli,* and OSPW stimulation as compared to the lowest concentration. A reduction in Pam_3CSK_4-stimulated NO production with increase in Cu-CPT22 concentration is seen but not significant. Pam_3CSK_4 and zymosan have previously induced NO response in RAW 264.7 cells (Cheng et al., 2012; Vicente et al., 2001). As Pam_3CSK_4 is a TLR1/2 agonist (Cheng et al., 2012), it was expected that the TLR1/2 inhibitor may reduce cell response. As such, my results are consistent with previous data showing RAW 264.7 cells stimulated with Pam_3CSK_4 were found to have a decrease in NO response with 4 μM Cu-CPT22 (Sang et al., 2018). As TLR2 can also exist in a heterodimer with TLR6 (Kawai and Akira, 2010), I wanted to further explore and compare the role of TLR2 in OSPW cell signaling using

zymosan. Durai et al. (2017) has shown that not only can Cu-CPT22 inhibit RAW 264.7 cell TNF-α secretion by a TLR1/2 agonist, but also shows significantly decreased TNF-α secretion with stimulation by a TLR2/6 agonist. Zymosan activates TLR2/6 (Underhill, 2003) and as seen here, zymosan induced TNF-α secretion. Zymosan-stimulated NO response was inhibited by Cu-CPT22 and here I use zymosan as another TLR agonist to compare to OSPW stimulation of RAW 264.7 cells.

Heat-killed *E. coli* contains more than one PAMP (Alexander and Rietschel, 2001; Coorens et al., 2017; Tükel et al., 2010) and may activate multiple TLRs. I see a significant reduction in heat-killed *E. coli*-stimulated NO response with the highest concentration of Cu-CPT22 as compared to the lowest concentration; however, despite significance, each Cu-CPT22 dose results in a higher nitrite concentration with heat-killed *E. coli* stimulation than stimulation with Pam$_3$CSK$_4$, zymosan, or OSPW. This may reflect the multiple PAMPs of heat-killed *E. coli* (Alexander and Rietschel, 2001; Coorens et al., 2017; Tükel et al., 2010) as activation of more than one TLR may increase NO response and would reflect a higher nitrite concentration at each inhibitor dose, as seen here.

Interestingly, 6.25% v/v OSPW stimulation of RAW 264.7 cells showed a dose-dependent decrease in NO response with increase in Cu-CPT22 concentration and Cu-CPT22 significantly inhibits NO production stimulated by OSPW. As Cu-CPT22 inhibits TLR1/2 (Cheng et al., 2012; Durai et al., 2017) and increased *tlr2* mRNA expression is associated with OSPW exposure (Paul et al., 2023), this suggests TLR2 may be activated by OSPW exposure and may have a role in OSPW-mediated cell signaling. In addition, OSPW-stimulated NO response is significantly and dramatically impacted by Cu-CPT22 inhibition which implies TLR2 may be involved in OSPW-mediated activation of RAW 264.7 cells.

Both TLR2 and TLR4 are implicated in OSPW activation of macrophage cells. This may be indicative of OSPW containing more than one agonist. Rachmawati et al. (2013) reports nickel ions and cobalt to have the capacity to activate cells and OSPW has been known to contain low concentrations of these metals (Phillips et al., 2020). Alternatively, another possibility is that one agonist may be activating more than one receptor as Francisco et al. (2022) reports that a TLR2/TLR4/MD-2 heterodimer forms and detects atypical LPS. As both TLR2 and TLR4 are implicated in OSPW bioactivity, this presents as an explanation of how one agonist may activate both TLRs.

One potential concern is possible off-target effects of TAK242 and Cu-CPT22 and the possibility of inhibiting stimulation by other TLR agonists. However, this concern is resolved as Kawamoto et al. (2008) demonstrates that NO response stimulated by Pam_3CSK_4 as well as TLR2/6, TLR3, TLR7, and TLR9 agonists is not significantly impacted by TAK242 inhibition. Durai et al. (2017) also showed that Cu-CPT22 does not significantly impact TNF-α secretion stimulated by LPS or a TLR3 agonist. This indicates that there is no overlap in inhibition of TLR4 and TLR2 agonists.

5.3.3 Comparison of TLR4-activated signaling to OSPW-mediated signaling

Pharmacological inhibitors were used to compare TLR4-activated signaling, stimulated by LPS (Kawamoto et al., 2008; Liu et al., 2014), to OSPW-stimulated signaling by assessing NO response. Aminoguanidine inhibits iNOS, which is involved in NO production (Salinas-Carmona et al., 2020) and acts as a pharmacological control. Aminoguanidine significantly inhibits NO production with LPS and OSPW stimulation which shows that NO production can be reduced by inhibiting iNOS.

The cell signaling proteins targeted here are implicated in LPS stimulation as well as OSPW stimulation as indicated by NO production; however, there are differences in the magnitude of NO response. Go 6976 significantly inhibits NO production from OSPW stimulation but not LPS stimulation, which reflects possible differences in cell signaling and activation of PKCα/βI. In addition, OSPW stimulation is dramatically impacted by Cardamonin, whereas LPS stimulation appears to be less impacted. Pharmacological inhibitors were serially diluted to assess dose-response effects with OSPW stimulation as compared to LPS stimulation. Increasing doses of all pharmacological inhibitors attenuates NO production from LPS and OSPW stimulation. Taken together, the OSPW-stimulated cell signaling pathway appears to activate the same signaling proteins as the LPS-stimulated signaling pathway, including proteins in the MyD88-dependent pathway such as IRAK1/4 and NF-κB (Ciesielska, Matyjek, and Kwiatkowska, 2021; Liu et al., 2014). Distal and proximal signaling proteins of the TLR4 pathway were targeted to differentiate LPS- and OSPW-mediated signaling, and no major differences were found.

The MyD88-dependent signaling pathway, which includes IRAK1/4 and NF-κB (Ciesielska, Matyjek, and Kwiatkowska, 2021; Liu et al., 2014), may potentially be activated by OSPW exposure as Cardamonin and IRAK1/4 Inhibitor I significantly inhibited OSPW-stimulated NO production. IRAK1/4 directly interacts with MyD88 (Ciesielska, Matyjek, and Kwiatkowska, 2021; Liu et al., 2014; Wang et al., 2009) and as IRAK4 is thought to be necessary for TIR domain signaling (Wang et al., 2009), this data suggests that OSPW may activate MyD88-dependent signaling. In addition, as the MyD88-dependent signaling pathway leads to the activation of NF-κB (Ciesielska, Matyjek, and Kwiatkowska, 2021; Liu et al., 2014), this also suggests OSPW may activate the MyD88-dependent signaling pathway. This is further

supported by earlier data seen in Chapter 4 as OSPW stimulation results in increased expression of pro-inflammatory genes *mip-2* and *mcp-1* that are upregulated by NF-κB activation (Liu et al., 2014; Qin et al., 2017; Singh, Anshita, and Ravichandiran, 2021). Thus, the decrease in OSPW-induced NO response by Cardamonin and IRAK1/4 Inhibitor I suggest OSPW stimulation activates the MyD88-dependent signaling pathway.

Go 6976 inhibits PKCα/βI (Qatsha et al., 1993; Wu et al., 2003) and as Go 6976 significantly reduces NO production from OSPW stimulation, it is likely specific PKC isoforms are involved in the OSPW-stimulated cell signaling pathway. PKCα has previously been implicated in TLR2, TLR3, and TLR4 signaling (Loegering and Lennartz, 2011; Zhou et al., 2015) and as OSPW-induced NO production significantly decreased with Go 6976, this signaling protein may be activated by OSPW stimulation. However, NO production is not significantly inhibited with LPS stimulation at the same concentration of Go 6976 which may indicate differences in cell signaling or signaling protein activation.

OSPW-stimulated NO production undergoes a dose-response decrease with increased U0126 concentration, which suggests MEK1/2 may be activated by OSPW stimulation. Previous results have noted that U0126 increases iNOS expression (Jin, Liu, and Nelin, 2015) and NO production (Koide et al., 2005) after LPS stimulation in RAW 264.7 cells. This contradicts the results seen here and as both studies used concentrations comparable to our work, this may be explained by differences in LPS concentration as Koide et al. (2005) uses 1 µg/mL LPS and Jin, Liu, and Nelin (2015) use 0.1 µg/mL LPS whereas I used 12.5 ng/mL LPS. The lower concentration of LPS used here may reflect the decrease in NO concentration with U0126.

When using pharmacological inhibitors, off-target effects need to be considered; for example, Go 6976 has been implicated in inhibiting the JAK/STAT pathway as Grandage et al.

(2006) reports Go 6976 to inhibit JAK2. As well, kinase inhibitors often result in off-target effects as kinases have comparable structures (Bello and Gujral, 2018) and so there may be off-target effects with IRAK1/4 Inhibitor I. However, these pharmacological inhibitors have been used in previous literature at similar concentrations (Table 3.3), except for IRAK1/4 Inhibitor I in which case a serial dilution reflects attenuation of NO response (Appendix Figure 1), and both low and high concentrations were used here to reflect attenuation of NO production. This allows us to assess pharmacological impact at more than one concentration and based on previous work (Table 3.3), instills confidence in these results. The conclusions made in this thesis are under the assumption off-target effects are minimal and cell viability is maintained.

5.3.4 Differential patterns of NO production with heat-killed E. coli, LPS, and OSPW

Differences in heat-killed *E. coli*-, LPS-, and OSPW-mediated NO production with inhibition of TLR4 or IRAK1/4 indicates that bioactive effects from OSPW are exerted majorly through TLR4 activation, and that OSPW-mediated cell signaling may differ from LPS-mediated cell signaling. This work also suggests that OSPW may activate signaling pathways outside of the MyD88-dependent signaling pathway.

TAK242 is used to investigate if receptors outside of TLR4 are inducing cell response. Heat-killed *E. coli* stimulation of TAK242-treated RAW 264.7 cells induce high levels of NO production at each concentration whereas LPS and OSPW stimulation induces a distinct dose-response effect. This is further reflected by the lower percent inhibition with heat-killed *E. coli* stimulation as compared to LPS and OSPW stimulation. As heat-killed *E. coli* contains more than one PAMP (Alexander and Rietschel, 2001; Coorens et al., 2017; Tükel et al., 2010), more than one cell receptor and cell signaling pathway may be activated and may explain the absence

of a pattern of inhibition. LPS is one PAMP that is specific for TLR4 (Kawamoto et al., 2008; Liu et al., 2014; Matsunaga et al., 2011; Takashima et al., 2009) and by serial diluting TAK242, we can see a distinct dose-response effect as TLR4 inhibition shows less NO production as concentration increases. 6.25% v/v OSPW stimulation of TAK242-inhibited cells revealed a similar pattern of inhibition to LPS-stimulated cells which suggests detection of OSPW is largely dependent on TLR4.

As IRAK4 is deemed critical for TLR signaling via MyD88 (Wang et al., 2009), IRAK1/4 Inhibitor I is used to investigate if the MyD88-dependent pathway is activated or if other signaling pathways may be inducing cell response, as NF-κB activation can result from TNF-α-activated or Ang II-activated signaling (Brasier, 2010). With IRAK1/4 Inhibitor I, a defined dose-response effect is seen with heat-killed *E. coli* stimulation. This demonstrates that IRAK1/4 may be critical in signaling stimulated by heat-killed *E. coli*, resulting in a robust, decreasing response with increasing inhibitor concentration. *E. coli* contains more than one bacterial component known to activate TLR signaling, such as lipoproteins and LPS (Alexander and Rietschel, 2001; Coorens et al., 2017; Tükel et al., 2010), and this may explain the higher NO response at each IRAK1/4 Inhibitor I concentration than seen with LPS stimulation. LPS stimulation shows low response at each IRAK1/4 Inhibitor I concentration which demonstrates the integral role of IRAK1/4 in LPS-stimulated signaling. The NO response profile of serially diluted TAK242 mirrors IRAK1/4 Inhibitor I with LPS stimulation as TLR4 is activated by LPS (Kawamoto et al., 2008; Liu et al., 2014) and both inhibited proteins are in relatively close proximity in the cell signaling pathway as IRAK1/4 is recruited to the submembrane TIRAP/MyD88 complex formed through TLR4 activation (Ciesielska, Matyjek, and Kwiatkowska, 2021; Liu et al., 2014; Wang et al., 2009). 6.25% v/v OSPW-stimulated NO

production is not as low as with LPS stimulation and is more comparable to heat-killed *E. coli* stimulation. As IRAK4 inhibition is thought to block TLR-activated MyD88-dependent signaling (Wang et al., 2009), this suggests OSPW is likely activating other cell signaling pathways which induces NO production. However, as indicated by the high percent inhibition, IRAK1/4 Inhibitor I is very effective in blocking activation with stimulation by all three stimuli and reflects the importance of IRAK1/4 in the associated signaling pathways.   Integrating this with data from the TAK242 serial dilution, the bioactive constituent of OSPW may mainly exert effects through TLR4 but may also activate signaling pathways outside of the MyD88-dependent signaling pathway. Alternatively, different structures of agonists can interact with and activate TLR4 (Peri & Calabrese, 2014), and it is possible that the bioactive constituent of OSPW could also differentially activate TLR4 as compared to activation by LPS and result in altered NO production. Regardless, stimulation by OSPW appears to mainly occur through TLR4 signaling and this work shows OSPW signaling differs from LPS-stimulated TLR4 signaling.

Environmental bacterial products may be found in OSPW and though OSPW is filtered, microbial products may not be removed (Choo-Yin, 2021). For example, if environmental LPS remained in filtered OSPW, the pro-inflammatory effects may be attributed to the presence of LPS. However, here I show that OSPW stimulation results in a different pattern of response as compared to LPS stimulation of mouse macrophage cells using IRAK1/4 Inhibitor I. This supports that OSPW bioactivity is not completely perpetuated by environmental LPS.

It should be noted that we are comparing 12.5 ng/mL of LPS and OD_{600} of 0.6 heat-killed *E. coli* to OSPW with an unknown concentration of agonists. The 6.25% v/v concentration was determined by serial diluting OSPW and identifying the concentration resulting in high bioactivity (data not provided). OSPW contaminants are diluted in nature as OSPW contains

water, and so comparing the concentration resulting in the high bioactivity allows us to best compare to concentrated cell stimuli. It should also be noted that differences in patterns of NO production between different stimuli with various concentrations of TAK242 and IRAK1/4 Inhibitor I were first discovered when determining ideal inhibitor concentrations through serial dilutions. Thus, data from Figure 5.11b and 5.12b are derived from Appendix Figure 1.

5.4 Future Directions

TLR4 can recognize many ligands with different chemical structures (Ciesielska, Matyjek, and Kwiatkowska, 2021; Liu et al., 2014; Peri & Calabrese, 2014; Rachmawati et al., 2013) and may be activated by OSPW as indicated by the above data. As signaling proteins may be involved in multiple cell signaling pathways, for example IRAK4 is known to be involved in interleukin-1 receptor (IL-1R) signaling as well as TLR signaling (Wang et al., 2009), exploring the activation of other receptors by OSPW may provide further understanding of OSPW-mediated macrophage activation. TLR1/2 also activates the MyD88-dependent signaling pathway (Kawai and Akira, 2010; Liu et al., 2014), and signaling proteins in this pathway are involved in the OSPW-stimulated signaling pathway as seen here so it presents as a feasible option for further exploration. In addition, receptors outside of the TLR family such as TNFR1, which binds TNF-α and can also activate NF-κB to induce pro-inflammatory effects (Brasier, 2010), may be potential receptors to explore in relation to OSPW-mediated bioactivity.

However, if more than one receptor is activated, then various agonists may be present in OSPW and should be explored. Currently, NAs are recognized as a prominent toxic OSPW constituent (Allen, 2008; Li et al., 2017), and treatments that decrease NA concentration result in decreased bioactivity (Arslan et al., 2023; Paul et al., 2023) which supports this. Certain metals

have been implicated in TLR4 activation (Schmidt et al., 2010; Rachmawati et al., 2013) and

OSPW is known to contain a variety of elements (Phillips et al., 2020), so the investigation of

inorganics in relation to bioactivity is also helpful to further understand the effects of OSPW.
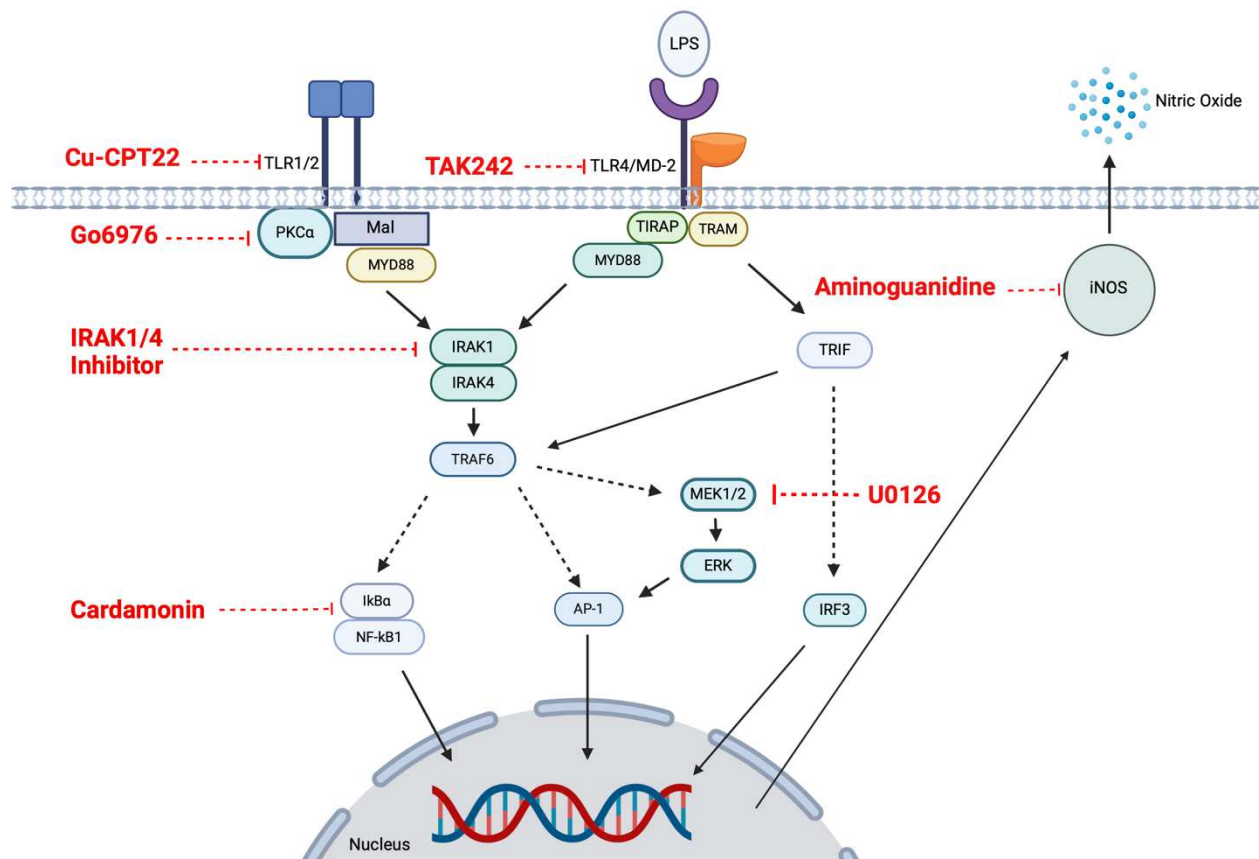
Figure 5.1. Model of TLR cell signaling pathways and associated signaling protein inhibitors. Black arrows are direct interactions, dotted arrows indicate indirect interactions, and red dotted lines reflect inhibition. Figure based on Bauerfeld and Samavati (2017), Ciesielska, Matyjek, and Kwiatkowska (2021), Duncia et al. (1998), Jones et al. (2007), Lester and Li (2014), Liu et al. (2014), Loegering and Lennartz (2011), Matsunaga et al. (2011), TOCRIS (n.d.), and Wang et al. (2009). Created with Biorender.com.

a)
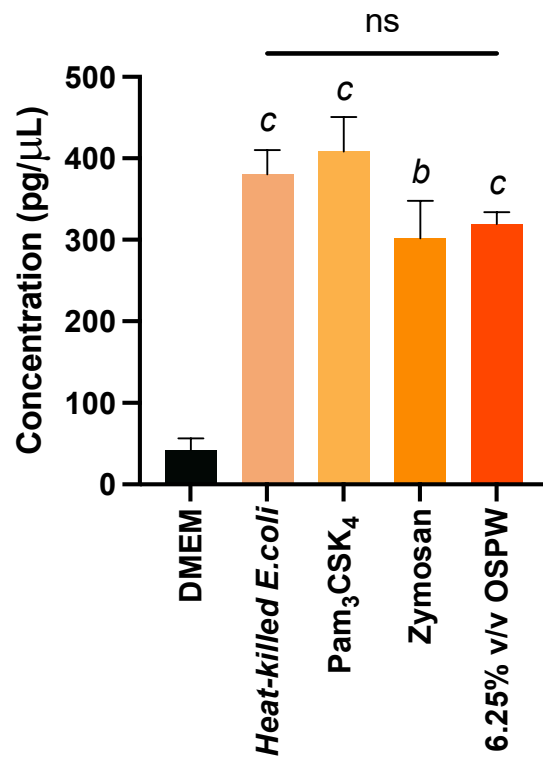
b)
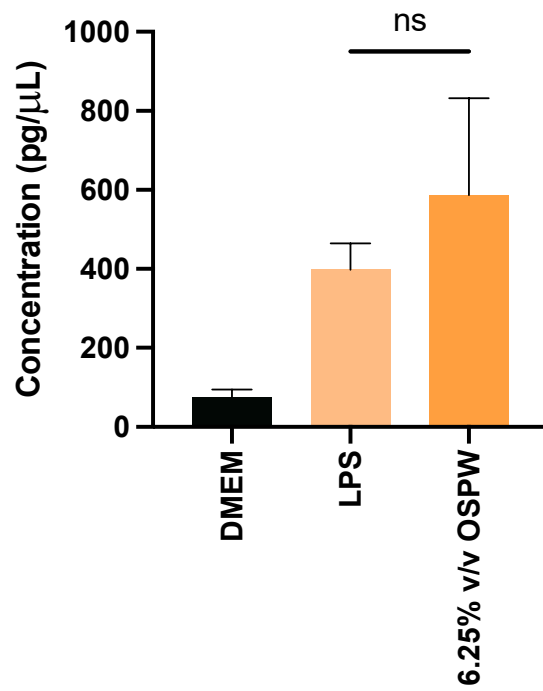
Figure 5.2. TNF-α secretion stimulated by TLR ligands. RAW 264.7 cells (300 000

cells/well) were exposed to heat-killed *E. coli* (a; n=3), Pam$_3$CSK$_4$ (a; n=3), zymosan (a; n=3),

LPS (b; n=3), and 6.25% v/v OSPW for 24 hours (ab;n=3). Significance was determined by one-

way ANOVA and Tukey's multiple comparisons test, and is depicted as * (p-value<0.05), ** (p-

value<0.01), or *** (p-value<0.001) while *a* (p<0.05), *b* (p-value<0.01), and *c* (p-value<0.001)

denotes significance compared to DMEM.

a)
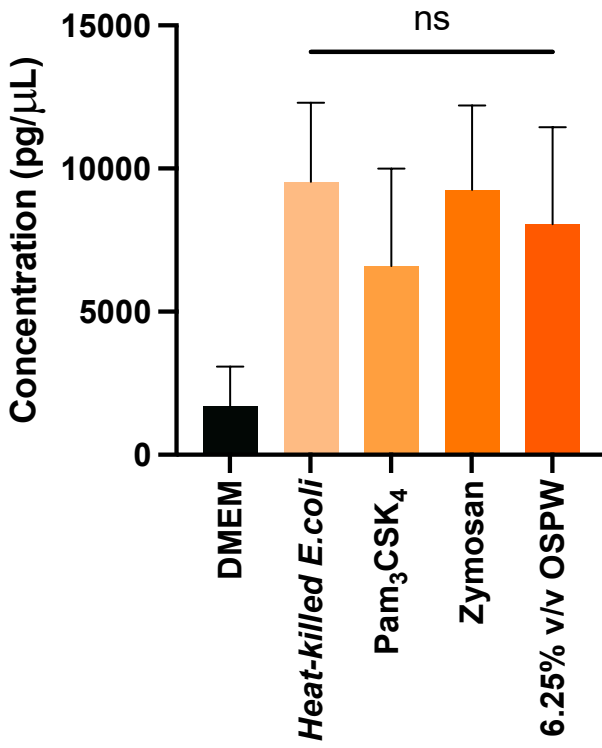
b)
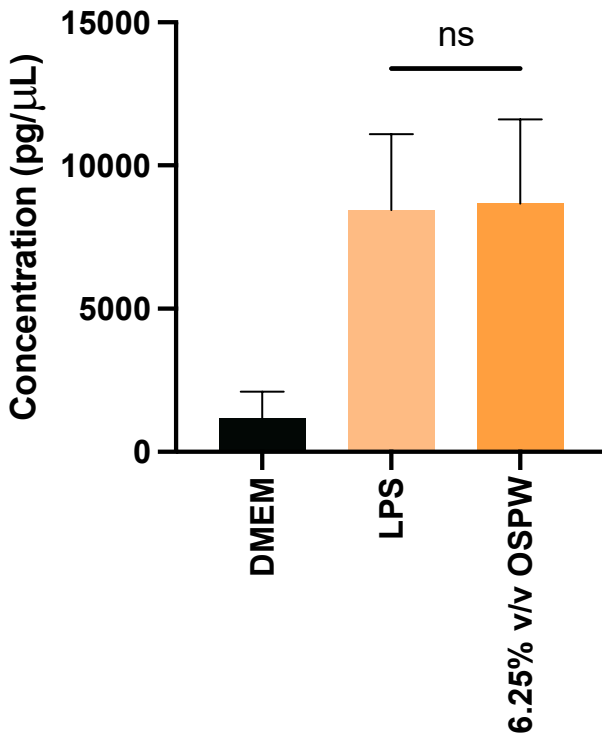
Figure 5.3. MCP-1 secretion stimulated by TLR ligands. RAW 264.7 cells (300 000 cells/well) were exposed to heat-killed *E. coli* (a; n=3), Pam$_3$CSK$_4$ (a; n=3), zymosan (a; n=3), LPS (b; n=3), and 6.25% v/v OSPW (ab; n=3) for 24 hours. Significance was determined by one-way ANOVA and Tukey's multiple comparisons test, and is depicted as * (p-value<0.05), ** (p-value<0.01), or *** (p-value<0.001) while *a* (p<0.05), *b* (p-value<0.01), and *c* (p-value<0.001) denotes significance compared to DMEM.
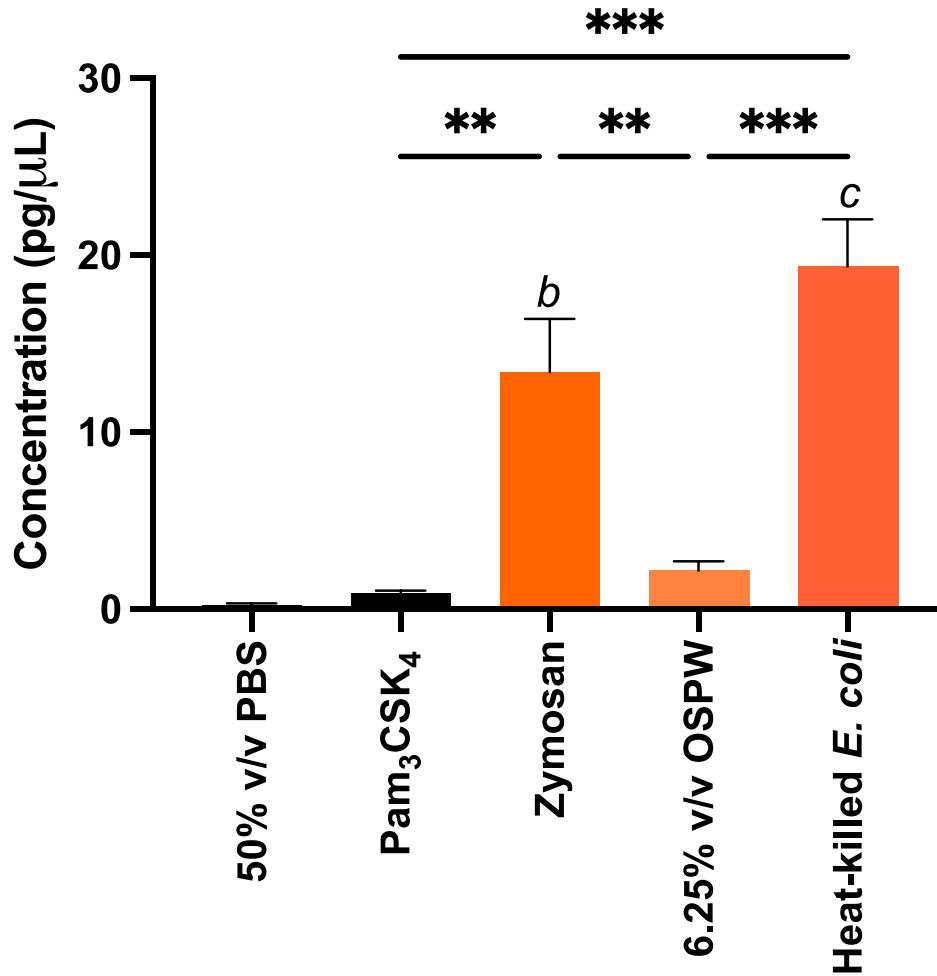
Figure 5.4. IL-2 secretion stimulated by TLR ligands. RAW 264.7 cells (300 000 cells/well) were exposed to Pam_3CSK_4, zymosan, heat-killed *E. coli*, LPS, and 6.25% v/v OSPW for 24 hours (n=3). Significance was determined by one-way ANOVA and Tukey's multiple comparisons test, and is depicted as * (p-value<0.05), ** (p-value<0.01), or *** (p-value<0.001) while *a* (p<0.05), *b* (p-value<0.01), and *c* (p-value<0.001) denotes significance compared to DMEM.

a)
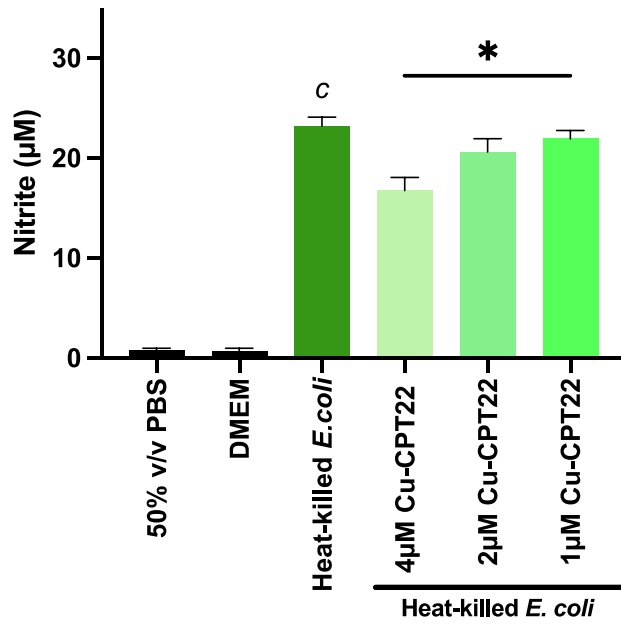
b)
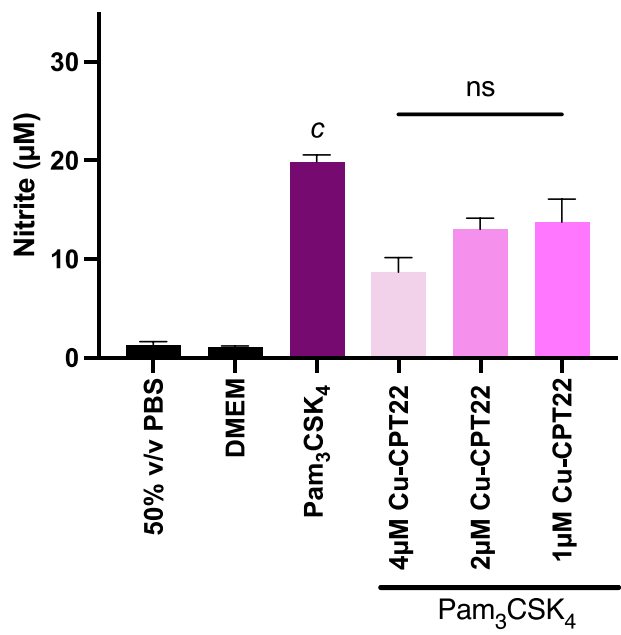
c)
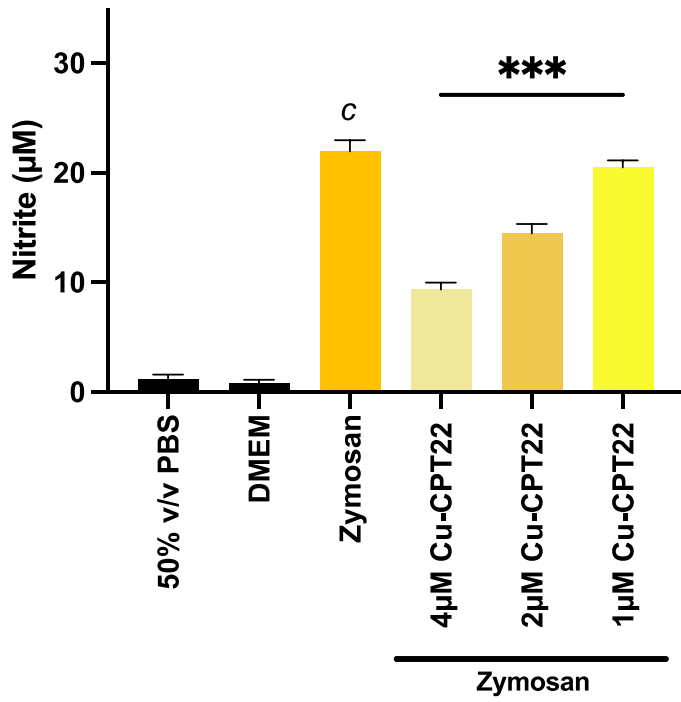
d)
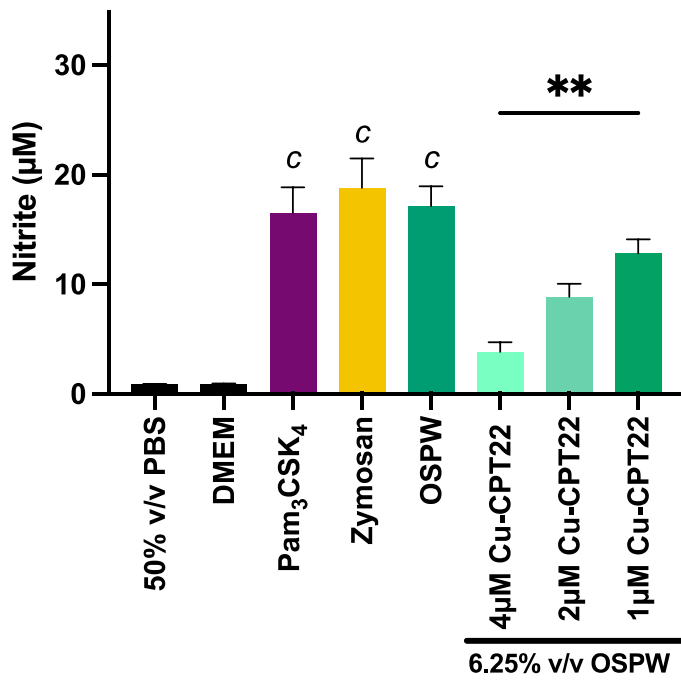
e)
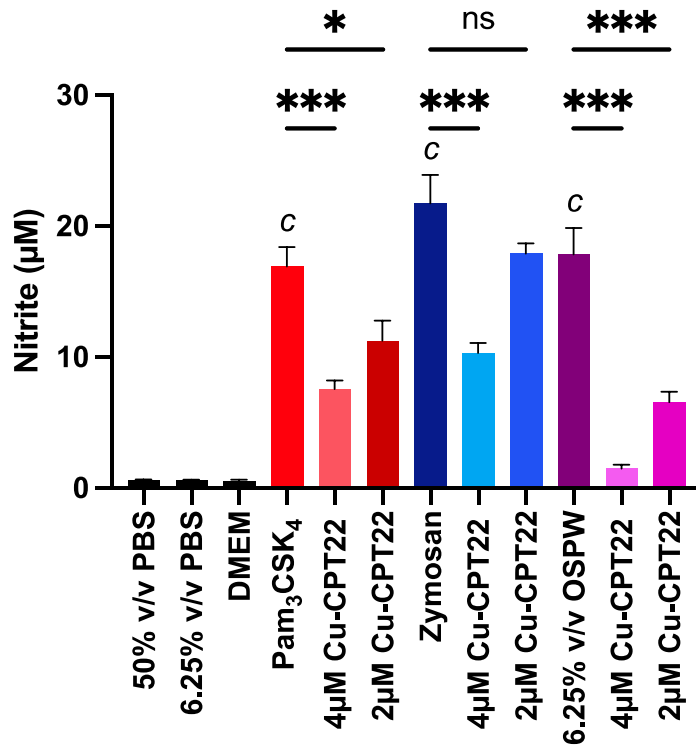
f)
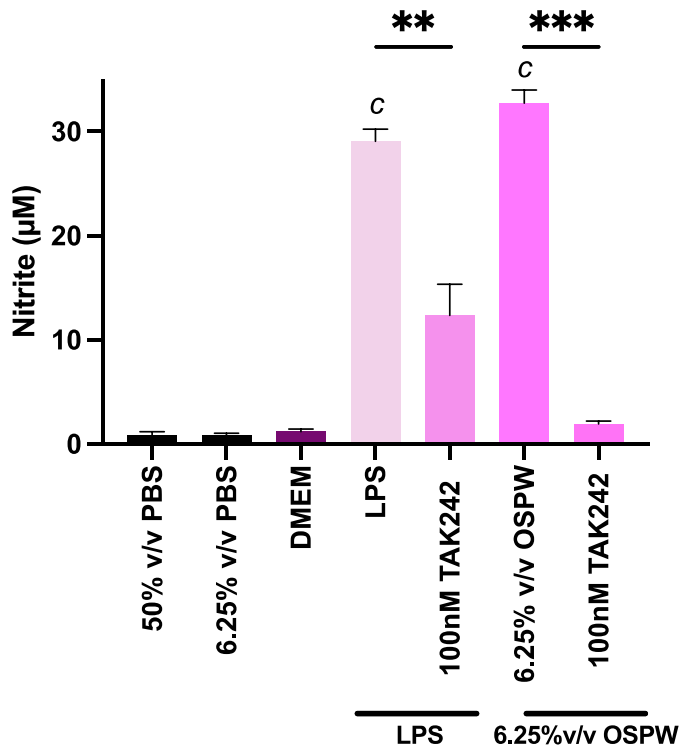
Figure 5.5. TLR1/2 inhibition of nitrite concentration with stimulation by heat-killed *E. coli*, LPS, or 6.25% v/v OSPW. RAW 264.7 cells (25 000 cells/well) were pre-treated with Cu-CPT22 or TAK242 for 2 hours and stimulated with heat-killed *E. coli* (a; n=3), Pam_3CSK_4 (b; n=3), zymosan (c; n=3), or 6.25% v/v OSPW (def; n=3) for 22 hours. Significance was determined by one-way ANOVA and Tukey's multiple comparisons test and is depicted as * (p-value<0.05), ** (p-value<0.01), or *** (p-value<0.001) while *a* (p<0.05), *b* (p-value<0.01), and *c* (p-value<0.001) denotes significance compared to DMEM.

a)
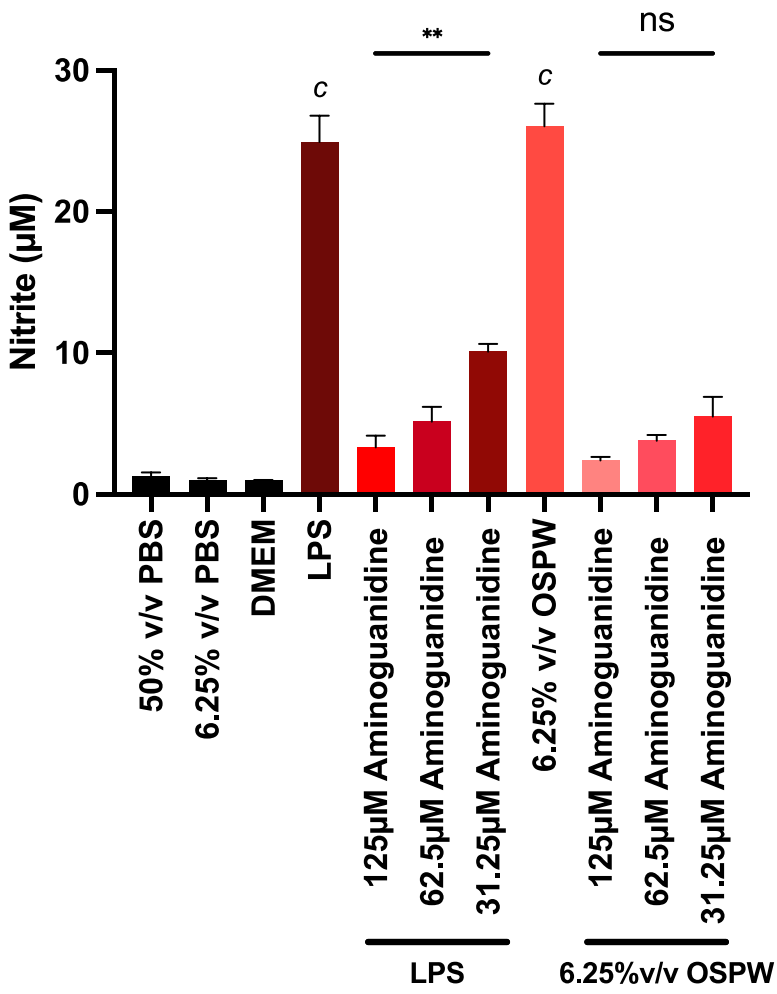
b)
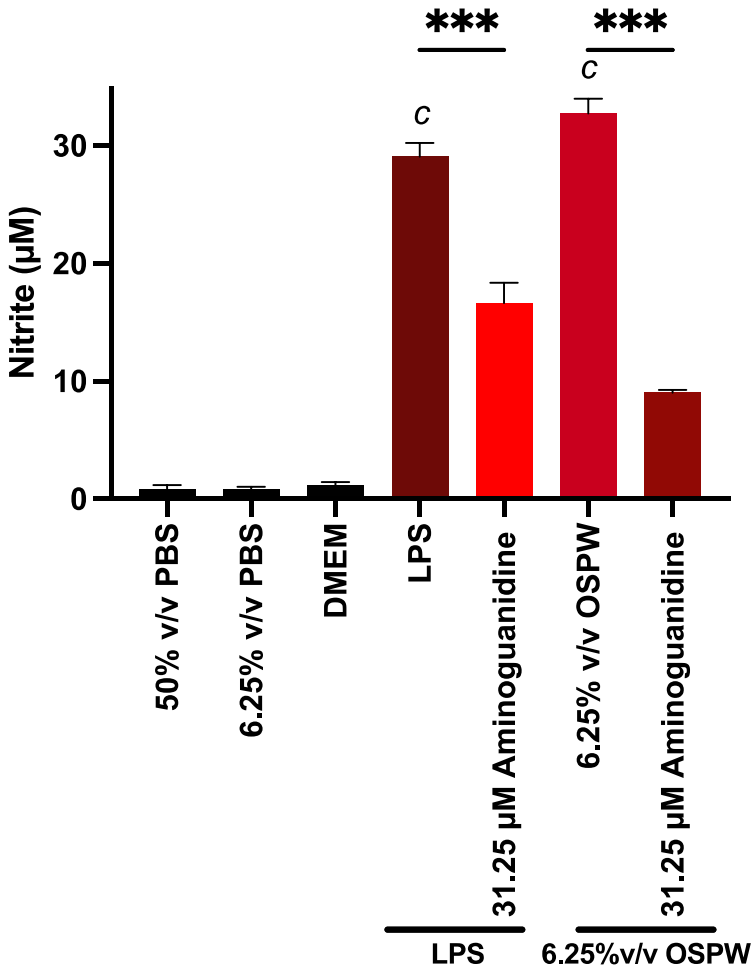
Figure 5.6. Aminoguanidine attenuates nitric oxide response. RAW 264.7 cells (100 000 cells/well) were pretreated with Aminoguanidine (ab; n=3) for 2 hours before stimulation with LPS (12.5 ng/mL) or 6.25% v/v OSPW for 22 hours. Significance was determined by one-way ANOVA and Tukey's multiple comparisons test. Bars display the average, error bars reflect SEM, * (p-value<0.05) or ** (p-value<0.01) or *** (p-value<0.001) depicts significance while *a* (p<0.05), *b* (p-value<0.01), and *c* (p-value<0.001) denotes significance compared to DMEM.

a)
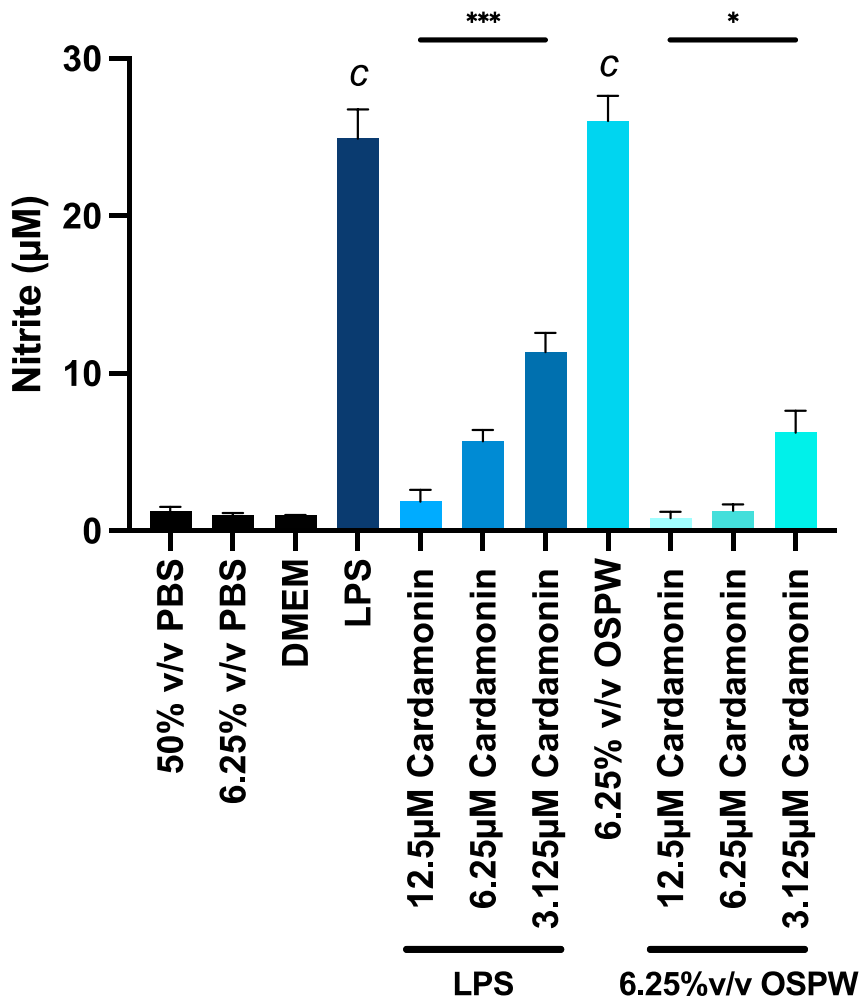
b)
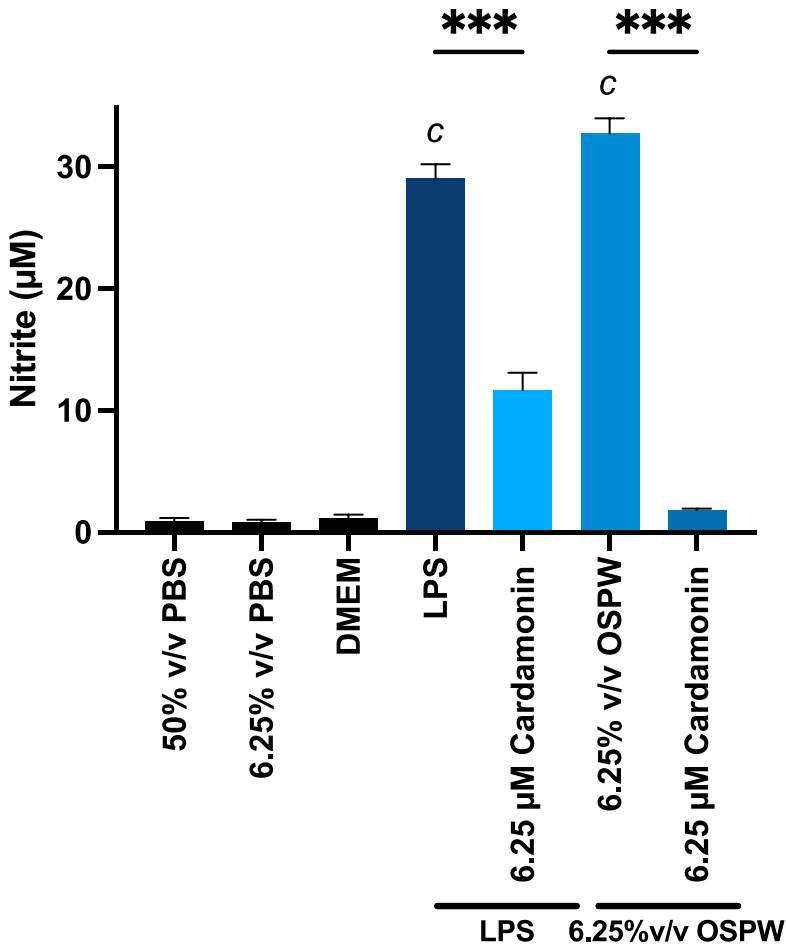
Figure 5.7. Cardamonin attenuates nitric oxide response. RAW 264.7 cells (100 000 cells/well) were pretreated with Cardamonin (ab; n=3) for 2 hours before stimulation with LPS (12.5 ng/mL) or 6.25% v/v OSPW for 22 hours. Significance was determined by one-way ANOVA and Tukey's multiple comparisons test. Bars display the average, error bars reflect SEM, * (p-value<0.05) or ** (p-value<0.01) or *** (p-value<0.001) depicts significance while *a* (p<0.05), *b* (p-value<0.01), and *c* (p-value<0.001) denotes significance compared to DMEM.

a)
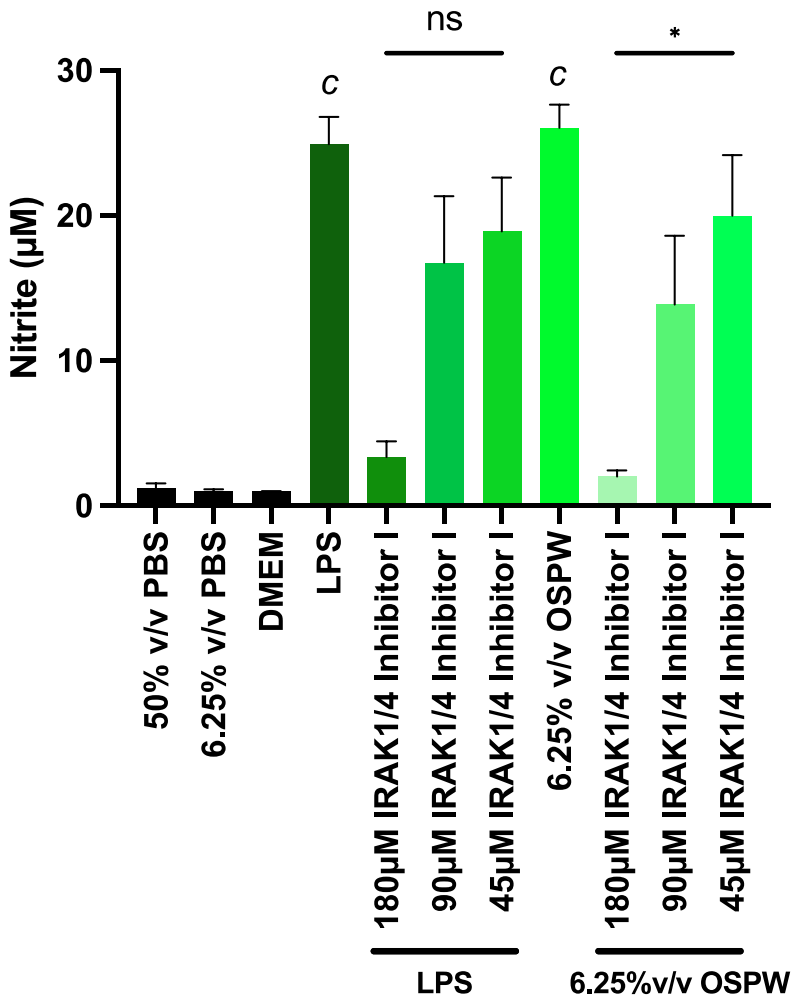
b)
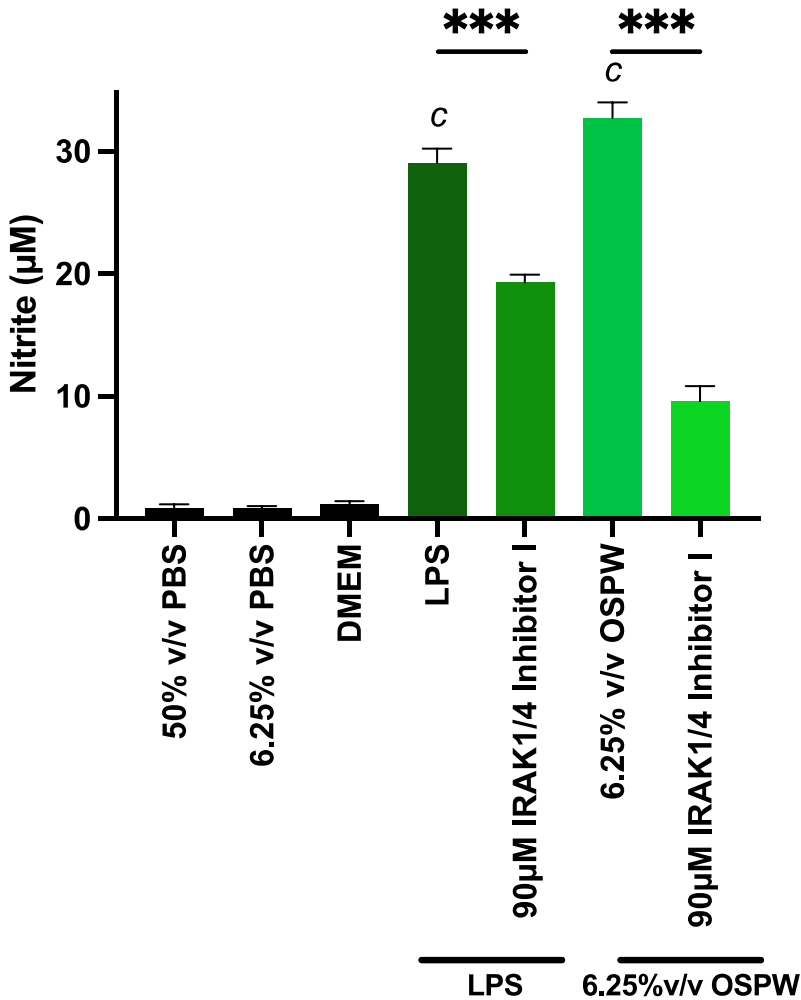
Figure 5.8. IRAK1/4 Inhibitor I attenuates nitric oxide response. RAW 264.7 cells (100 000 cells/well) were pretreated with IRAK1/4 Inhibitor I (ab; n=3) for 2 hours before stimulation with LPS (12.5 ng/mL) or 6.25% v/v OSPW for 22 hours. Significance was determined by one-way ANOVA and Tukey's multiple comparisons test. Bars display the average, error bars reflect SEM, * (p-value<0.05) or ** (p-value<0.01) or *** (p-value<0.001) depicts significance while *a* (p<0.05), *b* (p-value<0.01), and *c* (p-value<0.001) denotes significance compared to DMEM.
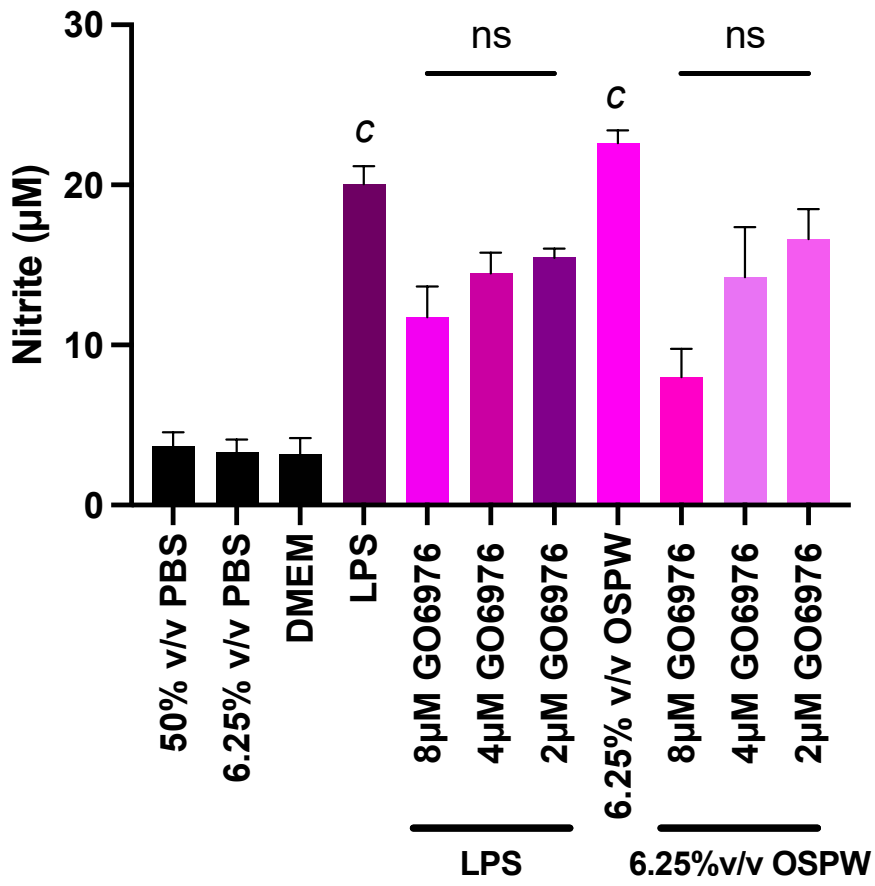
b)
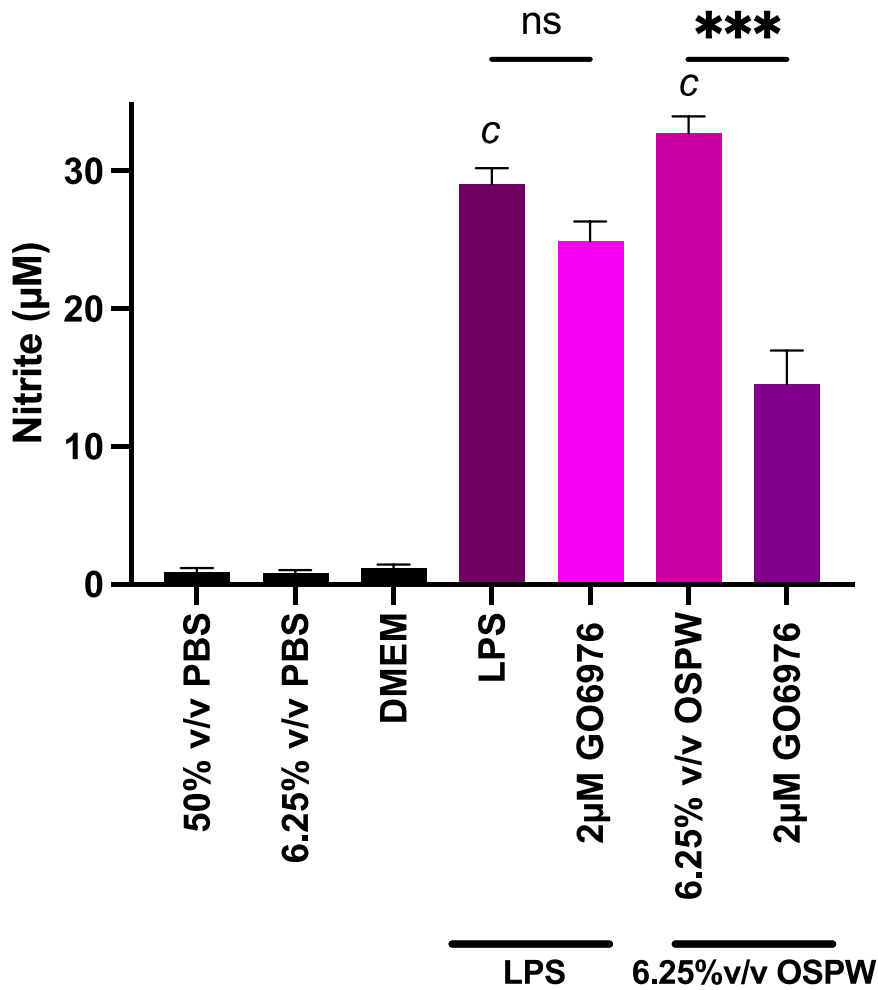
Figure 5.9. Go 6976 attenuates nitric oxide response. RAW 264.7 cells (100 000 cells/well) were pretreated with Go 6976 (ab; n=3) for 2 hours before stimulation with LPS (12.5 ng/mL) or 6.25% v/v OSPW for 22 hours. Significance was determined by one-way ANOVA and Tukey's multiple comparisons test. Bars display the average, error bars reflect SEM, * (p-value<0.05) or ** (p-value<0.01) or *** (p-value<0.001) depicts significance while *a* (p<0.05), *b* (p-value<0.01), and *c* (p-value<0.001) denotes significance compared to DMEM.

a)
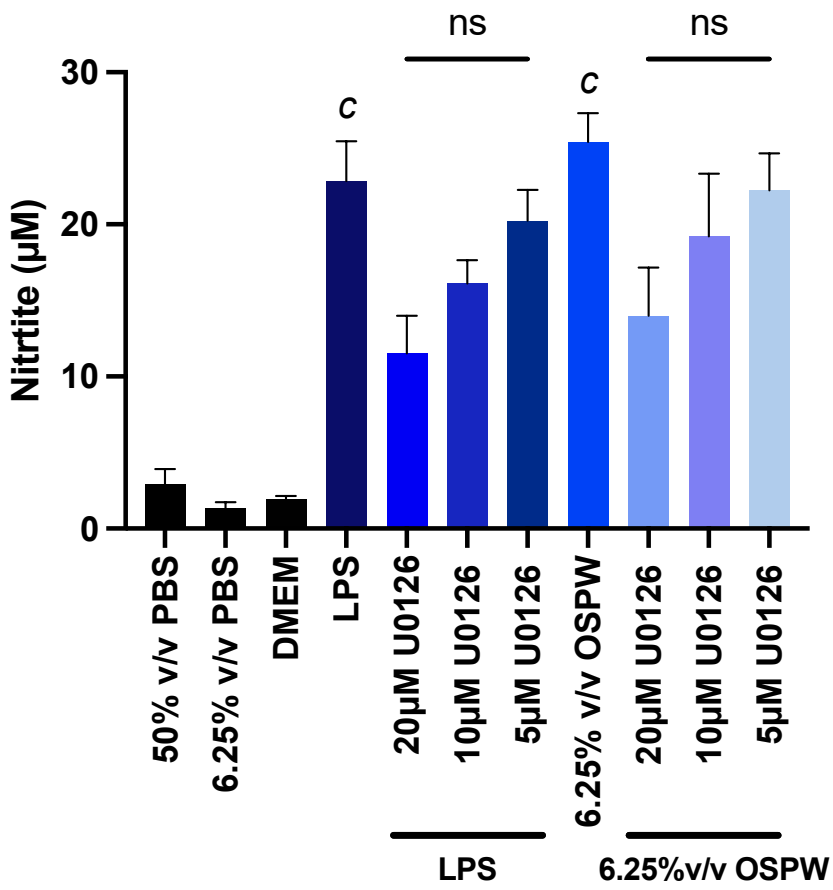
b)
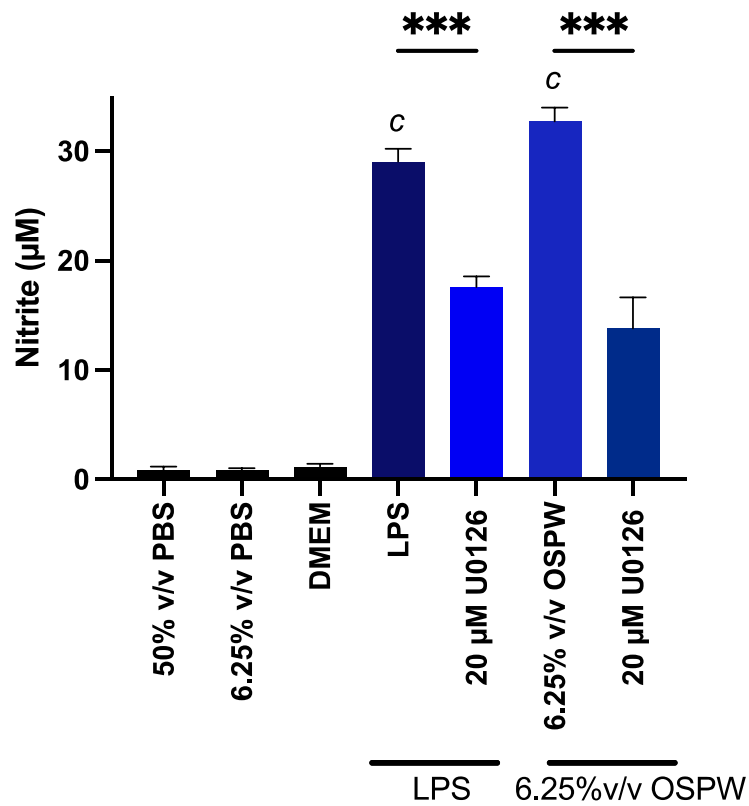
Figure 5.10. U0126 attenuates nitric oxide response. RAW 264.7 cells (100 000 cells/well) were pretreated with U0126 (ab; n=3) for 2 hours before stimulation with LPS (12.5 ng/mL) or 6.25% v/v OSPW for 22 hours. Significance was determined by one-way ANOVA and Tukey's multiple comparisons test. Bars display the average, error bars reflect SEM, * (p-value<0.05) or ** (p-value<0.01) or *** (p-value<0.001) depicts significance while *a* (p<0.05), *b* (p-value<0.01), and *c* (p-value<0.001) denotes significance compared to DMEM.

a)
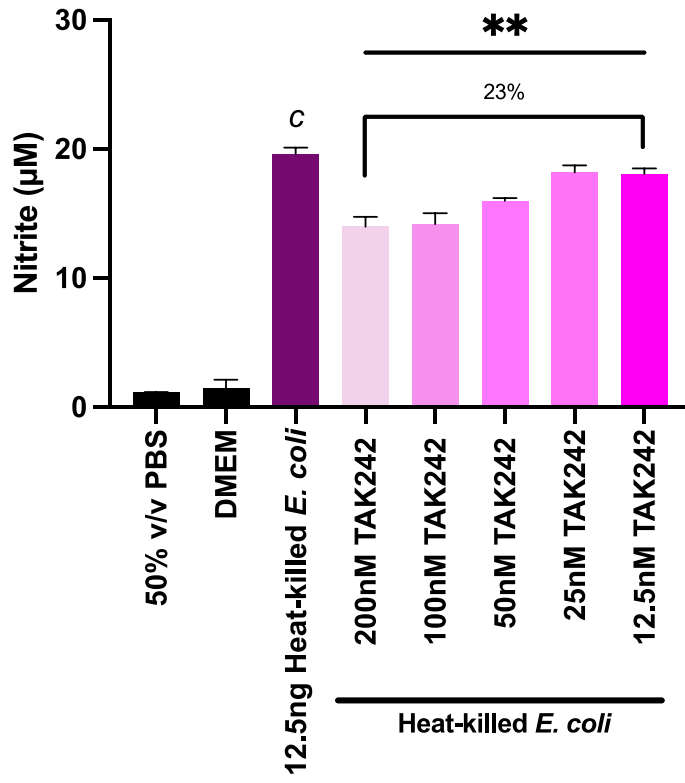
b)
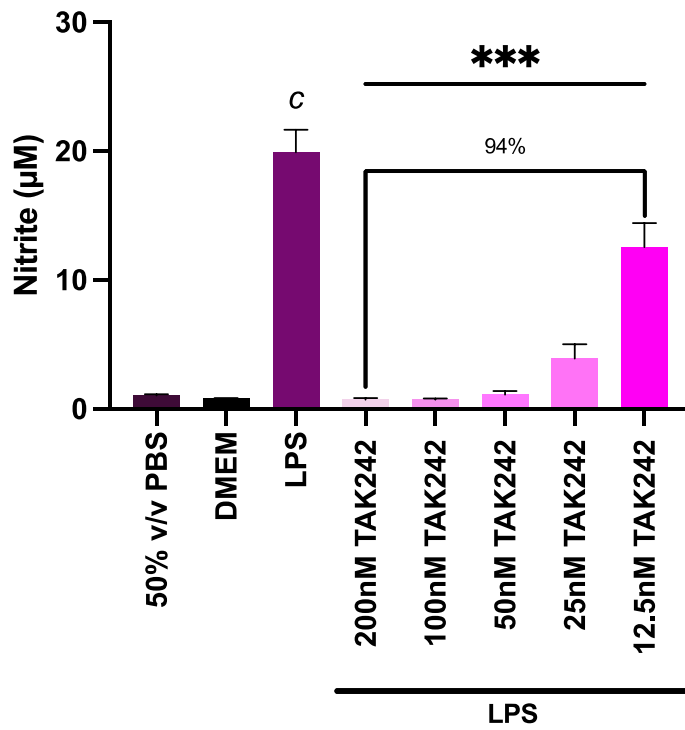
c)
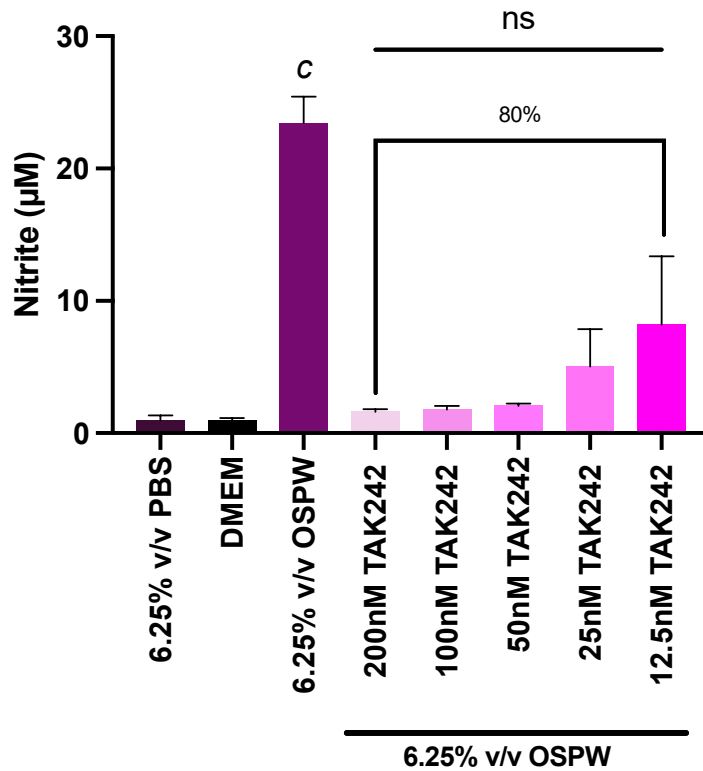
Figure 5.11. TAK242 inhibition of nitric oxide with stimulation by heat-killed *E. coli*, LPS, or 6.25% v/v OSPW. RAW 264.7 cells (100 000 cells/well) were pretreated with TAK242 for 2 hours and stimulated with heat-killed *E. coli* (a; n=3), LPS (b; n=3), and 6.25% v/v OSPW (c; n=3) for 22 hours. Percentage reflects percent inhibition between highest and lowest TAK242 concentrations. Significance was determined by one-way ANOVA and Tukey's multiple comparisons test, and significance is depicted as * (p-value<0.05), ** (p-value<0.01), or *** (p-value<0.001) while *a* (p<0.05), *b* (p-value<0.01), or *c* (p-value<0.001) denotes significance compared to DMEM.

a)

112
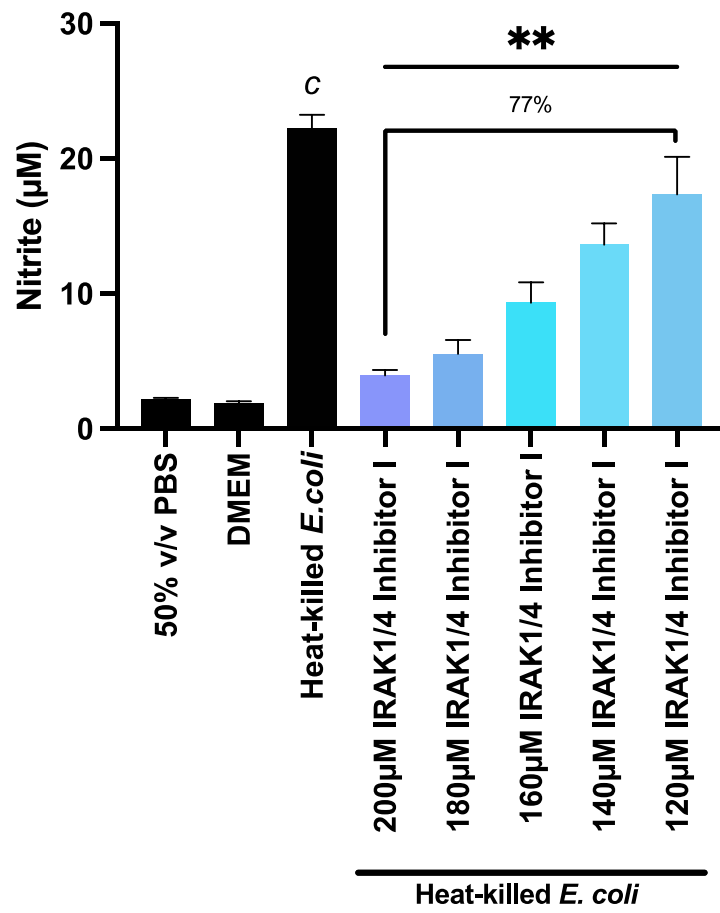
b)
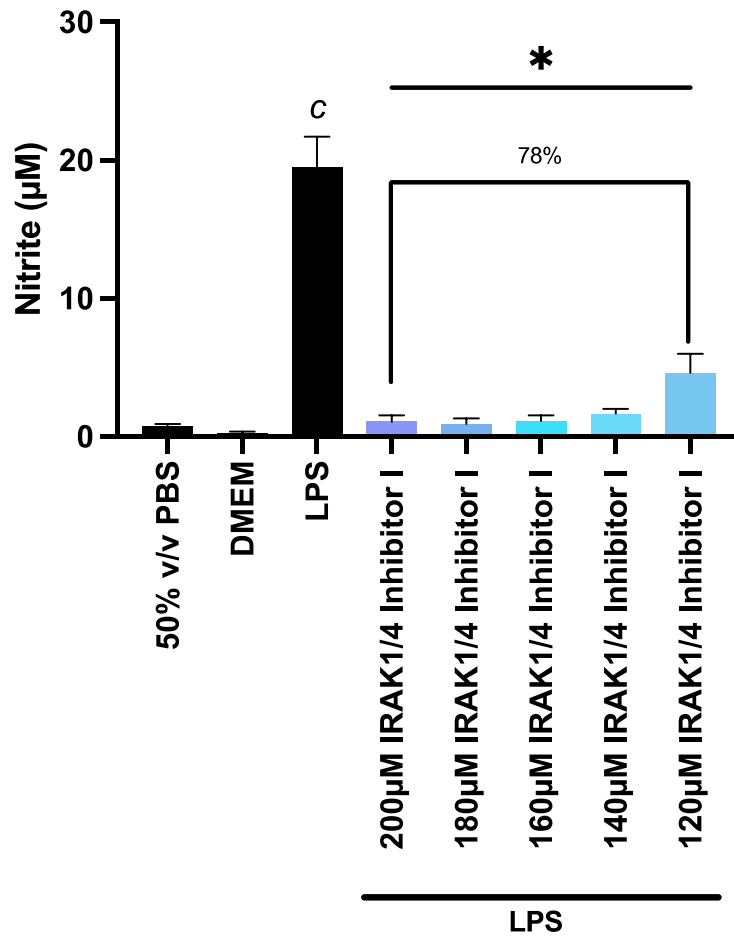
c)
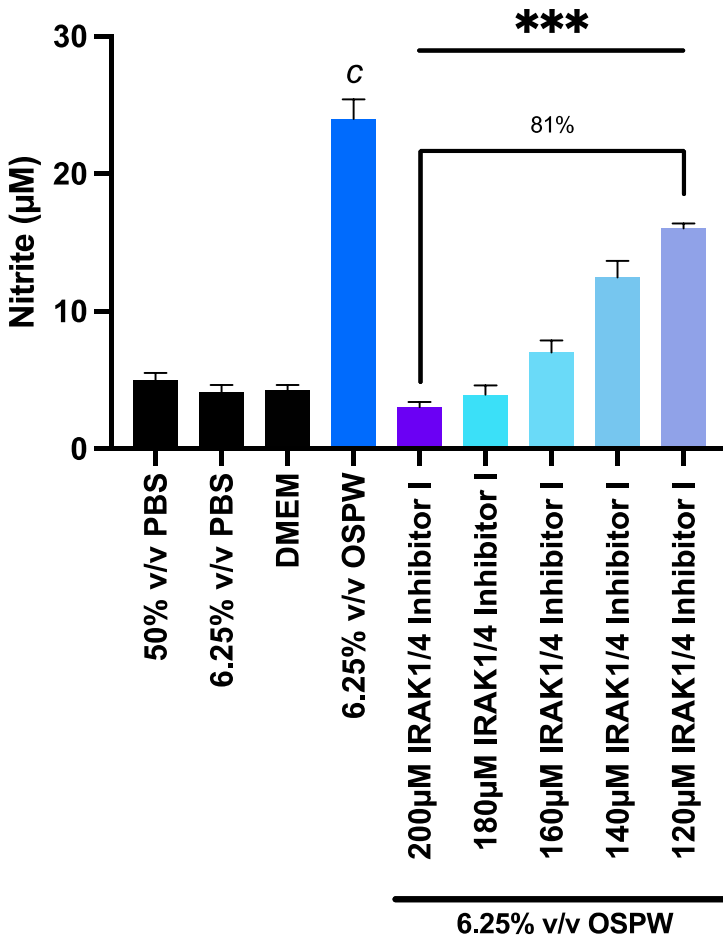
Figure 5.12. IRAK1/4 Inhibitor I inhibition of nitric oxide with stimulation by heat-killed *E. coli*, LPS, or 6.25% v/v OSPW. RAW 264.7 cells (100 000 cells/well) were pre-treated with IRAK1/4 Inhibitor I for 2 hours and stimulated with heat-killed *E. coli* (a; n=3), LPS (b; n=3), and 6.25% v/v OSPW (c; n=3) for 22 hours. Percentage reflects percent inhibition between highest and lowest IRAK1/4 Inhibitor I concentrations. Significance was determined by one-way ANOVA and Tukey's multiple comparisons test and is depicted as * (p-value<0.05), ** (p-value<0.01), or *** (p-value<0.001) while *a* (p<0.05), *b* (p-value<0.01), and *c* (p-value<0.001) denotes significance compared to DMEM.

Chapter VI

General Discussion

6.1 Summary

My thesis research showed differences in cytokine gene expression before and after electrooxidation and solar oxidation treatment of OSPW. Untreated OSPW exposures showed high cytokine gene expression, reflecting bioactivity, and solar and electrooxidation treatment reduced this associated bioactivity. In addition, I showed that the longer OSPW is treated, the lower the bioactivity. This demonstrates that treatments that remove NAs (Abdalrhman and El-Din, 2020; Abdalrhman, Zhang, and El-Din, 2019; Meng et al., 2021) also reduce bioactivity. Overall, this is supportive of NAs acting as the bioactive constituent as these treatments degrade NAs (Abdalrhman and El-Din, 2020; Abdalrhman, Zhang, and El-Din, 2019; Meng et al., 2021).

Using pharmacological inhibitors, I also showed that TLR4 and TLR1/2 are implicated in the detection of OSPW by RAW 264.7 cells. Furthermore, I showed how signaling proteins from the MyD88-dependent signaling pathway, such as NF-κB (Israf et al., 2007; Liu et al., 2014), are associated with the activation of RAW 264.7 cells by OSPW. Lastly, I outlined similarities and differences in NO response stimulated by OSPW, LPS, and heat-killed *E. coli* using pharmacological inhibitors at the receptor and kinase levels of cell signaling.

6.2 NAs as the Bioactive Constituent in OSPW

The RAW 264.7 macrophage cell-based biosensor system has previously shown bioactive or immunotoxic effects in response to OSPW exposures (Arslan et al., 2023; Fu et al., 2017;

Lillico et al., 2023; Phillips et al., 2020), and has been used to assess untreated and treated OSPW samples (Arslan et al., 2023; Lillico et al., 2023). For my thesis research, I used an *in vitro* RAW 264.7 macrophage cell biosensor system to assess untreated OSPW and electro- and solar oxidation-treated OSPW. I further demonstrated the efficacy and reliability of this biosensor tool as I successfully showed differences in bioactivity between untreated and treated OSPW. This research contributes to previous literature demonstrating the sensitivity and reliability of using the RAW 264.7 macrophage cell biosensor system as a successful evaluation method for OSPW treatment strategies (Lillico et al., 2023).

Our macrophage cell-based *in vitro* assay successfully showed a reduction in OSPW bioactivity after solar and electrooxidation treatment. As NAs are recognized as a toxic component of OSPW (Allen, 2008; Li et al., 2017) and NA species decrease over time with solar oxidation treatment (Suara et al., 2022), the decrease in bioactivity seen here further implies the bioactive component that is stimulating cells is AOP-sensitive, which further suggests NAs as the bioactive component of OSPW. As the bioactive component of OSPW can influence immune cell gene expression, it is important to understand how NAs interact with macrophage cells to influence a pro-inflammatory immune response.

6.3 OSPW Immunotoxicity

Previously, bioactivity has been understood as denoting a change from the inactive, basal state of macrophage cells to an active, pro-inflammatory state as indicated by pro-inflammatory biomolecule secretion (Lillico et al., 2023). My research shows the bioactivity of OSPW through changes in cytokine gene expression as well as increases in NO production and cytokine secretion. TNF-α and MCP-1 secretion is not significantly different between OSPW and the TLR agonists

and this indistinguishability shows how OSPW can propagate an immune response similar to immune system agonists. As OSPW is inducing a pro-inflammatory response comparable to pro-inflammatory stimuli, this suggests OSPW may adversely impact immune cells.

Immunotoxicity refers to "the adverse effects of foreign substances (xenobiotics) on the immune system" and Trizio et al. (1988) refers to immunopotentiation as a form of immunotoxicity. At first, the changes in gene expression were recognized more generally as bioactivity; but now, as we see the implication of TLR signaling in OSPW detection and identified changes in NO production and immune protein secretion, immunotoxicity more specifically reflects effects from OSPW exposure. Altogether, the implicated activation of TLRs by OSPW and tangible increases in pro-inflammatory cytokine secretion with OSPW exposure comparable to stimulation by TLR agonists blatantly reflects immunotoxicity. Though the impacts of OSPW on immune cells has previously been considered "bioactive" (Lillico et al., 2023), the data from this study provides evidence that suggests "immunotoxic" to be more accurate, though whole animal studies are necessary to support this.

The effects of OSPW on RAW 264.7 macrophage cells have previously been considered as immunotoxic (Fu et al., 2017; Phillips et al., 2020). OSPW demonstrated immunotoxicity as reflected by decreased cell viability with increasing NA concentration as well as changes in cytokine and stress gene expression (Fu et al., 2017). Inorganic fraction exposure has also shown immunotoxic effects as indicated by changes in cytokine and stress gene expression (Phillips et al., 2020). Immunotoxicity from OSPW exposure has also been recognized in another immune cell type, THP-1, by the increased secretion of pro-inflammatory cytokines (Paul et al., 2023).

My research provides further evidence of immunotoxic effects of OSPW, and as this research supports NAs as a potentiator of bioactivity, this suggests a role for NAs in OSPW-

mediated immunotoxicity. OSPW was recognized to be more immunotoxic at higher concentrations of NAs (Fu et al., 2017) and as we see OSPW-mediated bioactivity decrease with treatments that degrade NAs (Abdalrhman and El-Din, 2020; Abdalrhman, Zhang, and El-Din, 2019; Meng et al., 2021), this suggests that NAs may induce not just bioactive, but specifically immunotoxic effects.

6.4 TLR4 and TLR1/2 Implication in OSPW Detection

TLR1/2 and TLR4 were directly targeted via pharmacological inhibitors and this study shows that both TLRs are implicated in the detection of bioactive constituents of OSPW. RAW 264.7 macrophage cells stimulated with OSPW elicited a similar cytokine response as TLR4 and TLR1/2 agonists, which is consistent with the involvement of these TLRs in OSPW detection. This is also consistent with previous literature that has recognized TLR2 and TLR4 as facilitating inflammatory responses to particulate matter, which, like OSPW, may contain heavy metals, organics, and inorganics, in human umbilical vein endothelial cells (Le et al., 2019). This is also consistent with Paul et al. (2023) showing a significant increase in *tlr2* mRNA expression in THP-1 cells with OSPW exposure.

The overwhelming evidence of NA implication in OSPW immunotoxicity leads to the inevitable questions regarding how NAs or the pro-inflammatory constituent interacts with RAW 264.7 macrophage cells. One possibility includes ligand mimicry as molecules can be designed to consist of the same pattern as TLR4 or TLR2 agonists which successfully activate corresponding TLRs (Feng et al., 2019; Peri & Calabrese, 2014), and so molecules with similar patterns to TLR agonists may be found in OSPW and may result in the activation of TLRs (Choo-Yin, 2021). Another possibility includes differential activation of TLRs as Schmidt et al.

(2010) also demonstrates how TLR4 can be differentially activated based on molecular structure; for example, nickel can activate human TLR4 using specific histidines, but not mouse TLR4. This leads to a possibility that contaminants may differentially activate TLRs and that there may be interspecies differences in cellular detection/activation. An alternative explanation of both TLR1/2 and TLR4 inhibition impacting NO response may be heterodimer formation. TLR2 has been postulated to form heterodimers to increase the repertoire of potentially harmful stimuli detected (Farhat et al., 2008). For example, Francisco et al. (2022) shows that TLR2 and TLR4 can form heterodimers with specific stimuli in HEK 293 cells transfected with TLR4 or TLR2. Atypical LPS can be detected by a TLR2/TLR4/MD2 heterodimer and induce an inflammatory response in macrophages as indicated by changes in cytokine gene expression (Francisco et al., 2022). Further research is necessary to understand how TLR4 and TLR2 may potentially facilitate OSPW detection.

Though NAs are speculated to be the detectable, bioactive component of OSPW (Arslan et al., 2023; Paul et al., 2023), the possibility of other OSPW contaminants activating TLRs must be considered. TLR4 has been implicated in cell activation by metals such as nickel (Schmidt et al., 2010) and cobalt (Rachmawati et al., 2013). As OSPW contains these metallic contaminants (Li et al., 2017; Phillips et al., 2020), there is a possibility that these constituents may also impose immunotoxic effects on RAW 264.7 cells via TLR4 activation.

6.5 OSPW and MyD88-dependent Signaling

My research aimed to examine how cells detect immunotoxic constituents of OSPW by assessing signaling proteins in a well-known immune signaling pathway, the MyD88-dependent signaling pathway, and comparing NO response to the response induced by known TLR agonists

(Cheng et al., 2012; Ciesielska, Matyjek, and Kwiatkowska, 2021; Coorens et al., 2017; Kawamoto et al., 2008; Underhill, 2003). The MyD88-dependent signaling pathway appears to be a major propagator of OSPW-stimulated signaling as the inhibition of associated signaling proteins, like IRAK1/4 and NF-κB (Ciesielska, Matyjek, and Kwiatkowska, 2021; Liu et al., 2014), reduces immune cell NO response. In addition, OSPW-mediated signaling closely parallels TLR4-mediated signaling via LPS (Kawamoto et al., 2008; Liu et al., 2014; Matsunaga et al., 2011; Takashima et al., 2009) as indicated by NO responses from pharmacological inhibition. This is consistent with the association of TLR4 and TLR2 with OSPW-mediated signaling as both receptors can activate MyD88-dependent signaling (Ciesielska, Matyjek, and Kwiatkowska, 2021; Liu et al., 2014; Schenk, Belisle, and Modlin, 2009). IRAK4 is associated with MyD88-dependent signaling and it is proposed that by inhibiting this kinase, the TLR-activated MyD88-dependent pathway is also inhibited (Wang et al., 2009). As NO response is no longer seen with IRAK1/4 Inhibitor I inhibition and OSPW stimulation, this further supports the involvement of the MyD88-dependent signaling pathway in OSPW activation of immune cells. Altogether, it is likely that OSPW perpetuates cell signaling via the MyD88-dependent pathway, as does TLR4 (Ciesielska, Matyjek, and Kwiatkowska, 2021; Liu et al., 2014).

OSPW activation of RAW 264.7 cells also likely results in NF-κB activation as there is a lack of pro-inflammatory response with inhibition by Cardamonin, which inhibits NF-κB activity (Israf et al., 2007). OSPW-mediated upregulation of *mip-2* and *mcp-1*, which are associated with NF-κB (Liu et al., 2014; Qin et al., 2017; Singh, Anshita, and Ravichandiran, 2021), was seen in Chapter 4 and increased secretion of MIP-2 was shown in Chapter 5, which further supports an NF-κB-mediated response. This thesis supports that OSPW elicits an NF-κB-mediated cytokine response and NO response. Moving forward, investigating how OSPW impacts other genes

mediated by NF-κB will help to further elucidate OSPW immunotoxicity. However, as NO production is significantly reduced with inhibition by Go 6976 and OSPW stimulation but not LPS stimulation, this is indicative of possible differences in the signaling pathway activated by OSPW compared to LPS. PKCα is implicated at different points of signaling pathways of various TLRs and other immune receptors (Loegering and Lennartz, 2011) which may contribute to these results.

6.6 Multiple Bioactive Constituents of OSPW

Significantly heightened *tlr2* mRNA expression with OSPW exposure has previously been reported in THP-1 cells (Paul et al., 2023) and here, both TLR4 and TLR1/2 are implicated in OSPW activation of RAW 264.7 cells. As these TLRs recognize different, specific ligands (Kawai and Akira, 2010; Kawamoto et al., 2008; Liu et al., 2014; Tükel et al., 2010; Underhill, 2003), this also suggests that other, distinct bioactive components may be present. In addition, the comparison of NO response profiles shows differences that are not consistent with the activation of only one receptor. From these results, it is likely OSPW stimulation occurs mostly through TLR4 as indicated by the similarities to the response profile resulting from TAK242 inhibition and LPS stimulation as LPS stimulates TLR4 (Kawamoto et al., 2008; Liu et al., 2014; Matsunaga et al., 2011; Takashima et al., 2009). However, the NO response profile from IRAK1/4 Inhibitor I inhibition and OSPW stimulation is consistent with heat-killed *E. coli* stimulation which suggests that though OSPW detection may be mediated mainly via TLR4, OSPW-mediated signaling is not as IRAK4 is critical in TLR signaling (Wang et al., 2009). This may suggest other bioactive components are present in OSPW or OSPW may activate alternative cell signaling pathways.

Regardless, the difference between OSPW- and LPS-mediated signaling may indicate the presence of more than one bioactive OSPW component.

Differences in bioactivity or immunotoxicity have been documented in the organic and inorganic fractions of OSPW (Lillico et al., 2023; Phillips et al., 2020) which contain different components and further implicates more than one constituent in influencing OSPW immunotoxicity. Fu et al. (2017) demonstrated that immunotoxic effects from whole OSPW are not consistent with effects from only the organic fraction of OSPW which implies that another component must be enacting these effects. NAs are among the organic fraction of OSPW (Li et al., 2017) and previous literature has shown that the OSPW inorganic fraction has resulted in bioactive or immunotoxic effects (Lillico et al., 2023; Phillips et al., 2020). Exposure to the inorganic fraction resulted in changes in the expression of *inos* and *arg*, antimicrobial enzyme genes, as well as *gadd45*, a stress gene, in RAW 264.7 cells (Phillips et al., 2020). Exposure to the inorganic fraction of OSPW before and after the addition of a water cap showed differences in *inos* and cytokine gene expression as compared to the organic fraction (Lillico et al., 2023). These immunotoxic and bioactive changes are from exposure to the fraction without NAs (Lillico et al., 2023; Phillips et al., 2020) and suggest that the inorganic fraction may also impose bioactive effects on RAW 264.7 cells. Furthermore, both Phillips et al. (2020) and Lillico et al. (2023) demonstrated reciprocal effects on gene expression with exposure to the inorganic vs. organic fractions which further outlines differences elicited in bioactivity between different OSPW components. Overall, the implication of more than one immune receptor in OSPW detection by RAW 264.7 cells is evidenced here and the pro-inflammatory response induced by the inorganic fraction in RAW 264.7 cells (Lillico et al., 2023; Phillips et al., 2020) is suggestive of more than one bioactive component in OSPW.

Metals have been identified in the inorganic fraction of OSPW (Phillips et al., 2020) and specific metals have been found to activate TLR4 (Rachmawati et al., 2013; Schmidt et al., 2010). Cobalt has been associated with increased IL-8 secretion in TLR4/MD2-transfected HEK 293 cells (Rachmawati et al., 2013) and cobalt has been found in OSPW (Phillips et al., 2020). In addition, copper has been implicated in increased Il-8 secretion by HEK293 cells (Rachmawati et al., 2013) and copper in OSPW has previously been found to exceed Canadian Council of Ministers of the Environment guidelines (Li et al., 2017). As copper and cobalt are implicated in immune cell activation and both have previously been found in OSPW, these present as other possible constituents that may contribute to OSPW immunotoxicity.

With the possibility of multiple immunotoxic OSPW constituents, component interactions may impact the immunotoxic effects of OSPW (Fu et al., 2017; Phillips et al., 2020). Differences in RAW 264.7 cell viability and protein secretion between whole OSPW and organic fraction exposure suggests possible interactions between OSPW constituents (Fu et al., 2017). Fu et al. (2017) presents the possibility that the organic and inorganic fraction constituents may result in synergistic interactions that could influence immune cell response. Consistent with this, Phillips et al. (2020) demonstrated increases in stress gene expression when comparing whole OSPW to the inorganic fraction and organic fractions. Phillips et al. (2020) suggests OSPW may contain metallo-organic complexes that, once separated, may enact bioactive effects. Moving forward, it is important to investigate all OSPW constituents that may result in OSPW immunotoxicity.

6.7 Environmental Bacterial Components in OSPW

This work heavily suggests that one or more immunotoxic constituents influences macrophage cell activation in a TLR4-mediated way; however, environmental bacterial products may exist in OSPW and influence immunotoxicity. Though OSPW is filtered via a 0.45 μM filter, environmental bacterial products may also be found in OSPW as they may not be removed (Choo-Yin, 2021). If environmental bacterial products were to enact the majority of immunotoxicity seen here, then the NO response profile for serially diluted TAK242 with OSPW stimulation would be expected to resemble heat-killed *E. coli* stimulation as it contains more than one bacterial PAMP (Alexander and Rietschel, 2001; Coorens et al., 2017; Tükel et al., 2010). However, it more closely resembles only LPS stimulation which suggests that multiple environmental bacterial products are unlikely to activate RAW 264.7 cells and result in the immunotoxic effects seen here.

Building on, this critique can be modified to insinuate that all immunotoxicity can be attributed to environmental LPS. However, this is also unlikely because both TLR1/2 and TLR4 are implicated in OSPW activation of RAW 264.7 cells. It is seen here that Cu-CPT22 impacts OSPW stimulation of RAW 264.7 cells and if LPS within OSPW is stimulating immune cells, then other components must also be present to stimulate TLR1/2 as it is inhibited by Cu-CPT22 (Cheng et al., 2012). Therefore, as this work compares OSPW to TLR agonists, the idea of bacterial products inciting OSPW immunotoxicity is possible but unlikely to be the main factor.

6.8 Future Directions

The *in vitro* RAW 264.7 macrophage cell assay is a sensitive, reliable tool that can be used to monitor immunotoxicity of untreated OSPW over time and assess the immunotoxicity of treated

OSPW. This assay can be used to assess and compare the efficacy of other AOP treatments as well as assess and compare other sources of OSPW. In addition, the impact of OSPW on stress genes could also be explored as other studies have shown OSPW-mediated effects on stress genes in RAW 264.7 cells (Fu et al., 2017; Phillips et al., 2020). Understanding how cells are impacted outside of immune functions will give a well-rounded understanding on how OSPW impacts mammalian cells.

Further investigation of other immunotoxic constituents, like the inorganic fraction, is necessary to fully understand the immunotoxic effects of OSPW. Phillips et al. (2020) demonstrates immunotoxic effects of the inorganic fraction and as metals found in this fraction have the capacity to activate immune receptors (Phillips et al., 2020; Rachmawati et al., 2013), this fraction should be further investigated. The immunotoxic effects of metals, specifically copper, cobalt, palladium, and nickel, should be explored. It is important to understand all constituents that lead to immunotoxicity in RAW 264.7 cells so treatments can be designed to eliminate these constituents. This will allow OSPW to be properly remediated and returned to the environment. In addition, understanding how metals may adversely impact immune cells will further contribute to our current understanding of how mammalian cells perceive contaminated waters and guide remediation strategies.

Exploring other immune receptors activated by OSPW will better elucidate the immunotoxic constituents of OSPW. Immune receptors like other TLRs, TNFR1, and IL-1R could be targeted using pharmacological inhibitors to determine if they are involved in OSPW-mediated stimulation of RAW 264.7 cells as OSPW-activated signaling proteins are involved in overlapping cell signaling pathways (Brasier, 2010; Liu et al., 2014; Wang et al., 2009). This will expand our understanding of immunotoxicants and how they impact mammalian cells.

Overall, further research is required to fully understand the immunotoxicity incited by OSPW, and to ultimately remediate and return it to the environment. Understanding how environmental contaminants interact with immune cells and how immune cells respond will give us a comprehensive understanding that we can apply to treatment methods.

References

Abbas, A. K., Trotta, E., R. Simeonov, D., Marson, A., & Bluestone, J. A. (2018). Revisiting IL-2: Biology and therapeutic prospects. *Science Immunology*, 3(25), eaat1482.

Abdalrhman, A. S., & El-Din, M. G. (2020). Degradation of organics in real oil sands process water by electro-oxidation using graphite and dimensionally stable anodes. *Chemical Engineering Journal*, 389, 124406.

Abdalrhman, A. S., Zhang, Y., & El-Din, M. G. (2019). Electro-oxidation by graphite anode for naphthenic acids degradation, biodegradability enhancement and toxicity reduction. *Science of The Total Environment*, 671, 270-279.

Afzal, A., Drzewicz, P., Pérez-Estrada, L. A., Chen, Y., Martin, J. W., & Gamal El-Din, M. (2012). Effect of molecular structure on the relative reactivity of naphthenic acids in the UV/H2O2 advanced oxidation process. *Environmental Science & Technology*, 46(19), 10727-10734.

Alberts, M. E., Wong, J., Hindle, R., Degenhardt, D., Krygier, R., Turner, R. J., & Muench, D. G. (2021). Detection of naphthenic acid uptake into root and shoot tissues indicates a direct role for plants in the remediation of oil sands process-affected water. *Science of The Total Environment*, 795, 148857.

Alexander, C., & Rietschel, E. T. (2001). Bacterial lipopolysaccharides and innate immunity. *Journal of Endotoxin Research*, 7(3), 167-202.

Allen, E. W. (2008). Process water treatment in Canada's oil sands industry: I. Target pollutants and treatment objectives. *Journal of Environmental Engineering and Science*, 7, 123-138.

Anderson, J., Wiseman, S. B., Moustafa, A., El-Din, M. G., Liber, K., & Giesy, J. P. (2012). Effects of exposure to oil sands process-affected water from experimental reclamation ponds on *Chironomus dilutus*. *Water Research,* 46(6), 1662-1672.

Armstrong, S. A., Headley, J. V., Peru, K. M., & Germida, J. J. (2007). Phytotoxicity of oil sands naphthenic acids and dissipation from systems planted with emergent aquatic macrophytes. *Journal of Environmental Science and Health*, Part A, 43(1), 36-42.

Arslan, M., Ganiyu, S. O., Lillico, D. M., Stafford, J. L., & El-Din, M. G. (2023). Fate of dissolved organics and generated sulfate ions during biofiltration of oil sands process water pretreated with sulfate radical advanced oxidation process. *Chemical Engineering Journal*, 458, 141390.

Arunachalam, A. R., Samuel, S. S., Mani, A., Maynard, J. P., Stayer, K. M., Dybbro, E., Narayanan, S., Biswas, A., Pathan, S., Soni, K., Kamal, A. H., Ambati, C. S., Putluri, N., Desai, M. S., & Thevananther, S. (2023). P2Y2 purinergic receptor gene deletion protects mice from bacterial endotoxin and sepsis-associated liver injury and mortality. *American Journal of Physiology Gastrointestinal and Liver Physiology*, 325(5), G471-G491.

Baker, L. F., Ciborowski, J. J., & MacKinnon, M. D. (2012). Petroleum coke and soft tailings sediment in constructed wetlands may contribute to the uptake of trace metals by algae and aquatic invertebrates. *Science of the Total Environment*, 414, 177-186.

Balaberda, A. L., & Ulrich, A. C. (2021). Persulfate oxidation coupled with biodegradation by Pseudomonas fluorescens enhances naphthenic acid remediation and toxicity reduction. *Microorganisms*, 9(7), 1502.

Bandow, K., Kusuyama, J., Shamoto, M., Kakimoto, K., Ohnishi, T., & Matsuguchi, T. (2012). LPS-induced chemokine expression in both MyD88-dependent and -independent manners is regulated by Cot/Tpl2-ERK axis in macrophages. *FEBS letters,* 586(10), 1540-1546.

Barrow, K., Escher, B. I., Hicks, K. A., König, M., Schlichting, R., & Arlos, M. J. (2023). Water quality monitoring with in vitro bioassays to compare untreated oil sands process-affected water with unimpacted rivers*. Environmental Science: Water Research & Technology*, 9(8), 2008-2020.

Bartlett, A. J., Frank, R. A., Gillis, P. L., Parrott, J. L., Marentette, J. R., Brown, L. R., Hooey, T., Vanderveen, R., McInnis, R., Brunswick, P., Shang, D., Headley, J. V., Peru, K. M., & Hewitt, L. M. (2017). Toxicity of naphthenic acids to invertebrates: Extracts from oil sands process-affected water versus commercial mixtures. *Environmental Pollution*, 227, 271-279.

Bauerfeld, C., & Samavati, L. (2017). Role of MEK1 in TLR4 Mediated Signaling. *Journal of Cell Signaling*, 2(1), 135.

Bello, T., & Gujral, T. S. (2018). KInhibition: A Kinase Inhibitor Selection Portal. *iScience*, 8, 49-53.

Brasier, A. R. (2010). The nuclear factor-κB–interleukin-6 signalling pathway mediating vascular inflammation. *Cardiovascular Research*, 86(2), 211-218.

Brown, L. D., & Ulrich, A. C. (2015). Oil sands naphthenic acids: A review of properties, measurement, and treatment. *Chemosphere*, 127, 276-290.

Burger, J., & Gochfeld, M. (2001). On developing bioindicators for human and ecological health. *Environmental Monitoring and Assessment*, 66, 23-46.

Cheng, K., Wang, X., Zhang, S., & Yin, H. (2012). Discovery of Small-Molecule Inhibitors of the TLR1/TLR2 Complex. *Angewandte Chemie International Edition*, 51(49), 12246-12249.

Choo-Yin, Y.Y. (2021). Monitoring macrophage immune gene expression profiles as an early indicator system for examining the bioactivity of oil sands process affected waters [Unpublished master's thesis, University of Alberta]. University of Alberta.

Ciesielska, A., Matyjek, M., & Kwiatkowska, K. (2021). TLR4 and CD14 trafficking and its influence on LPS-induced pro-inflammatory signaling. *Cellular and Molecular Life Sciences*, 78, 1233-1261.

Clemente, J. S., MacKinnon, M. D., & Fedorak, P. M. (2004). Aerobic biodegradation of two commercial naphthenic acids preparations. *Environmental Science & Technology*, 38(4), 1009-1016.

Colavecchia, M. V., Backus, S. M., Hodson, P. V., & Parrott, J. L. (2004). Toxicity of oil sands to early life stages of fathead minnows (Pimephales promelas). *Environmental Toxicology and Chemistry*, 23(7), 1709-1718.

Connors, K. A., Brill, J. L., Norberg-King, T., Barron, M. G., Carr, G., & Belanger, S. E. (2022). Daphnia magna and Ceriodaphnia dubia have similar sensitivity in standard acute and chronic toxicity tests. *Environmental Toxicology and Chemistry*, 41(1), 134-147.

Coorens, M., Schneider, V. A., de Groot, A. M., van Dijk, A., Meijerink, M., Wells, J. M., Scheenstra, M. R., Veldhuizen, E. J., & Haagsman, H. P. (2017). Cathelicidins Inhibit Escherichia coli–Induced TLR2 and TLR4 Activation in a Viability-Dependent Manner. *The Journal of Immunology*, 199(4), 1418-1428.

de Campos, G. Y., Oliveira, R. A., Oliveira-Brito, P. K. M., Roque-Barreira, M. C., & da Silva, T. A. (2020). Pro-inflammatory response ensured by LPS and Pam3CSK4 in RAW 264.7 cells did not improve a fungistatic effect on Cryptococcus gattii infection. *PeerJ*, 8:e10295.

Duncia, J. V., Santella, J. B., Higley, C. A., Pitts, W. J., Wityak, J., Frietze, W. E., Rankin, F. W.,
Sun, J. H., Earl, R. A., Tabaka, A. C., Teleha, C. A., Blom, K. F., Favata, M. F., Manos, E. J.,
Daulerio, A. J., Stradley, D. A., Horiuchi, K., Copeland, R. A., Scherle, P. A., Trzaskos, J. M.,
Magolda, R. L., Trainor, G. L., Wexler, R. R., Hobbs, F. W., & Olson, R. E. (1998). MEK
inhibitors: the chemistry and biological activity of U0126, its analogs, and cyclization
products. *Bioorganic & Medicinal Chemistry Letters*, 8(20), 2839-2844.

Durai, P., Shin, H. J., Achek, A., Kwon, H. K., Govindaraj, R. G., Panneerselvam, S., Yesudhas,
D., Choi, J., No, K. T., & Choi, S. (2017). Toll-like receptor 2 antagonists identified through
virtual screening and experimental validation. *The FEBS Journal*, 284(14), 2264-2283.

Elvidge, C. K., Robinson, C. E., Caza, R. A., Hewitt, L. M., Frank, R. A., & Orihel, D. M.
(2023). Chemical communication in wood frog (Rana sylvatica) tadpoles is influenced by
early-life exposure to naphthenic acid fraction compounds. *Aquatic Toxicology*, 257, 106435.

Falvo, J. V., Tsytsykova, A. V., & Goldfeld, A. E. (2010). Transcriptional Control of the TNF
Gene. *TNF Pathophysiology*, 11, 27-60.

Farhat, K., Riekenberg, S., Heine, H., Debarry, J., Lang, R., Mages, J., Buwitt-Beckmann, U.,
Roschmann, K., Jung, G., Wiesmuller, K. H., & Ulmer, A. J. (2008). Heterodimerization of
TLR2 with TLR1 or TLR6 expands the ligand spectrum but does not lead to differential
signaling. *Journal of Leucocyte Biology,* 83(3), 692-701.

Feng, Y., Mu, R., Wang, Z., Xing, P., Zhang, J., Dong, L., & Wang, C. (2019). A toll-like
receptor agonist mimicking microbial signal to generate tumor-suppressive macrophages.
Nature Communications, 10, 2272.

Fernie, K. J., Marteinson, S. C., Chen, D., Eng, A., Harner, T., Smits, J. E., & Soos, C. (2018).
Elevated exposure, uptake and accumulation of polycyclic aromatic hydrocarbons by nestling

tree swallows (Tachycineta bicolor) through multiple exposure routes in active mining-related areas of the Athabasca oil sands region. *Science of the Total Environment*, 624, 250-261.

Folwell, B. D., McGenity, T. J., & Whitby, C. (2016). Biofilm and planktonic bacterial and fungal communities transforming high-molecular-weight polycyclic aromatic hydrocarbons. *Applied and Environmental Microbiology*, 82(8), 2288-2299.

Francisco, S., Billod, J. M., Merino, J., Punzón, C., Gallego, A., Arranz, A., Martin-Santamaria, S., & Fresno, M. (2022). Induction of TLR4/TLR2 Interaction and Heterodimer Formation by Low Endotoxic Atypical LPS. *Frontiers in Immunology*, 12, 748303.

Frank, R. A., Fischer, K., Kavanagh, R., Burnison, B. K., Arsenault, G., Headley, J. V., Peru, K. M., Van Der Kraak, G., & Solomon, K. R. (2009). Effect of carboxylic acid content on the acute toxicity of oil sands naphthenic acids. *Environmental Science & Technology*, 43(2), 266-271.

Frank, R. A., Kavanagh, R., Burnison, B. K., Arsenault, G., Headley, J. V., Peru, K. M., Van Der Kraak, G., & Solomon, K. R. (2008). Toxicity assessment of collected fractions from an extracted naphthenic acid mixture. *Chemosphere*, 72(9), 1309-1314.

Fu, L., Li, C., Lillico, D. M., Phillips, N. A., El-Din, M. G., Belosevic, M., & Stafford, J. L. (2017). Comparison of the acute immunotoxicity of nonfractionated and fractionated oil sands process-affected water using mammalian macrophages. *Environmental Science & Technology*, 51(15), 8624-8634.

Gagioti, S., Scavone, C., & Bevilacqua, E. (2000). Participation of the mouse implanting trophoblast in nitric oxide production during pregnancy. *Biology of Reproduction*, 62(2), 260-268.

Ganiyu, S. O., & El-Din, M. G. (2020). Insight into in-situ radical and non-radical oxidative degradation of organic compounds in complex real matrix during electrooxidation with boron doped diamond electrode: A case study of oil sands process water treatment. *Applied Catalysis B: Environmental*, 279, 119366.

Garcia-Garcia, E., Ge, J. Q., Oladiran, A., Montgomery, B., El-Din, M. G., Perez-Estrada, L. C., Stafford, J. L., Martin, J. W., & Belosevic, M. (2011). Ozone treatment ameliorates oil sands process water toxicity to the mammalian immune system. *Water research*, 45(18), 5849-5857.

Gentes, M. L., Waldner, C., Papp, Z., & Smits, J. E. (2006). Effects of oil sands tailings compounds and harsh weather on mortality rates, growth and detoxification efforts in nestling tree swallows (Tachycineta bicolor). *Environmental Pollution,* 142(1), 24-33.

Gentes, M. L., Waldner, C., Papp, Z., & Smits, J. E. (2007). Effects of exposure to naphthenic acids in tree swallows (Tachycineta bicolor) on the Athabasca oil sands, Alberta, Canada. *Journal of Toxicology and Environmental Health*, Part A, 70(14), 1182-1190.

Giesy, J. P., Anderson, J. C., & Wiseman, S. B. (2010). Alberta oil sands development. *Proceedings of the National Academy of Sciences*, 107(3), 951-952.

Girbl, T., Lenn, T., Perez, L., Rolas, L., Barkaway, A., Thiriot, A., del Fresno, C., Lynam, E., Hub, E., Thelen, M., Graham, G., Alon, R., Sancho, D., von Andrian, U. H., Voisin, M. B., Rot, A., & Nourshargh, S. (2018). Distinct Compartmentalization of the Chemokines CXCL1 and CXCL2 and the Atypical Receptor ACKR1 Determine Discrete Stages of Neutrophil Diapedesis. *Immunity,* 49(6), 1062-1076.

Godwin, C. M., Smits, J. E., & Barclay, R. M. (2016). Metals and metalloids in nestling tree swallows and their dietary items near oilsands mine operations in Northern Alberta. *Science of the Total Environment*, 562, 714-723.

Grandage, V. L., Everington, T., Linch, D. C., & Khwaja, A. (2006). Gö6976 is a potent inhibitor of the JAK 2 and FLT3 tyrosine kinases with significant activity in primary acute myeloid leukaemia cells. *British Journal of Haematology*, 135(3), 303-316.

Granucci, F., Vizzardelli, C., Pavelka, N., Feau, S., Persico, M., Virzi, E., Rescigno, M., Moro, G., & Ricciardi-Castagnoli, P. (2001). Inducible IL-2 production by dendritic cells revealed by global gene expression analysis. *Nature Immunology*, 2(9), 882-888.

Griffiths, M. J., Messent, M., MacAllister, R. J., & Evans, T. W. (1993). Aminoguanidine selectively inhibits inducible nitric oxide synthase. *British Journal of Pharmacology*, 110(3), 963-968.

Gurney, K. E., Williams, T. D., Smits, J. E., Wayland, M., Trudeau, S., & Bendell-Young, L. I. (2005). Impact of oil-sands based wetlands on the growth of mallard (Anas platyrhynchos) ducklings. *Environmental Toxicology and Chemistry*, 24(2), 457-463.

He, Y., Wiseman, S. B., Zhang, X., Hecker, M., Jones, P. D., El-Din, M. G., Martin, J. W., & Giesy, J. P. (2010). Ozonation attenuates the steroidogenic disruptive effects of sediment free oil sands process water in the H295R cell line. *Chemosphere*, 80(5), 578-584.

Hersikorn, B. D., & Smits, J. E. (2011). Compromised metamorphosis and thyroid hormone changes in wood frogs (Lithobates sylvaticus) raised on reclaimed wetlands on the Athabasca oil sands. *Environmental Pollution*, 159(2), 596-601.

Hewitt, L. M., Roy, J. W., Rowland, S. J., Bickerton, G., DeSilva, A., Headley, J. V., Milestone, C. B., Scarlett, A. G., Brown, S., Spencer, C., West, C. E., Peru, K. M., Grapentine, L., Ahad, J. M., Pakdel, H., & Frank, R. A. (2020). Advances in distinguishing groundwater influenced by oil sands process-affected water (OSPW) from natural bitumen-influenced groundwaters. *Environmental Science & Technology*, 54(3), 1522-1532.

Holowenko, F. M., MacKinnon, M. D., & Fedorak, P. M. (2002). Characterization of naphthenic acids in oil sands wastewaters by gas chromatography-mass spectrometry. *Water Research*, 36(11), 2843-2855.

Honda, M., & Suzuki, N. (2020). Toxicities of polycyclic aromatic hydrocarbons for aquatic animals. *International Journal of Environmental Research and Public Health*, 17(4), 1363.

Hussain, N. A., & Stafford, J. L. (2023). Abiotic and biotic constituents of oil sands process-affected waters. *Journal of Environmental Sciences*, 127, 169-186.

Israf, D. A., Khaizurin, T. A., Syahida, A., Lajis, N. H., & Khozirah, S. (2007). Cardamonin inhibits COX and iNOS expression via inhibition of p65NF-κB nuclear translocation and Iκ-B phosphorylation in RAW 264.7 macrophage cells. *Molecular Immunology*, 44(5), 673-679.

Jankowska-Kieltyka, M., Roman, A., Mikrut, M., Kowalska, M., van Eldik, R., & Nalepa, I. (2021). Metabolic Response of RAW 264.7 Macrophages to Exposure to Crude Particulate Matter and a Reduced Content of Organic Matter. *Toxics*, 9, 205.

Jin, Y., Liu, Y., & Nelin, L. D. (2015). Extracellular signal-regulated kinase mediates expression of arginase II but not inducible nitric-oxide synthase in lipopolysaccharide-stimulated macrophages. *Journal of Biological Chemistry,* 290(4), 2099-2111.

Jones, D., Scarlett, A. G., West, C. E., & Rowland, S. J. (2011). Toxicity of individual naphthenic acids to *Vibrio fischeri. Environmental Science & Technology*, 45(22), 9776-9782.

Jones, E., Adcock, I. M., Ahmed, B. Y., & Punchard, N. A. (2007). Modulation of LPS stimulated NF-kappaB mediated Nitric Oxide production by PKCε and JAK2 in RAW macrophages. *Journal of Inflammation*, 4, 23.

Kavanagh, R. J., Frank, R. A., Burnison, B. K., Young, R. F., Fedorak, P. M., Solomon, K. R., & Van Der Kraak, G. (2012). Fathead minnow (Pimephales promelas) reproduction is impaired when exposed to a naphthenic acid extract. *Aquatic Toxicology*, 116, 34-42.

Kavanagh, R. J., Frank, R. A., Oakes, K. D., Servos, M. R., Young, R. F., Fedorak, P. M., MacKinnon, M. D., Solomon, K. R., Dixon, D. G., & Van Der Kraak, G. (2011). Fathead minnow (Pimephales promelas) reproduction is impaired in aged oil sands process-affected waters. *Aquatic Toxicology*, 101(1), 214-220.

Kawai, T., & Akira, S. (2010). The role of pattern-recognition receptors in innate immunity: update on Toll-like receptors. *Nature immunology*, 11(5), 373-384.

Kawamoto, T., Ii, M., Kitazaki, T., Iizawa, Y., & Kimura, H. (2008). TAK-242 selectively suppresses Toll-like receptor 4-signaling mediated by the intracellular domain. *European Journal of Pharmacology*, 584(1), 40-48.

Kinley, C. M., McQueen, A. D., & Rodgers Jr, J. H. (2016). Comparative responses of freshwater organisms to exposures of a commercial naphthenic acid. *Chemosphere*, 153, 170-178.

Klamerth, N., Moreira, J., Li, C., Singh, A., McPhedran, K. N., Chelme-Ayala, P., Belosevic, M., & El-Din, M. G. (2015). Effect of ozonation on the naphthenic acids' speciation and toxicity of pH-dependent organic extracts of oil sands process-affected water. *Science of the Total Environment,* 506, 66-75.

Koide, N., Ito, H., Mu, M. M., Sugiyama, T., Hassan, F., Islam, S., Mori, I., Yoshida, T., & Yokochi, T. (2005). Inhibition of extracellular signal-regulated kinase 1/2 augments nitric oxide production in lipopolysaccharide-stimulated RAW264.7 macrophage cells. *FEMS Immunology & Medical Microbiology*, 45(2), 213-219.

Kong, L., Smith, W., & Hao, D. (2019). Overview of RAW264.7 for osteoclastogensis study: Phenotype and stimuli. *Journal of Cellular and Molecular Medicine*, 23(5), 3077-3087.

Kurek, J., Kirk, J. L., Muir, D. C., Wang, X., Evans, M. S., & Smol, J. P. (2013). Legacy of a half century of Athabasca oil sands development recorded by lake ecosystems. *Proceedings of the National Academy of Sciences*, 110(5), 1761-1766.

Lari, E., Steinkey, D., Razmara, P., Mohaddes, E., & Pyle, G. G. (2019). Oil sands process-affected water impairs the olfactory system of rainbow trout (Oncorhynchus mykiss). *Ecotoxicology and Environmental Safety*, 170, 62-67.

Lari, E., Wiseman, S., Mohaddes, E., Morandi, G., Alharbi, H., & Pyle, G. G. (2016). Determining the effect of oil sands process-affected water on grazing behaviour of Daphnia magna, long-term consequences, and mechanism. *Chemosphere*, 146, 362-370.

Le, Y., Hu, X., Zhu, J., Wang, C., Yang, Z., & Lu, D. (2019). Ambient fine particulate matter induces inflammatory responses of vascular endothelial cells through activating TLR-mediated pathway. *Toxicology and Industrial Health*, 35(10), 670-678.

Leclair, L. A., Pohler, L., Wiseman, S. B., He, Y., Arens, C. J., Giesy, J. P., Scully, S., Wagner, B. D., van den Heuvel, M. R., & Hogan, N. S. (2015). In vitro assessment of endocrine disrupting potential of naphthenic acid fractions derived from oil sands-influenced water. *Environmental Science & Technology*, 49(9), 5743-5752.

Lei, J., Yin, X., Shang, H., & Jiang, Y. (2019). IP-10 is highly involved in HIV infection. *Cytokine*, 115, 97-103.

Lester, S. N., & Li, K. (2014). Toll-like Receptors in Antiviral Innate Immunity. *Journal of Molecular Biology,* 426(6), 1246-1264.

Li, C., Fu, L., Stafford, J., Belosevic, M., & El-Din, M. G. (2017). The toxicity of oil sands process-affected water (OSPW): A critical review. *Science of the Total Environment*, 601-602, 1785-1802.

Lillico, D. M., Hussain, N. A., Choo-Yin, Y. Y., Qin, R., How, Z. T., El-Din, M. G., & Stafford, J. L. (2023). Using immune cell-based bioactivity assays to compare the inflammatory activities of oil sands process-affected waters from a pilot scale demonstration pit lake. *Journal of Environmental Sciences*, 128, 55-70.

Lister, A., Nero, V., Farwell, A., Dixon, D. G., & Van Der Kraak, G. (2008). Reproductive and stress hormone levels in goldfish (Carassius auratus) exposed to oil sands process-affected water. *Aquatic Toxicology,* 87(3), 170-177.

Liu, M., Guo, S., Hibbert, J. M., Jain, V., Singh, N., Wilson, N. O., & Stiles, J. K. (2011). CXCL10/IP-10 in infectious diseases pathogenesis and potential therapeutic implications. *Cytokine & Growth Factor Reviews*, 22(3), 121-130.

Liu, Y., Yin, H., Zhao, M., & Lu, Q. (2014). TLR2 and TLR4 in Autoimmune Diseases: A Comprehensive Review. *Clinical Reviews in Allergy & Immunology*, 47, 136-147.

Lo, C. C., Brownlee, B. G., & Bunce, N. J. (2006). Mass spectrometric and toxicological assays of Athabasca oil sands naphthenic acids. *Water Research*, 40(4), 655-664.

Loegering, D. J., & Lennartz, M. R. (2011). Protein kinase C and Toll-Like Receptor Signaling. *Enzyme Research*, 2011, 537821.

Mahaffey, A., & Dubé, M. (2017). Review of the composition and toxicity of oil sands process-affected water. *Environmental Reviews*, 25(1), 97-114.

Makene, V. W., & Pool, E. J. (2015). The assessment of inflammatory activity and toxicity of treated sewage using RAW264.7 cells. *Water and Environment Journal*, 29(3), 353-359.

Marentette, J. R., Frank, R. A., Hewitt, L. M., Gillis, P. L., Bartlett, A. J., Brunswick, P., Shang, D., & Parrott, J. L. (2015). Sensitivity of walleye (Sander vitreus) and fathead minnow (Pimephales promelas) early-life stages to naphthenic acid fraction components extracted from fresh oil sands process-affected waters. *Environmental Pollution*, 207, 59-67.

Masztalerz, A., Van Rooijen, N., Den Otter, W., & Everse, L. A. (2003). Mechanisms of macrophage cytotoxicity in IL-2 and IL-12 mediated tumour regression. *Cancer Immunology, Immunotherapy*, 52, 235-242.

Matsunaga, N., Tsuchimori, N., Matsumoto, T., & Ii, M. (2011). TAK-242 (Resatorvid), a Small-Molecule Inhibitor of Toll-like receptor (TLR) 4 signaling, Binds Selectively to TLR4 and Interferes with Interactions between TLR4 and Its Adaptor Molecules. *Molecular Pharmacology*, 79(1), 34-41.

McQueen, A. D., Kinley, C. M., Hendrikse, M., Gaspari, D. P., Calomeni, A. J., Iwinski, K. J., Castle, J. W., Haakensen, M. C., Peru, K. M., Headley, J. V., & Rodgers Jr, J. H. (2017). A risk-based approach for identifying constituents of concern in oil sands process-affected water from the Athabasca Oil Sands region. *Chemosphere*, 173, 340-350.

Melvin, S. D., & Trudeau, V. L. (2012). Growth, development and incidence of deformities in amphibian larvae exposed as embryos to naphthenic acid concentrations detected in the Canadian oil sands region. *Environmental Pollution,* 167, 178-183.

Meng, L., How, Z. T., Ganiyu, S. O., & El-Din, M. G. (2021). Solar photocatalytic treatment of model and real oil sands process water naphthenic acids by bismuth tungstate: Effect of

catalyst morphology and cations on the degradation kinetics and pathways. *Journal of Hazardous Materials*, 413, 125396.

Morandi, G. D., Wiseman, S. B., Pereira, A., Mankidy, R., Gault, I. G., Martin, J. W., & Giesy, J. P. (2015). Effects-directed analysis of dissolved organic compounds in oil sands process-affected water. *Environmental Science & Technology*, 49(20), 12395-12404.

Movasseghi, A. R., Rodríguez-Estival, J., & Smits, J. E. (2017). Thyroid pathology in deer mice (Peromyscus maniculata) from a reclaimed mine site on the athabasca oil sands. *Environmental Pollution*, 222, 42-49.

Parameswaran, N., & Patial, S. (2010). Tumor Necrosis Factor-α Signaling in Macrophages. *Critical Reviews in Eukaryotic Gene Expression*, 20(2), 87-103.

Paul, S., Hussain, N. A., Lillico, D. M., Suara, M. A., Ganiyu, S. O., El-Din, M. G., & Stafford, J. L. (2023). Examining the immunotoxicity of oil sands process affected waters using a human macrophage cell line. *Toxicology*, 153680.

Peri, F., & Calabrese, V. (2014). Toll-like receptor 4 (TLR4) Modulation by Synthetic and Natural Compounds: An Update. *Journal of Medicinal Chemistry*, 57(9), 3612-3622.

Peters, L. E., MacKinnon, M., Van Meer, T., van den Heuvel, M. R., & Dixon, D. G. (2007). Effects of oil sands process-affected waters and naphthenic acids on yellow perch (Perca flavescens) and Japanese medaka (Orizias latipes) embryonic development. *Chemosphere*, 67(11), 2177-2183.

Phillips, N. A., Lillico, D. M., Qin, R., McAllister, M., El-Din, M. G., Belosevic, M., & Stafford, J. L. (2020). Inorganic fraction of oil sands process-affected water induces mammalian macrophage stress gene expression and acutely modulates immune cell functional markers at both the gene and protein levels. *Toxicology in Vitro*, 66, 104875.

Platchek, M., Lu, Q., Tran, H., & Xie, W. (2020). Comparative Analysis of Multiple

    Immunoassays for Cytokine Profiling in Drug Discovery. *SLAS Discovery*, 25(10), 1197-

    1213.

Pool, E. J., & Magcwebeba, T. U. (2009). The Screening of River Water for Immunotoxicity

    Using an In Vitro Whole Blood Culture Assay. *Water, Air, and Soil Pollution*, 200, 25-31.

Powers, J. P., Li, S., Jaen, J. C., Liu, J., Walker, N. P., Wang, Z., & Wesche, H. (2006). Discovery

    and initial SAR of inhibitors of interleukin-1 receptor-associated kinase-4. *Bioorganic &*

    Medicinal Chemistry Letters, 16(11), 2842-2845.

Qatsha, K. A., Rudolph, C., Marme, D., Schächtele, C., & May, W. S. (1993). Gö 6976, a

    selective inhibitor of protein kinase C, is a potent antagonist of human immunodeficiency

    virus 1 induction from latent/low-level-producing reservoir cells in vitro. *Proceedings of the*

    National Academy of Sciences, 90(10), 4674-4678.

Qin, C. C., Liu, Y. N., Hu, Y., Yang, Y., & Chen, Z. (2017). Macrophage inflammatory protein-2

    as mediator of inflammation in acute liver injury. *World Journal of Gastroenterology*, 23(17),

    3043-3052.

Quinlan, P. J., & Tam, K. C. (2015). Water treatment technologies for the remediation of

    naphthenic acids in oil sands process-affected water. *Chemical Engineering Journal*, 279,

    696-714.

Rachmawati, D., Bontkes, H. J., Verstege, M. I., Muris, J., von Blomberg, B. M. E., Scheper, R.

    J., & van Hoogstraten, I. M. (2013). Transition metal sensing by Toll-like receptor-4: next to

    nickel, cobalt and palladium are potent human dendritic cell stimulators. *Contact Dermatitis*,

    68(6), 331-338.

Reyes-Maldonado, R., Marie, B., & Ramírez, A. (2021). Rearing methods and life cycle characteristics of Chironomus sp. Florida (Chironomidae: Diptera): A rapid-developing species for laboratory studies. *Plos one*, 16(2), e0247382.

Rundle, K. I., Sharaf, M. S., Stevens, D., Kamunde, C., & Van Den Heuvel, M. R. (2018). Oil sands derived naphthenic acids are oxidative uncouplers and impair electron transport in isolated mitochondria. *Environmental Science & Technology,* 52(18), 10803-10811.

Rundle, K. I., Sharaf, M. S., Stevens, D., Kamunde, C., & Van Den Heuvel, M. R. (2021). Adamantane carboxylic acids demonstrate mitochondrial toxicity consistent with oil sands-derived naphthenic acids. *Environmental Advances*, 5, 100092.

Salinas-Carmona, M. C., Longoria-Lozano, O., Garza-Esquivel, H. R., Lopez-Ulloa, J., Reyes-Carrillo, J., & Vázquez-Marmolejo, A. V. (2020). Inducible nitric oxide synthase blockade with aminoguanidine, protects mice infected with Nocardia brasiliensis from actinomycetoma development. *PLoS Neglected Tropical Diseases*, 14(10), e0008775.

Samarpita, S., Kim, J. Y., Rasool, M. K., & Kim, K. S. (2020). Investigation of toll-like receptor (TLR) 4 inhibitor TAK-242 as a new potential anti-rheumatoid arthritis drug. *Arthritis Research & Therapy*, 22, 1-10.

Sang, W., Zhong, Z., Linghu, K., Xiong, W., Tse, A. K. W., Cheang, W. S., Yu, H., & Wang, Y. (2018). Siegesbeckia pubescens Makino inhibits Pam_3CSK_4-induced inflammation in RAW 264.7 macrophages through suppressing TLR1/TLR2-mediated NF-κB activation. *Chinese Medicine*, 13, 37.

Sato, M., Sano, H., Iwaki, D., Kudo, K., Konishi, M., Takahashi, H., Takahashi, T., Imaizumi, H., Asai, Y., & Kuroki, Y. (2003). Direct Binding of Toll-like Receptor 2 to Zymosan, and

Zymosan-induced NF-κB Activation and TNF-α Secretion Are Down-Regulated by Lung

Collectin Surfactant Protein A. *The Journal of Immunology*, 171(1), 417-425.

Scarlett, A. G., Reinardy, H. C., Henry, T. B., West, C. E., Frank, R. A., Hewitt, L. M., &

Rowland, S. J. (2013). Acute toxicity of aromatic and non-aromatic fractions of naphthenic

acids extracted from oil sands process-affected water to larval zebrafish. *Chemosphere*, 93(2),

415-420.

Schenk, M., Belisle, J. T., & Modlin, R. L. (2009). TLR2 Looks at Lipoproteins. *Immunity*,

31(6), 847-849.

Schmidt, M., Raghavan, B., Müller, V., Vogl, T., Fejer, G., Tchaptchet, S., Keck, S., Kalis, C.,

Nielson, P. J., Galanos, C., Roth, J., Skerra, A., Martin, S. F., Freudenberg, M. A., & Goebeler,

M. (2010). Crucial role for human Toll-like receptor 4 in the development of contact allergy to

nickel. *Nature Immunology*, 11(9), 814-819.

Scott, A. C., Zubot, W., MacKinnon, M. D., Smith, D. W., & Fedorak, P. M. (2008). Ozonation of

oil sands process water removes naphthenic acids and toxicity. *Chemosphere*, 71(1), 156-160.

Singh, S., Anshita, D., & Ravichandiran, V. (2021). MCP-1: Function, regulation, and

involvement in disease. *International Immunopharmacology*, 101, 107598.

Stow, J. L., Low, P. C., Offenhäuser, C., & Sangermani, D. (2009). Cytokine secretion in

macrophages and other cells: pathways and mediators. *Immunobiology*, 214(7), 601-612.

Suara, M. A., Ganiyu, S. O., Paul, S., Stafford, J. L., & El-Din, M. G. (2022). Solar-activated

zinc oxide photocatalytic treatment of real oil sands process water: Effect of treatment

parameters on naphthenic acids, polyaromatic hydrocarbons and acute toxicity removal.

Science of The Total Environment, 819, 153029.

Taciak, B., Białasek, M., Braniewska, A., Sas, Z., Sawicka, P., Kiraga, Ł., Rygiel, T., & Król, M.

    (2018). Evaluation of phenotypic and functional stability of RAW 264.7 cell line through

    serial passages. *PloS ONE,* 13(6), e0198943.

Takahashi, A., Yamamoto, N., & Murakami, A. (2011). Cardamonin suppresses nitric oxide

    production via blocking the IFN-γ/STAT pathway in endotoxin-challenged peritoneal

    macrophages of ICR mice. *Life Sciences*, 89(9-10), 337-342.

Takashima, K., Matsunaga, N., Yoshimatsu, M., Hazeki, K., Kaisho, T., Uekata, M., Hazeki, O.,

    Akira, S., Iizawa, Y., & Ii, M. (2009). Analysis of binding site for the novel small-molecule

    TLR4 signal transduction inhibitor TAK-242 and its therapeutic effect on mouse sepsis model.

    British Journal of Pharmacology, 157(7), 1250-1262.

Tanaka, T., Narazaki, M., & Kishimoto, T. (2014). IL-6 in Inflammation, Immunity, and Disease.

    Cold Spring Harbor Perspectives in Biology, 6(10), a016295.

Taylor, P. R., Martinez-Pomares, L., Stacey, M., Lin, H. H., Brown, G. D., & Gordon, S. (2005).

    Macrophage Receptors and Immune Recognition. *Annual Reviews of Immunology*, 23, 901-

    944.

Thomas, P. J., Newell, E. E., Eccles, K., Holloway, A. C., Idowu, I., Xia, Z., Hassan, E., Tomy,

    G., & Quenneville, C. (2021). Co-exposures to trace elements and polycyclic aromatic

    compounds (PACs) impacts North American river otter (Lontra canadensis) baculum.

    Chemosphere, 265, 128920.

TOCRIS. (n.d.). Toll-like Receptor Signaling Pathway. https://www.tocris.com/pathways/toll-

    like-receptor-signaling-pathway

Trizio, D., Basketter, D. A., Botham, P. A., Graepel, P. H., Lambre, C., Magda, S. J., Pal, T. M., Riley, A. J., Ronneberger, H., Van Sittert, N. J., & Bontinck, W. J. (1988). Identification of immunotoxic effects of chemicals and assessment of their relevance to man. *Food and Chemical Toxicology*, 26(6), 527-539.

Tükel, Ç., Nishimori, J. H., Wilson, R. P., Winter, M. G., Keestra, A. M., Van Putten, J. P., & Bäumler, A. J. (2010). Toll-like receptors 1 and 2 cooperatively mediate immune responses to curli, a common amyloid from enterobacterial biofilms. *Cellular Microbiology*, 12(10), 1495-1505.

Underhill, D. M. (2003). Macrophage recognition of zymosan particles. *Journal of Endotoxin Research*, 9(3), 176-180.

Van den Heuvel, M. R., Hogan, N. S., Roloson, S. D., & Van Der Kraak, G. J. (2012). Reproductive development of yellow perch (Perca flavescens) exposed to oil sands–affected waters. *Environmental Toxicology and Chemistry*, 31(3), 654-662.

Varanasi, U., Stein, J. E., Nishimoto, M., Reichert, W. L., & Collier, T. K. (1987). Chemical carcinogenesis in feral fish: uptake, activation, and detoxication of organic xenobiotics. *Environmental Health Perspectives*, 71, 155-170.

Varin, A., & Gordon, S. (2009). Alternative activation of macrophages: immune function and cellular biology. *Immunobiology,* 214, 630-641.

Varol, C., Mildner, A., & Jung, S. (2015). Macrophages: development and tissue specialization. *Annual Review of Immunology*, 33, 643-675.

Vicente, A. M., Guillén, M. I., & Alcaraz, M. J. (2001). Modulation of haem oxygenase-1 expression by nitric oxide and leukotrienes in zymosan-activated macrophages. *British Journal of Pharmacology*, 133(6), 920-926.

Wang, Z., Wesche, H., Stevens, T., Walker, N., & Yeh, W. C. (2009). IRAK-4 Inhibitors for

    Inflammation. *Current Topics in Medicinal Chemistry*, 9(8), 724-737.

Wayland, M., Headley, J. V., Peru, K. M., Crosley, R., & Brownlee, B. G. (2008). Levels of

    polycyclic aromatic hydrocarbons and dibenzothiophenes in wetland sediments and aquatic

    insects in the oil sands area of Northeastern Alberta, Canada. *Environmental Monitoring and*

    Assessment, 136, 167-182.

Wolff, D. J., Lubeskie, A., & Li, C. (1997). Inactivation and Recovery of Nitric Oxide Synthetic

    Capability in Cytokine-Induced RAW 264.7 Cells Treated with "Irreversible" NO Synthase

    Inhibitors. *Archives of Biochemistry and Biophysics,* 338(1), 73-82.

Wu, C. H., Chang, C. H., Lin, H. C., Chen, C. M., Lin, C. H., & Lee, H. M. (2003). Role of

    protein kinase C in BSA-AGE-mediated inducible nitric oxide synthase expression in RAW

    264.7 macrophages. *Biochemical Pharmacology,* 66(2), 203-212.

Yadav, A., Saini, V., & Arora, S. (2010). MCP-1: Chemoattractant with a role beyond immunity:

    A review. *Clinica Chimica Acta*, 411(21-22), 1570-1579.

Zelante, T., Fric, J., Wong, A. Y., & Ricciardi-Castagnoli, P. (2012). Interleukin-2 production by

    dendritic cells and its immuno-regulatory functions. *Frontiers in Immunology*, 3, 161.

Zhang, Q., Liu, M., Li, L., Chen, M., Puno, P. T., Bao, W., Zheng, H., Wen, X., Cheng, H., Fung,

    H., Wong, T., Zhao, Z., Lyu, A., Han, Q., & Sun, H. (2021). Cordyceps polysaccharide marker

    CCP modulates immune responses via highly selective TLR4/MyD88/p38 axis. *Carbohydrate*

    Polymers, 271, 118443.

Zhou, X., Ye, Y., Sun, Y., Li, X., Wang, W., Privratsky, B., Tan, S., Zhou, Z., Huang, C., Wei, Y.

    Q., Birnbaumer, L., Singh, B. B., & Wu, M. (2015). Transient Receptor Potential Channel 1

Deficiency Impairs Host Defense and Proinflammatory Responses to Bacterial Infection by

Regulating Protein Kinase Cα Signaling. *Molecular and Cellular Biology*, 35(16), 2729-2739.

Zubot, W., MacKinnon, M. D., Chelme-Ayala, P., Smith, D. W., & El-Din, M. G. (2012).

Petroleum coke adsorption as a water management option for oil sands process-affected water.

Science of the Total Environment, 427-428, 364-372.

a)
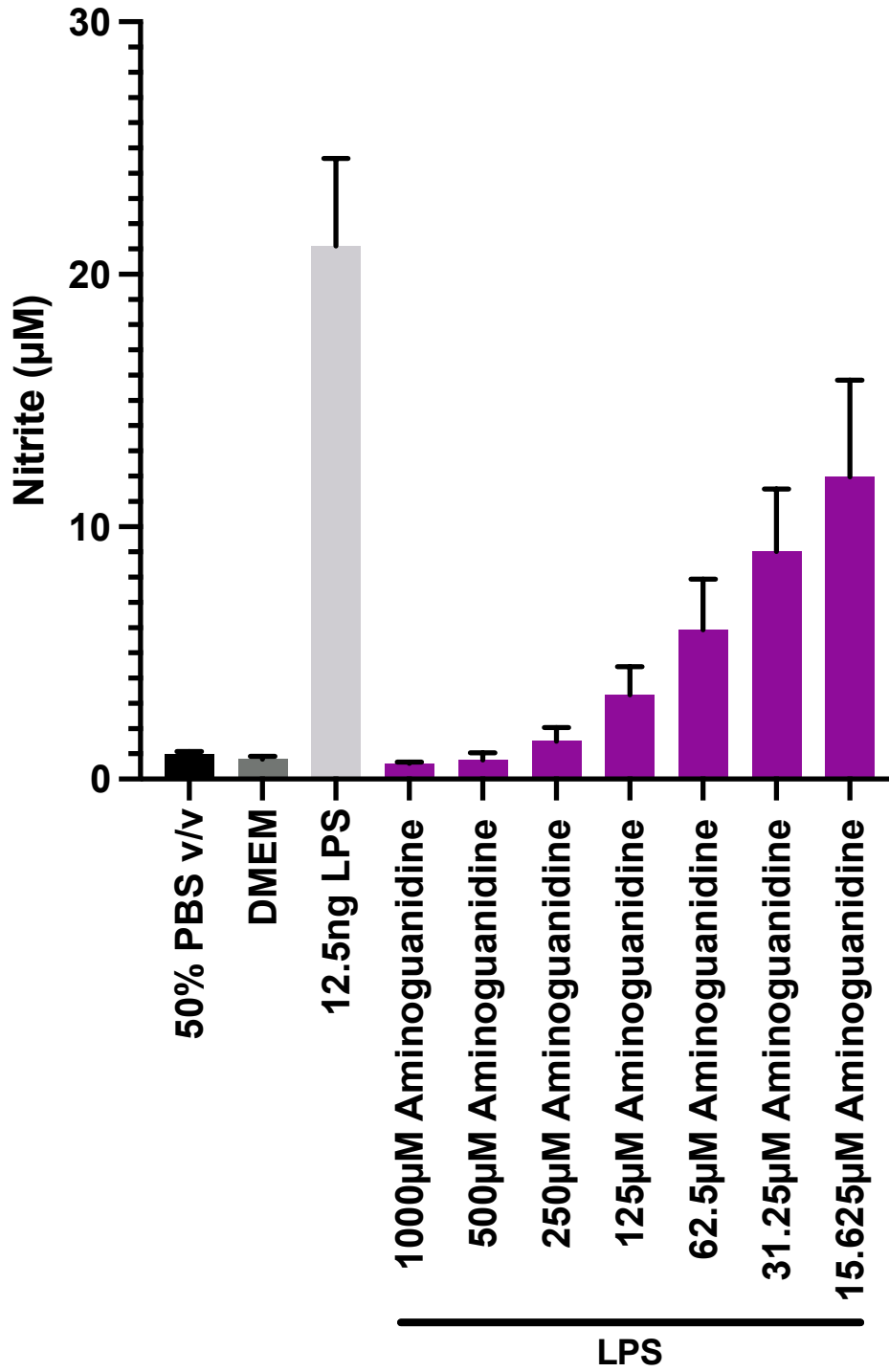
b)
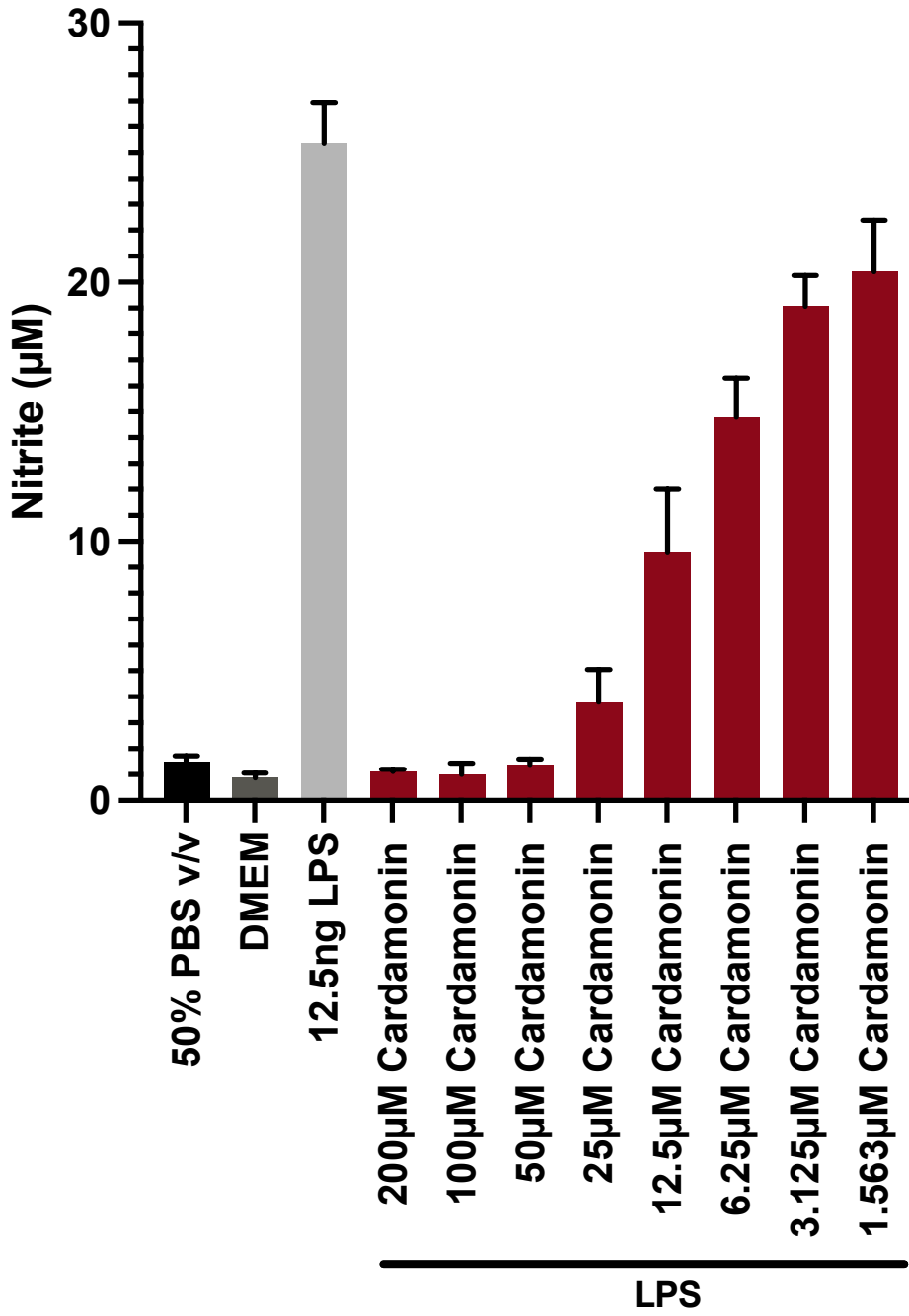
c)
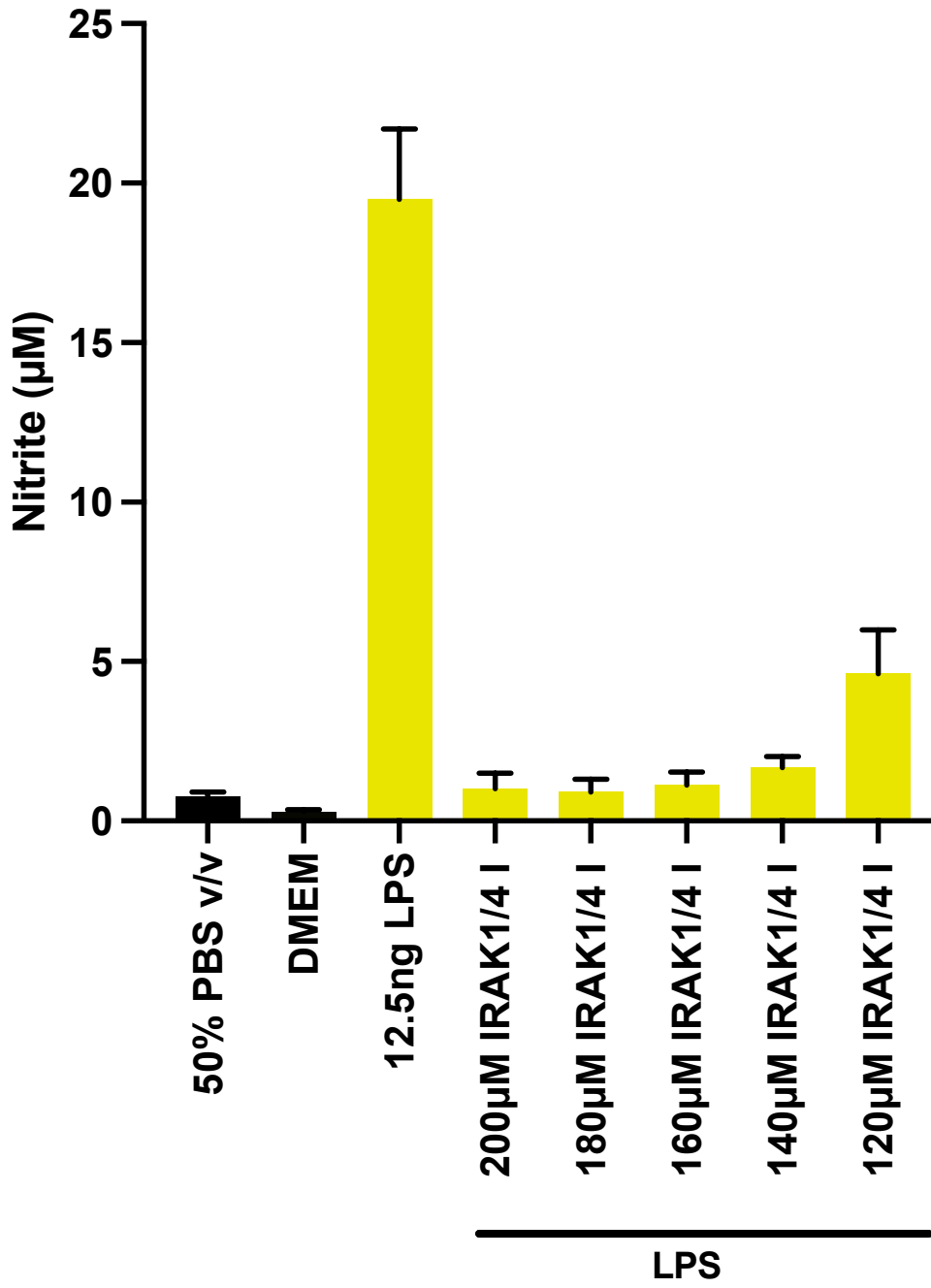
d)

e)
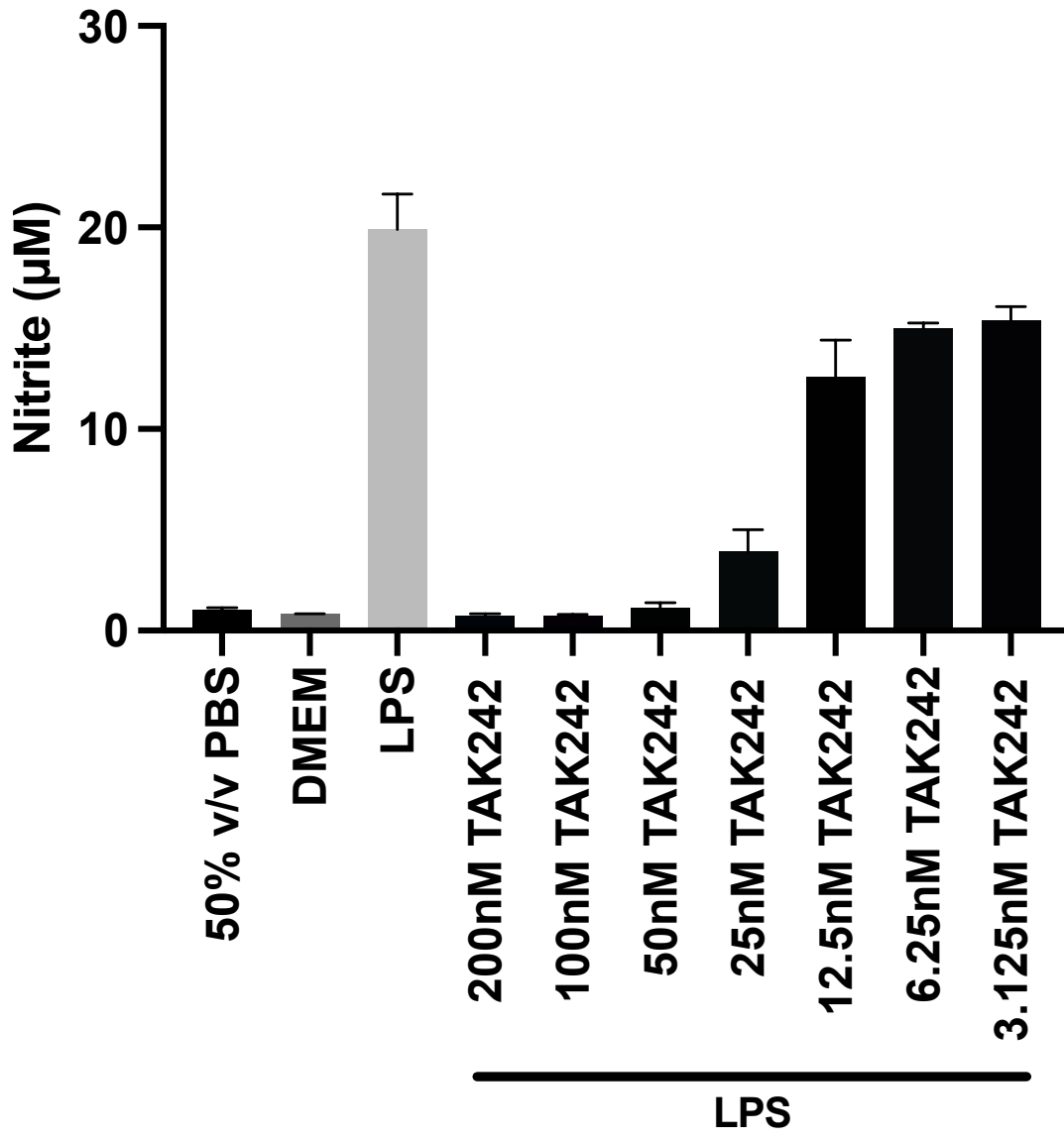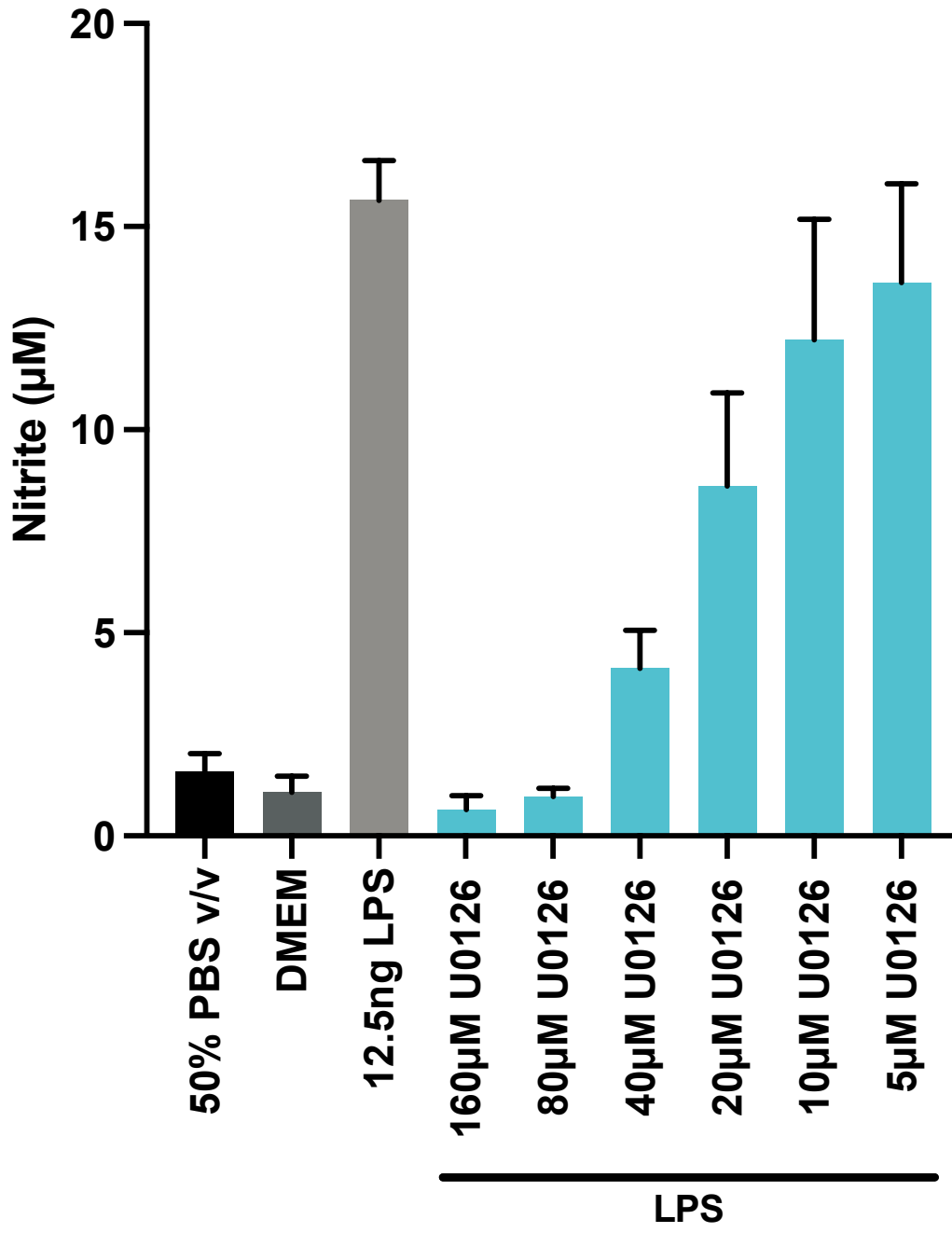
Appendix Figure 1. Serial dilutions of pharmacological inhibitors at various concentrations with LPS stimulation. RAW 264.7 cells (100 000 cells/well) were pretreated with Aminoguanidine (a; n=3), Cardamonin (b; n=3), IRAK1/4 Inhibitor I (c; n=3), TAK242 (d; n=3), or U0126 (e; n=3) for 2 hours before stimulation with LPS (12.5 ng/mL) for 22 hours. Positive and negative controls were exposed for 24 hours.